VIBRATIONAL RELAXATION OF DIATOMIC MOLECULES AT HIGH TEMPERATURES

A Thesis presented by

STEPHEN JAMES COLGAN

in partial fulfilment of the requirements

for the degree of

DOCTOR OF PHILOSOPHY.

Department of Chemistry,
Imperial College of Science and Technology,
London. S.W.7.

August, 1968.

ABSTRACT.

This thesis describes the use of light emission from sulphur dioxide to measure vibrational relaxation times (vibrational energy transfer rates) in shock heated gas mixtures. Chapter 1 surveys the principles underlying the theory of vibrational energy transfer in gases and summarises the practical methods available for the measurement of relaxation times in the shock tube.

The description of the shock tube and the experimental techniques used in this work are given in Chapter 2.

The analysis of the sulphur dioxide emission to give vibrational relaxation times is set out in Chapter 3. It is shown that the observed decrease in the relaxation time of nitrogen behind incident shock waves, contrary to the expected behaviour, is due solely to boundary layer formation in the shock tube. The results have been corrected accordingly; they then fall in line with the determinations of other workers.

In Chapter 4 the vibrational relaxation times of nitrogen with the following collision partners are given: N_2, H_2, He, D_2, Ar, Kr (at 2500^{oK}); SO_2 ($1800 - 2500^{oK}$); O_2, HCl, DCl, H_2O, D_2O (2500^{oK}); and CH_4, CD_4 (2250^{oK}). The first six partners have been correlated successfully with the Schwartz, Slawsky and Herzfeld theory and also with Millikan and White's semi-empirical formula. The results for the remaining collision partners have been interpreted in terms of near resonant vibration-vibration energy transfer processes. Energy transfer from the rotational modes of all these molecules does not contribute significantly to the rate of vibrational relaxation.

In Chapter 5 the use of a laser schlieren system to follow the density gradient due to vibrational relaxation is described. Relaxation times obtained for $N_2 - H_2$ mixtures are in accord with other results. A modification is suggested to improve the sensitivity of the system.

ACKNOWLEDGEMENTS.

I wish to register my appreciation to Dr. Bryan P. Levitt for his guidance and supervision at all times during this work and to thank Professor R.M. Barrer F.R.S. for providing research facilities in the Department of Chemistry at Imperial College. I acknowledge helpful discussions on the theoretical aspects of the work with Dr. J.L. Stretton (C.E.R.L. Leatherhead).

I thank the Science Research Council for my Research Studentship; they also provided a Special Research Grant for the apparatus used. The work was also partially supported by the European Research Office of the United States Army under contracts DA-91-59-EUC-3360/4113 and DAJA 37-67-C-0735. The later stages of the work was greatly aided by the Literature Information Service provided through a Chemical Society/OSTI project.

I thank Mr. D. Alger and the Instrument Section of this Department for their help with the electronic equipment, Mr. H. Cobley and the Workshop staff for construction of the shock tube itself, and Mr. A. Madell and the Glassblowing section for construction of the glassware, particularly the high speed pumping line.

I thank Messrs. British Sidac Ltd. for a gift of diaphragm material, the Institute of Computer Science, University of London, for the use of their ATLAS computer, and the Centre for Computing and Automation at Imperial College for the use of their I.B.M. 7090/4 computer.

CONTENTS.

NOMENCLATURE

The letter sequences T-V, V-V, R-V, etc. quoted throughout the thesis refer to the processes for the transfer of energy between the internal modes of two molecules during a collision.

e.g. T-V : translation → vibration energy transfer.

V-V : vibration → vibration energy transfer.

R-R : rotation → rotation energy transfer.

Vibrational relaxation times are quoted as $P\tau(A\text{-}B)$. This refers to the transfer of energy from molecule B to the vibrations of molecule A.

$P\tau(A\text{-}B)_T$ refers specifically to the transfer of energy in the T-V process between molecules A and B. Similarly relaxation times with the subscripts R or V refer to the R-V and V-V processes respectively.

CHAPTER 1.

ENERGY TRANSFER IN GASES.

1-1) INTRODUCTION.

All chemical reactions involve the transfer of molecular energy. The investigation of energy transfer processes involves many aspects of the physical sciences. In solids, energy transfer is governed by the vibrational modes of molecules fixed in the crystal lattice. In liquids this symmetry is lost; interpretation of results is rendered difficult by the complex interaction of molecules in close proximity. Energy transfer in gases takes place by simple collisions whose character is well established by the kinetic theory.

1-2) GENERAL PRINCIPLES FOR GASES.

Gas molecules may gain or lose energy by two distinct processes - either through the absorption or emission of radiation or during collisions with other particles. When molecules collide, four types of energy may be exchanged during the period of interaction - translational, rotational, vibrational and electronic energy.

The probabilities of energy transfer for these processes are governed by Ehrenfest's adiabatic principle (1). Consider an oscillatory motion described by a set of quantum numbers. The motion is perturbed by changing an external parameter. If the change is small during the period of the oscillation, the quantum number will be unaltered by the perturbation (adiabatic). If the change is large, i.e. the perturbation is fast, there is a finite probability that the quantum number will change as a result of the perturbation (non-adiabatic). In this case, the perturbation is the

collision itself and so for effective energy transfer the time of interaction during the collision must be small compared to the period of oscillation associated with the molecular energy change under consideration.

Translational quanta are so small that the transfer of translational energy between molecules on collision may be treated using classical mechanics. The probability of energy transfer is unity.

Rotational quanta are also small and the period of oscillation, i.e. rotation, is of the same order as the collision time. The probability of rotational energy transfer is thus high; for diatomic gases at room temperature it requires only about 10 collisions. Hydrogen, with its lower moment of inertia, is an exception; it requires about 300 collisions at room temperature (2).

The measurements described in this thesis are on a time scale which is much longer than the time required for the equilibration of translational and rotational energy. These parameters are always considered to be in equilibrium during the period of measurement.

Ehrenfest's principle may be applied to vibrational energy transfer. When the period of interaction of the colliding species is short compared to the period of the vibration, energy transfer becomes probable.

The average period of interaction for the collision may be written as xv^{-1} where x represents the interaction distance between the species and v is the mean molecular velocity. As the period of vibration is $\frac{1}{\nu}$ where ν is the frequency of the oscillator then it may be stated that energy transfer is probable only when

$$\nu\, xv^{-1} \ll 1$$

A similar conclusion may be obtained by considering the collisions classically.

For a typical diatomic molecule at 300^{oK}, $\nu \simeq$ 1000 cms^{-1}, $x \simeq 10^{-8}$cm., $\nu \simeq 3.10^{4}$cm.sec.$^{-1}$ and hence $\nu x v^{-1} = 10$. A velocity at least 10 times the average is thus required for energy transfer. The proportion of these collisions is governed by the Maxwell-Boltzmann[1] distribution of velocities and is small. The probability of energy transfer is correspondingly low. For O_2 at 300^{oK}, $2x10^{7}$ collisions are required (2). The proportion of energetic collisions increases rapidly with temperature; the probability of vibrational energy transfer increases accordingly.

The period of oscillation associated with an electronic energy change is so short that direct electronic-translational energy transfer is forbidden. Collisional transfer of electronic energy often occurs by internal conversion.

The advent of the laser as well as of problems associated with supersonic combustion, shock initiated detonations etc. has stimulated interest in these energy transfer processes. As vibrational energy transfer takes several thousand collisions its importance is felt in many fields - chemical kinetics, dissociation (2,3,4).

Although much is known about the translation - vibration (T-V) processes, as yet relatively little is known about (V-V) and (R-V) processes. Various reviews have considered the problems associated with energy transfer (4-11). The article by Lambert (7) gives a clear account of (V-V) energy transfer.

1-3) DEFINITION OF VIBRATIONAL RELAXATION.

When a gas at equilibrium is perturbed, the rate at which any parameter

A adjusts itself to its new surroundings is given by:

$$\frac{d(\Delta A)}{dt} = \frac{-(\Delta A)}{\tau} \qquad (1\text{-}1)$$

where ΔA represents the deviation of A from its final equilibrium value.

This re-adjustment is known as a relaxation process and τ is the relaxation time characteristic of the rate of change of A. From this definition it is also the time required for (ΔA) to be reduced to $^1/_{e}$th. of its value.

For a vibrational perturbation (1-1) becomes:

$$\frac{d(E_{VIB})}{dt} = \frac{-\left(E_{VIB}(Eq) - E_{VIB}\right)}{\tau} \qquad (1\text{-}2)$$

where E_{VIB} is the vibrational energy and $E_{VIB}(Eq)$ is the equilibrium vibrational energy. This equation holds for a two level system. Landau and Teller (12) have also shown that a system of multilevel harmonic oscillators may be described by (1-2) provided that (1) the change in quantum number on collision is $0, \pm 1$, and (2) the transition probabilities per collision K_{xy} (for a change in quantum number $x \rightarrow y$) are in the ratio of the vibrational quantum numbers, i.e.

$$K_{01} : K_{12} : K_{23} = 1 : 2 : 3 \ldots\ldots$$

When the translational temperature is changing, $E_{VIB}(Eq)$ becomes $E_{VIB}(T)$ -the equilibrium vibrational energy corresponding to the instantaneous translational temperature (T.). The relaxation time τ in the Landau-Teller equation (1-2) is a function of the translational temperature of the gas. It increases in value as T is reduced. Behind incident shock waves, T falls during the vibrational relaxation. The energy supplied to the

relaxing mode is taken from the translational and rotational energy of the molecule. The instantaneous value of τ should therefore increase as relaxation proceeds. This will be described as "Landau-Teller" behaviour. Apparent deviations from this behaviour will be discussed in Chapter 3.

As vibrational relaxation times are the result of two-body collisions, they are inversely proportional to the pressure of the gas. Relaxation times are referred to a standard pressure of one atmosphere and are normally expressed in the units of atmosphere-seconds (atm. sec.) The relaxation time τ is related to the probability of energy transfer per collision, P_{xy}, and to the number of collisions required for the transfer of a quantum of energy, Z_{xy}.

$$P_{010} = \left[\tau (1 - e^{-h\nu/kT}) Z \right]^{-1}$$

$$P_{01} = 1/Z_{01}$$

where Z, the gas collision rate at one atmosphere, is given by

$$Z = 4 n \sigma^2 \left(\frac{\pi kT}{M} \right)^{1/2}$$

n = no. of molecules per cm^3 at 1 atm.

σ = collision diameter.

M = reduced mass.

1-4) THEORETICAL TREATMENTS OF VIBRATIONAL RELAXATION.

The first comprehensive theory of vibrational relaxation was given by Landau and Teller. (12). Their classical calculations considered only T-V transfer and coupled an exponential interaction potential between the colliding molecules to the most favoured approach velocity for energy transfer. This last factor was obtained from an examination of the Maxwell distribution of velocities.

Many of the parameters in the theory were unknown and no absolute calculations were made. The theory did, however, predict the correct temperature dependence of relaxation times viz:

$$\log_{10} P\tau \propto T^{-1/3} + \text{constant.}$$

Schwartz, Slawsky and Herzfeld (SSH) (13) derived a quantum mechanical theory using Jackson and Mott's (14) "distorted wave" method. This treats the problem as a stream of plane waves striking a scattering vibrator. Most of the waves are scattered elastically; the small inelastic contribution corresponds to a change in the vibrational quantum number of the scatterer i.e. to vibrational energy transfer. The solution to the Schrodinger eqn. for the distorted wave is obtained by perturbation theory. This solution is valid only when the perturbation is small, i.e. when the probability of energy transfer is small.

The derivation of the theory has been described in great detail in the book by Herzfeld and Litovitz (15). The theory may be extended to include the effect of resonant or near resonant energy transfer (V-V). The effect of rotation (R-V) has not been treated.

The basic SSH theory may be summarised as follows. The calculation for the number of collisions required to de-excite a vibrational mode from quantum level 1 to level 0, Z_{10}, is divided into three parts Z_0, Z_{OSC}, Z_{TR} where

$$Z_{10} = Z_0 \cdot Z_{OSC} \cdot Z_{TR} .$$

Z_0 is a steric factor which is estimated to account for the proportion of head-on to the total number of collisions which can influence energy transfer. Its value for a diatom-atom collision is taken as $1/3$. Z_{OSC} contains terms mainly describing the molecular weight and reduced mass of the colliding

particles. It is independent of temperature. Z_{TR} is dependent on both temperature and vibrational frequency. It takes into account, if necessary, resonant or near-resonant V-V transfer.

To enable the equations to be interpreted, the interaction potential between the colliding molecules must be expressed as an exponential. This can lead to uncertainties in the exact application of the theory. Another important parameter required in SSH calculations is the characteristic length, L, used in the exponential repulsion term between the colliding molecules. L is normally about $\cdot 2\text{Å}$ for most molecules: a small error in its computation is magnified in the calculations for Z_{10}. Herzfeld and Litovitz give various methods both for calculating L from viscosity data and for modifying data from Lennard-Jones type potentials to fit the exponential repulsion term.

The original theory is very successful in predicting vibrational relaxation times. It has since been modified in many ways, e.g. in the inclusion of a 3-dimensional analysis using a Morse oscillator (16) or an angular dependent potential (17). Benson et al. (18, 19) have examined in detail the coupling between the atoms in a collision between a hard sphere and a diatomic molecule. Recently Hartmann and Slawsky (20) have compared the various forms of intermolecular potential available when calculating relaxation times in chlorine. Shin (21) has given methods for the calculation of the steric factor Z_0.

Tanczos (22) extended SSH theory to collisions between polyatomic molecules. The polyatomic molecules are considered as "breathing spheres" where the movements of the surface atoms in the vibrations are separated

from the translational motion involved in the collision. This modified theory is mainly concerned with an accurate calculation of Z_{OSC} for the polyatoms. This is the factor that describes the motions of the surface atoms. When a diatomic molecule is treated using the breathing sphere model, the derived Z_{OSC} is equal to that obtained from the original SSH theory.

Stretton (23) has used this model as a basis for the comparison between calculated and measured relaxation times in a series of hydrocarbons and their halogenated derivatives. One notable point arising from Stretton's work is that the characteristic length, L, best suited to the calculations is almost identical for all these molecules. (1.8Å).

Millikan and White (24) have deduced a semi-empirical correlation for the experimental relaxation times of diatomic molecules with various collision partners:

$$\log_{10} P\tau = 5.10^{-4} \cdot \mu^{\frac{1}{2}} \cdot \Theta^{4/3} \left[T^{-1/3} - .015 \mu^{\frac{1}{4}} \right] - 8.00 \qquad (1\text{-}3)$$

where $P\tau$ is in atm.sec.

$$\Theta = \frac{h\nu}{k} \quad , \quad \mu = \text{reduced mass of the collision pair in a.m.u.}$$

The relaxation times predicted depend only on the temperature, reduced mass and on the vibrational frequency of the oscillator. The equation is remarkably accurate for a wide range of gases. If, as Stretton suggests, the characteristic length for all collisions is similar, this result is not surprising.

If the SSH equations are arranged in the same form as (1-3), the exponents of T, μ and ν are approximately $-\frac{1}{3}$, $\frac{1}{3}$ and $\frac{2}{3}$ respectively: equation (1-3) gives them as $-\frac{1}{3}$, $\frac{1}{2}$ and $\frac{4}{3}$. An accurate determination of the

exponent for μ forms part of the work to be described here.

Losev and Osipov (25) have also correlated relaxation times empirically in terms of Landau-Teller and SSH theories. Good agreement is reported where only T-V transfer is involved.

There are several gases for which the simple SSH and Millikan and White theories fail e.g. air (V-V coupling between N_2-O_2), CH_4 (rotation), O_2-O (chemical interaction). These deviations from the theoretical predictions are discussed further in section (1-5) below.

1-5) DEVIATIONS FROM "SSH" T-V THEORY.

Where the collision partner is diatomic or polyatomic, the observed relaxation time is often much lower than that predicted by assuming only (T-V) energy transfer. The more complex SSH theory mentioned in sect. (1-4) which includes (V-V) transfer has been applied fairly successfully to these gas mixtures in which (V-V) processes are important.

Rapp et. al. (e.g. 26, 27) have developed a separate theory of resonant/near-resonant (V-V) energy transfer based on the lines of (T-V) transfer. Although mathematically different to SSH theory, the final results are roughly equivalent. No theory however is yet in the position to give an adequate account of multiple quantum transfers; these seem to be underestimated in both theories.

SSH theory is notably incorrect in predicting the ratio of relaxation times in molecules containing either hydrogen or deuterium e.g. CH_4/CD_4, HCl/DCl (28, 29). This has been ascribed to the coupling of rotation in the transfer of energy in the collision. For molecules with low moments of inertia, the high peripheral angular velocity can be comparable to the

translational approach velocity of the colliding molecules. Collisions in which rotational energy is transfered to vibrational energy directly may thus contribute to the overall relaxation.

Lambert and Salter (30) examined the effect that the number of hydrogen atoms substituted in organic molecules had on the vibrational relaxation times. By plotting log Z_{01} against the lowest vibrational frequency of the molecule they found that points for compounds fell on different plots according to the number of hydrogen atoms they contained. The plots were linear and the slopes decreased as the number of hydrogen atoms per molecule increased.

(R-V) energy transfer has often been cited as the explanation for the molecules on the Lambert-Salter plot. However for these molecules the Z_{OSC} factor in the SSH theory contains terms very dependent on the number of hydrogen atoms in the molecule. It is possible that the theory is inaccurate in its consideration of vibrations such as $H\text{-}CX_3$.

Cottrell et.al. (31) and Bradley-Moore (32) have considered the interaction of a classical rotator with a quantised oscillator. They have applied their theories with some success to the hydrogen containing molecules on the Lambert-Salter plot. Nikitin (33) has recently published a theory of vibrational relaxation which accounts for the effects of rotation. Good agreement with the practical measurements on HI are claimed.

Another intractable effect is that of chemical interaction between the colliding species. This has been used by Callear and Williams (34) to explain the anomalously fast relaxation of nitric oxide with various hydrides and deuterides. The fast vibrational relaxation of oxygen by O atoms

obtained by Kiefer and Lutz (35) has also been described in terms of incipient chemical bonding - "sticky collisions".

In summary therefore, the modified SSH theory provides an adequate basis for formal vibrational relaxation calculations. Millikan and White's formula also predicts the rate of many T-V processes. Rotational and chemical effects are, as yet, not fully understood; a more comprehensive theory with their inclusion is required.

1-6) EXPERIMENTAL METHODS OF DETERMINING RELAXATION TIMES.

For a complete understanding of energy transfer, an adequate knowledge of the variation of relaxation times over a wide temperature range is required. Almost all high temperature work has been performed in shock-tubes and the results have, in general, confirmed measurements at lower temperatures. Room temperature methods of measurement - the ultrasonic interferometer, the spectrophone, "kinetic spectroscopy" (flash photolysis) etc. have been reviewed in the monograph by Cottrell and McCoubrey (2).

1-7) THE SHOCK TUBE.

Consider a tube of gas closed at one end by a piston which is capable of acceleration to a velocity greater than the speed of sound in the gas. If the piston is considered accelerating in small increments, then the pressure wave propagating through the medium at each step progressively compresses the gas. Each "step-wave" travels through the gas faster than its predecessor and a shock wave is produced when these steps coalesce. As the shock front travels normally down the tube, the hot compressed gas is pushed out behind it at the velocity of the piston. See fig. (1-1) (a).

In fig. (1-1) (b) an equivalent process where the passage of gas at a

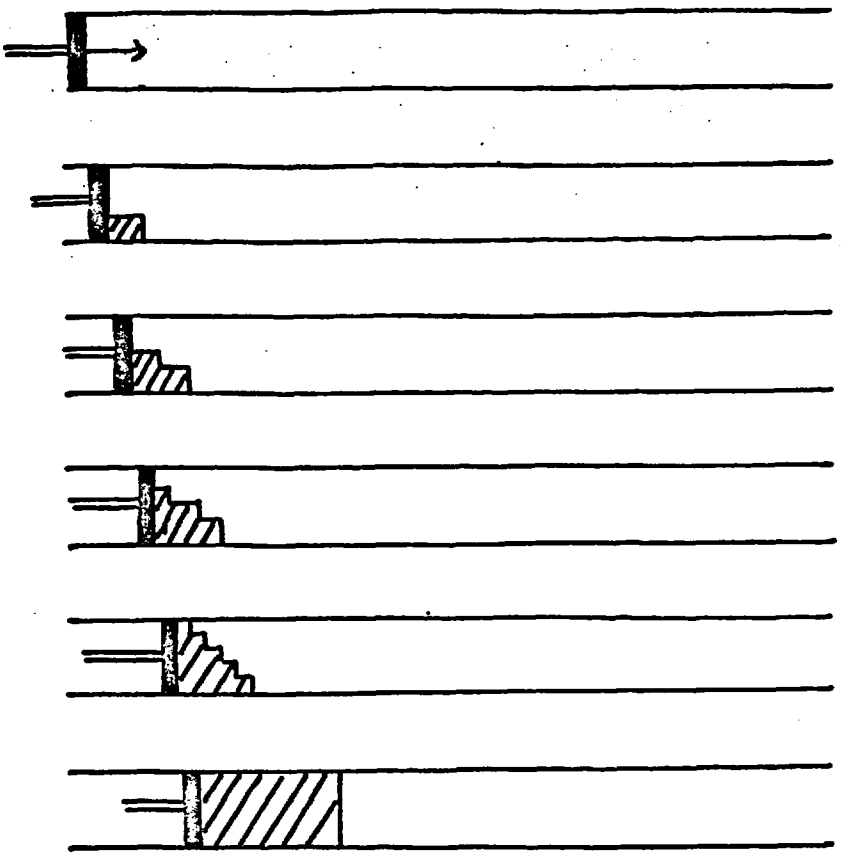

FIG. 1-1 (a)

FORMATION OF A SHOCK WAVE (AFTER BECKER).

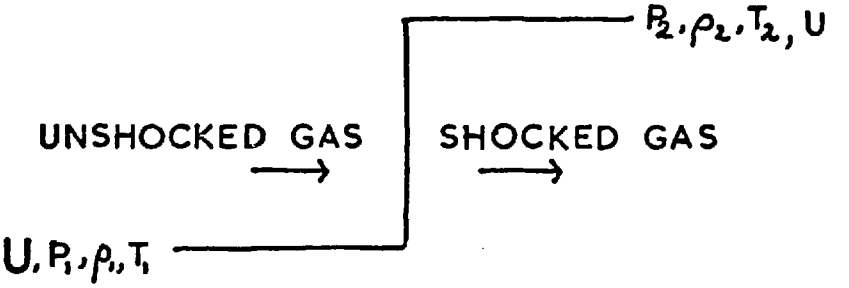

FIG. 1-1 (b)

PASSAGE OF GAS THROUGH A STATIONARY SHOCK FRONT

constant rate through unit area of a stationary shock front is considered. Equations governing the physical parameters of the shocked and unshocked gas may be written in terms of the conservation of mass, energy, momentum and in terms of the general gas law:

$$\rho_1 U = \rho_2 u \qquad (1\text{-}4)$$ Conservation of mass

$$\rho_1 U^2 + P_1 = \rho_2 u^2 + P_2 \qquad (1\text{-}5)$$ " " momentum

$$\tfrac{1}{2} U^2 + H_1 = \tfrac{1}{2} u^2 + H_2 \qquad (1\text{-}6)$$ " " energy.

$$\frac{P_1}{\rho_1} = D_1 R_1 T \; ; \; \frac{P_2}{\rho_2} = D_2 R T_2 \qquad (1\text{-}7)$$ General gas law.

(Notation as in fig. (1-1) (b)).

A solution to these equations in terms of the shocked gas temperature, pressure and density requires a knowledge of all the unshocked gas parameters, the enthalpy as a function of temperature as well as one other variable of the shocked gas. Normally the measured shock velocity, U, is chosen as this variable and the solution of equations (1-4) - (1-7) may be obtained. The calculations are easy but tedious and are normally carried out on a computer.

When an ideal monatomic gas is shocked, the temperature behind the front remains constant in the absence of ionisation. There are no relaxation processes to make the internal energy of the gas time dependent. In a gas undergoing relaxation behind the shock front, the shocked gas enthalpy increases due to the contribution from the relaxing modes and the temperature falls: the shocked gas is adiabatic and nearly at constant pressure.

For nitrogen undergoing relaxation at about 2500°K, the equilibrium temperature is several hundred degrees below the temperature behind the front. In this context it is possible to consider the separation of the translational,

rotational and vibrational temperatures as relaxation proceeds. Such a process is illustrated in fig. (1-2) (a). Although the effect of vibrational relaxation can mean up to a 10-15% change in the translational temperature and density, the effect on pressure is much smaller. This is illustrated in fig. (2-2) (b) (c).

By monitoring the change in these variables, the shock tube provides a useful tool for obtaining relaxation times. Its advantages are that by selecting the shock strength any desired temperature range may be studied. The one dimensional flow down the tube provides a time scale for the measurement of these processes. However as the gas under observation has been compressed and set in motion by the shock wave, the laboratory time scale will not coincide with the internal time scale of the reactions taking place in the tube.

For ideal flow $t_1 = t_g / (\rho_2 / \rho_1)$ so the time scale is compressed. t_1 is laboratory time; t_g is gas particle time.

One of the major disadvantages of the shock tube is that the gas is never completely inviscid and a boundary layer of cold gas builds up behind the shock front adjacent to the walls of the shock tube. This effect is worst at low pressures in small diameter shock tubes and any rate measurements made under these conditions must be corrected very carefully.

1-8) RELAXATION MEASUREMENTS IN SHOCK TUBES.

All relaxation times measured in shock tubes have been obtained by monitoring the change in temperature, density or vibrational energy of the shocked gas. Density measuring techniques - the Mach-Zender interferometer, the X-ray densitometer etc. have been described in the books written on shock

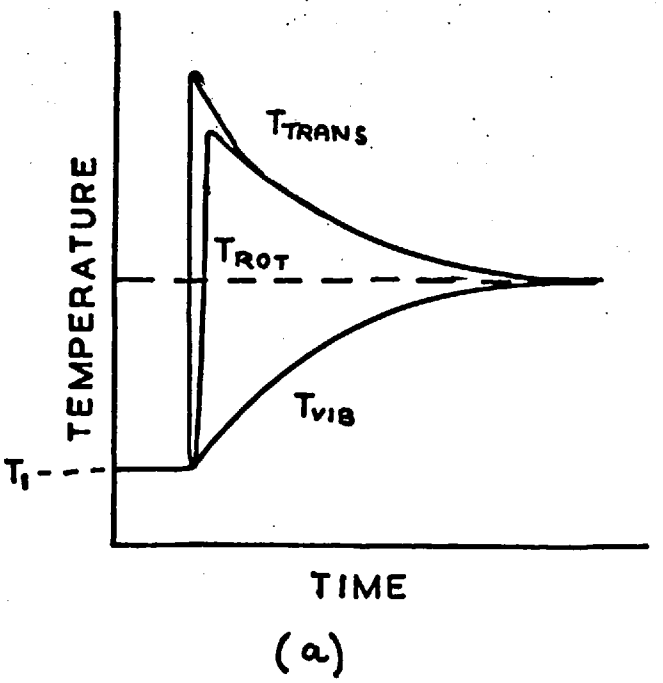

(a)

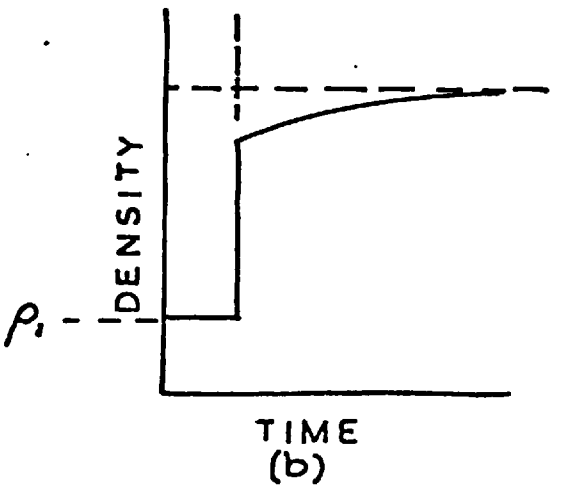

(b)

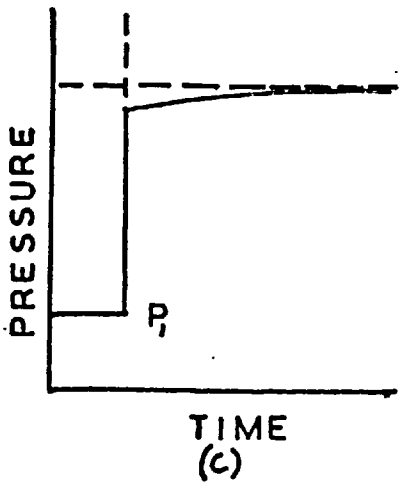

(c)

VARIATION OF TEMPERATURE, DENSITY, PRESSURE IN A RELAXING GAS BEHIND A SHOCK WAVE

FIG. 1-2

tube techniques (36, 37, 38). Kiefer and Lutz (39, 40, 41) have recently used a continuous gas laser as a narrow beam source of light to obtain quantitative schlieren measurements of the density gradient behind shock fronts.

The line reversal technique for determining relaxation times developed by Gaydon et.al. (42) monitors the emission from an ionised metal atom and compares it to the brightness temperature of a calibrated light source. The population of the electronically excited metal atoms has been shown to be in equilibrium with the vibrational energy of the relaxing gas. There has been considerable discussion whether the relaxation times infered from this technique are correct. Results obtained using both chromium and sodium as the ionised atom are however in excellent agreement with those obtained by other methods (37).

The recent advent of fast rise-time infra-red detectors has enabled many measurements of relaxation times in I-R active molecules to be made directly (43). The intensity of an infra-red vibration-rotation band is a function of the population of the level corresponding to the band. A record of the intensity against time gives the relaxation time for that particular vibration. This technique should enable the relative contributions of each separate vibration to the relaxation of a polyatomic molecule to be determined.

The method used to determine relaxation times in this thesis was developed from the work of Levitt and Sheen (44-47) on the characteristics of the light emission from shock-heated sulphur dioxide. This emission has been shown to depend on the translational temperature of the gas. When a small proportion of SO_2 is added to a relaxing gas e.g. N_2, the emission provides

a very sensitive method of following the fall in translational temperature due to relaxation.

Two or three interesting points arose from Levitt and Sheen's preliminary work on this emission tracer technique. The instantaneous rate of vibrational relaxation of nitrogen apparently decreased as relaxation went to completion, unlike the expected increase in $P\tau$ for Landau-Teller behaviour. Secondly a short investigation of the vibrational relaxation of N_2 indicated that an SO_2 molecule was more efficient in transfering energy than a nitrogen molecule itself. On (T-V) energy transfer theory the heavier SO_2 molecule should be a less efficient collision partner.

The initial objectives in this work were thus:

(1) the improvement of the translational temperature tracer technique to obtain more accurate relaxation times.

(2) an explanation for the observed decrease in $P\tau$ during a single relaxation.

(3) an explanation for the high efficiency of the SO_2 molecule.

A survey of the literature has shown that although much work has been performed on the relaxation of pure nitrogen, surprisingly little is known about the efficiencies of various collision partners. The third and main objective of this work has been the measurement of these efficiencies with special reference to the relative contributions from the various (T-V), (V-V) and (R-V) processes.

CHAPTER 2.

EXPERIMENTAL METHODS.

2-1) INTRODUCTION.

The shock tube built for this work is of conventional design, similar to the tube already in operation in this Department. The driver section contains hydrogen at high pressure; the test section contains the gas to be shock heated. A shock wave is generated when a plastic diaphragm set between driver and test sections ruptures. The driver gas expands into the test section.

At the far end of the test section remote from the driver section the shock bursts a thin diaphragm and is dissipated in the dump tank. The volume of this tank is sufficiently large to prevent the formation of reflected shocks or high static gas pressures. The dump tank also removes diaphragm fragments and spent test gas.

The metalwork and construction of the tube, window mountings and seals are almost identical to those described by Sheen (48) but the pumping system and electronics have been improved.

2-2) DRIVER SECTION.

This was constructed from 5' of 2" o.d. round brass tubing closed at one end. It is designed to withstand up to 1000 p.s.i. A flat face place was soldered normally to the axis of the tube; it was recessed to hold an "O" ring vacuum seal. The plate is provided with locating dowels to align the tube to a similar plate on the downstream section. The diaphragms are clamped between these plates, vacuum sealed by the "O" rings. The section is mounted on rollers to enable it to be moved easily to change diaphragms.

It is connected by a flexible line to a vacuum pump to remove air before admitting the driver gas.

Hydrogen (B.O.C. cylinder grade) was taken by a two stage regulator with a high pressure outlet (0.-600 p.s.i.) (British Industrial Gases) into the tube by a W.S.A. microneedle valve. Driver pressures in the range 50 - 250 p.s.i. were employed; pressure was measured with three Budenberg vacuum gauges : 0-100, 0-400, 0-1000 p.s.i. These gauges are provided with spring loaded cut-offs which protected them against excessive pressures.

In use, the hydrogen pressure was increased until the diaphragms burst either spontaneously or by the action of a blunt plunger. This was operated by a piston which could be set into motion by applying the driver gas pressure.

2-3) TEST SECTION.

A square tube: 9' long, internal section $1\frac{1}{2}$", wall thickness $\frac{1}{4}$", was constructed by soldering together two lengths of brass angle. The tube is reinforced with metal straps at 1' intervals. Face plates at either end connect to the driver section and to the dump tank.

The hot gas was observed through three pairs of window holes reamed in the vertical faces of the tube. These holes, at stations A, B and C (see fig. 2-1) are situated near the dump tank end of the tube to provide adequate test-time observation of the shocked gas.

A short, round section stainless steel manifold (2" o.d.) between test and driver sections has valves to admit air after a run and to a connection to the glass vacuum line. The change in profile from round to square section was machined so as to avoid any sharp edges which would impede gas flow. The whole section is rigidly bolted to the bench to damp the recoil after

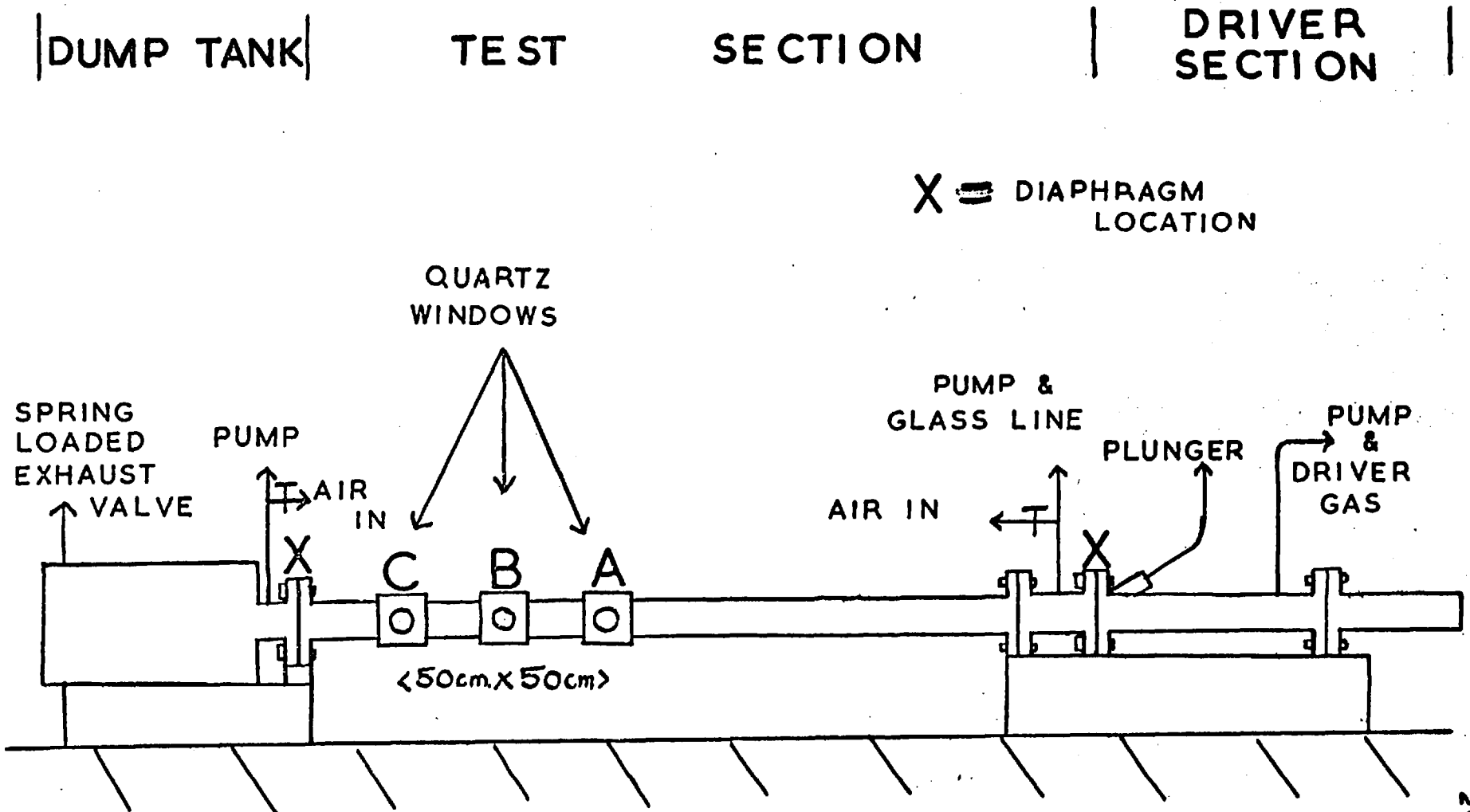

FIG. 2-1 THE SHOCK TUBE

firing the shock.

2-4) WINDOWS.

Quartz discs, 1" diameter, $\frac{1}{4}$" thick (Thermal Syndicate Ltd.) were cemented in circular brass mounts with Araldite to form a vacuum tight seal. The mounts are screwed into flat face plates, pairs of which are bolted together either side of the tube. The windows fit into the reamed holes at A, B and C. Vacuum sealing is afforded by "O" rings: the use of double "O" rings gave a better seal than the system previously used (48) (see fig. 2-2).

The mounts are screwed into the face plates to such a depth so that when fitted in position, the quartz windows are flush with the inside of the shock tube. To assist in this adjustment, windows were set up one at a time by bolting to a dummy face plate. The screw tensions were adjusted until the plate was .060" away from the shock tube wall. The mount was then adjusted in its screw fitting until the window was felt to be flush inside the tube. When this operation was completed for each pair of windows, the dummy plates were discarded and the windows bolted together with the plates again .060" away from the tube.

2-5) DUMP TANK.

A 9" diameter stainless steel tank, 22" in length with a short 6" x 2" o.d. linking tube and face plate is aligned with the downstream section at the end remote from the driver. The tank is closed at one end. At the other, the face plate and its mate on the test section were recessed to take "O" rings. These hold thin diaphragms in a vacuum tight seal. A line is provided to evacuate the tank; it is fitted with a valve to admit air. A spring loaded

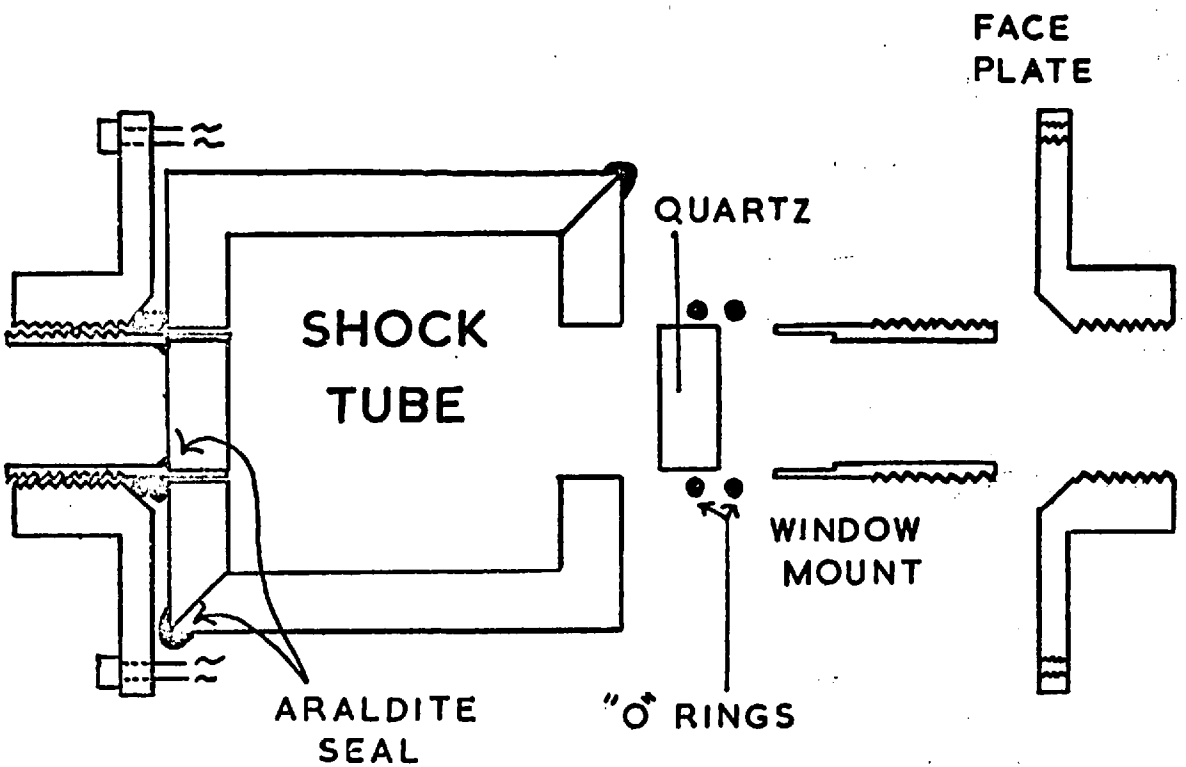

FIG. 2-2 SHOCK TUBE WINDOW SECTION

safety valve set to open at about 5 p.s.i. above atmospheric pressure is included in the end of the tank. The dump tank unit can be moved back and forth on a metal beam bolted to the bench.

2-6) DIAPHRAGMS.

Sets of diaphragms were clamped in the tube at either end of the test section. At the driver section I.C.I. Melinex type "O" or "S" in varying thicknesses was used according to the shock strength required. Melinex tears rather than shatters. The finite opening time of the "petals" delays the formation of the shock. To keep this to a minimum, the diaphragm thicknesses were chosen so that they were always used at or near their spontaneous bursting point.

Water desorbing from the Melinex surface increased the time required to reach a working vacuum. To reduce this effect thin guard diaphragms of plastic coated, water resistant cellophane (British Sidac type MXXT) were used. MXXT diaphragms were also used at the dump tank end.

2-7) THE PUMPING SYSTEM.

The driver section and dump tank were evacuated with a N.G.N. type P.S.R. 12 oil pump. The P.S.R. 12 has two separate pumping chambers in parallel, a nominal capacity of 360 litres/min. and reaches a vacuum of about 10^{-2} torr. in about one minute. The downstream section was evacuated via a glass line with a Klemperer single stage mercury diffusion pump backed by a second, three stage pump and another P.S.R. 12 oil pump. In conjunction with the diffusion pump an ultimate vacuum of 5.10^{-5} torr. could be obtained in the tube within about one hour. The permanent gas leak rate to the test section is about 1·5 microns/minute.

2-8) THE VACUUM LINE.

A glass line joins the test section to the vacuum pumps, connection being made through a glass to metal seal. Two ball and socket joints absorb any movement when the shock is fired. The line is divided into two limbs: one for pressure measurement, the other for gas handling and storage.

Large 25 mm. bore taps are used between the shock tube and pumps to increase pumping speed. Between the test section and pumps, wide bore glass tubing with few bends and of short length also kept pumping time to a minimum. The test section is isolated from the glass line with a Saunders diaphragm valve. These valves are operated by a cam clamp action and were found to be suitable for vacuum purposes. Apiezon L grease was used on all vacuum taps. A diagram of the vacuum line is given in fig. 2-3.

2-9) PRESSURE MEASURING LINE.

For the range 0-760 torr. a glass spiral gauge was used for pressure measurements. The mirror on the gauge was quartz coated by Messrs. Optical Works Ltd. to prevent loss of reflectivity due to the corrosive action of the gases. From 1-35 torr. a silicon oil manometer (Hopkin and Williams silicon oil type MS550, density 1·09 $gm.ml^{-1}$) was used. This oil suffers from the disadvantage of "wetting" the sides of the manometer, however it is relatively inert to chemical reaction.

At lower pressures a Pirani gauge, 10^{-1} - 10^{-4} torr., and a McLeod gauge, 10^{-1} - 10^{-6} torr., were available. The Pirani gauge wire was manufactured from a 100 watt tungsten light bulb filament and is operated in a Wheatstone bridge configuration. The out of balance current, dependent on the gas pressure, is indicated on a 50 μa. meter. The stable bridge

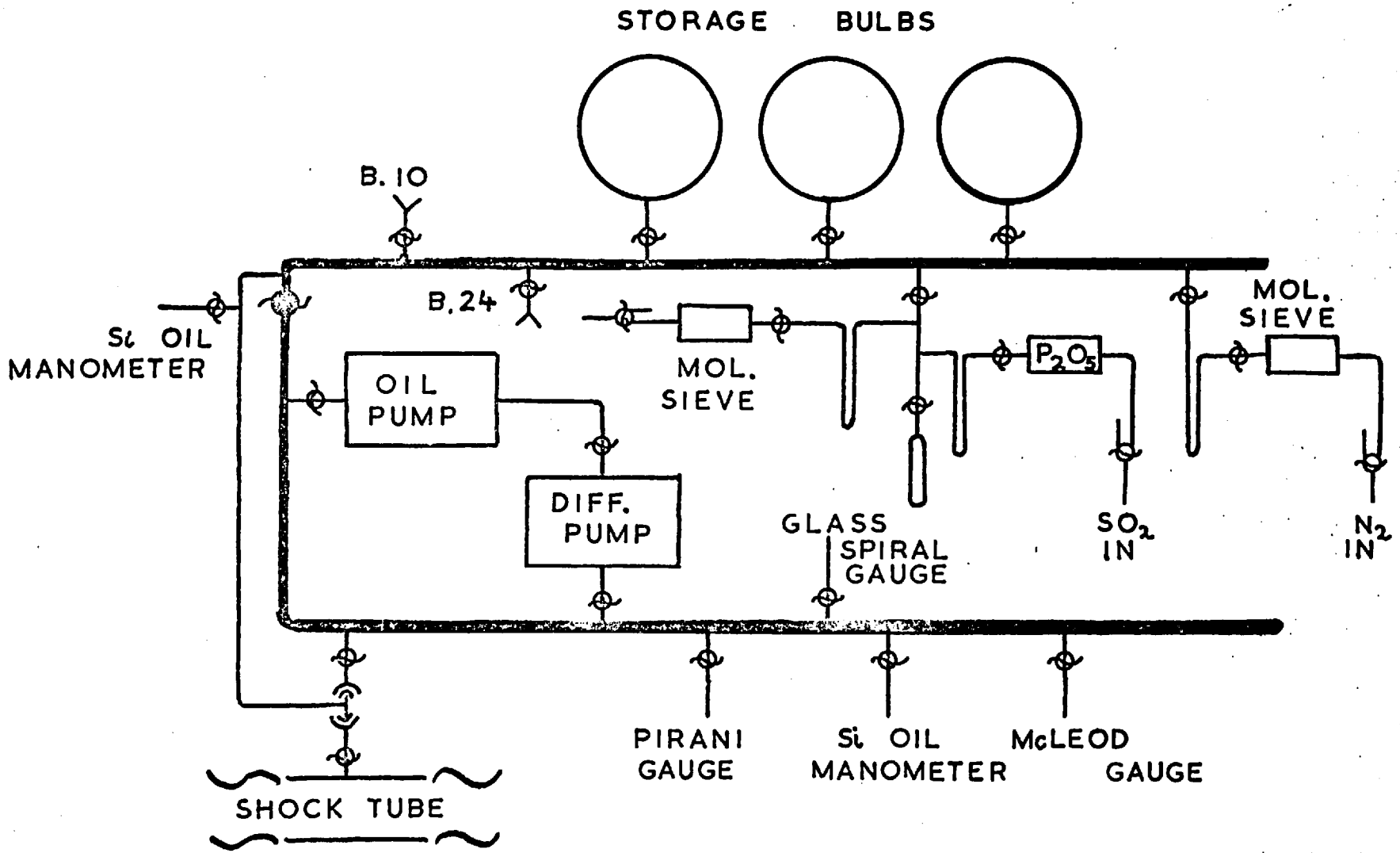

FIG. 2-3 THE VACUUM LINE

voltage is taken from the 300 volt.H.T. supply provided for the electronic circuits. The gauge was found to be more reliable than its commercial equivalent.

2-10) GAS HANDLING AND STORAGE LINE.

Gases were purified, stored and metered into the shock tube on the gas handling line. Facilities for drying the input gases over molecular sieves (Linde type 5A) or phosphorus pentoxide are provided. Test gas mixtures were made up in the reverse order of partial pressures except for the mixtures containing H_2O or D_2O. In these mixtures the remaining gases were premixed before admittance to the storage bulb which already contained the H_2O or D_2O.

Mixing was accomplished by the turbulent action obtained by passing the gases into the flasks with a high pressure gradient; in any case mixtures were usually left overnight before use. To prevent wastage of test gas, samples were admitted into the shock tube via a thin bypass line fitted with an additional oil manometer.

2-11) GAS PREPARATION.

All gases except HCl and DCl were obtained from cylinders or bulbs from commercial sources. The materials used, their sources, quoted purities and handling techniques are summarised in Table 2-1.

2-11-a) Preparation of HCl and DCl.

HCl and DCl were initially prepared to the method of De Vries and Klein (49) by the action of H_2O or D_2O on silicon tetrachloride. Silicon tetrachloride was distilled under vacuum and condensed in a cold trap at -196° c. H_2O or D_2O which had previously been degassed was condensed into

TABLE 2-1

Gas preparation.

GAS	SUPPLIER	PURITY	PREPARATION
N_2	B.O.C. cylinder	> 99·9%	Over molecular sieve, and thro' liquid N_2 trap.
O_2			
H_2			
Ar			
D_2	Matheson cylinder	99·5%	"
CH_4	"	99·95%	"
Kr	B.O.C. 1½ litre bulb	≃ 100%	Used direct
He			
CD_4	Merck ½ litre bulb	99%	"
H_2O	Fresh distilled	-	Degassed and distilled
D_2O	Norsk Hydro Co.	99·7%	"
SO_2	Hopkin and Williams syphon	Impurities 400 ppm.	Frozen, pumped on, melted, repeat and vacuum distilled.
NH_3	I.C.I cylinder	99·9%	Thro' KOH column into liquid N_2 trap. Pellet of Na to remove H_2O. 1st. fraction discarded.

Comment on Table 2-1

The purities have been taken from the manufacturers quoted specifications. Apart from the work described in section (2-12) p.38, no tests were employed to check these specifications.

The deuterium was made available by Professor G. Wilkinson F.R.S., Inorganic Chemistry Dept., Imperial College; the NH_3 by Dr. E.D. Brown of the Organic Chemistry Dept.

the frozen Si Cl_4 and the liquid N_2 replaced by a bath at -80°c. The evolving gas was condensed at -196°c and purified by successive distillation between traps at -196°c and-80°c. The frozen product was evacuated each time to less than 10^{-4} torr. The pure gas was stored in a one litre bulb.

A more convenient method of DCl preparation was used in the later stages of the work. D_2SO_4 (CIBA, 99% pure) was dropped onto NaCl under vacuum and the evolving DCl was trapped and purified as before.

2-12) GAS IMPURITIES.

Gas impurities have long been regarded as a source of error in relaxation measurements (2) and efforts were made to minimise this effect. As a check on the purity of the mixtures, especially with respect to any water present, a sample of test gas (SO_2- N_2) was taken from the shock tube and subjected to mass spectral analysis. The presence of a small amount of background emission in the M.S.9 spectrometer prevents the detection of small amounts of impurities; however a comparison of the scans of both background and sample set a maximum water content of 300 p.p.m.

This level is insufficient to effect measured relaxation times significantly at 2-3000°K. This point is more fully discussed in Chapter 4 where relaxation measurements of nitrogen in the presence of water vapour are described.

2-13) ELECTRONICS.

The light emitted by the shock heated gas was measured by a photomultiplier. Pulses from the luminous shock front obtained from photomultipliers at A and C were amplified and used to start and stop the gates of a Racal (SA 535) microsecond chronometer. From the distance AC, the shock velocity was thus

determined by the indicated transit time.

Quantitative emission measurements were made at B. The output from an E.M.I. 9558Q photomultiplier was displayed on a photographed single sweep of an oscilloscope.

The three photomultipliers and attendant electronics are supported in light-proof boxes on an optical bench mechanically independent of the shock tube. Light from the emission was collimated at each station by two pairs of razor blade slits; one pair on each of the windows, the other across the entrance to the photomultiplier boxes.

The distance between the timing slits AC is exactly 1 metre. The slits at B are $\frac{1}{2}$ metre from A and C. The slits for the timing photomultipliers were ·5 mm. in width. For the quantitative measurements at B, a slit of ·1 x 1·25 cms. was used on the shock tube window; one of dimensions ·29 x 1·2 or ·29 x 2·4 cms. across the photomultiplier. The electronics are shown schematically in fig. (2-4).

2-14) TIMING PHOTOMULTIPLIERS.

Light at stations A and C fell onto R.C.A. 931A photo tubes to be amplified as electrical pulses prior to admittance to the chronometer start/stop gates. The electronic circuit is shown in fig. (2-5). The H.T. bias for the dynode chain was taken from a Power Designs Inc. power pack (0-2012V. 15 m.a.). The +300 volt stabilized supply was built by the Department's Instrument Section.

The light emission produced a low impedance signal across the anode load resistor. This was amplified by a X25 pentode stage and was fed into a cathode follower. Coaxial cable took the approximately ·5 volt low

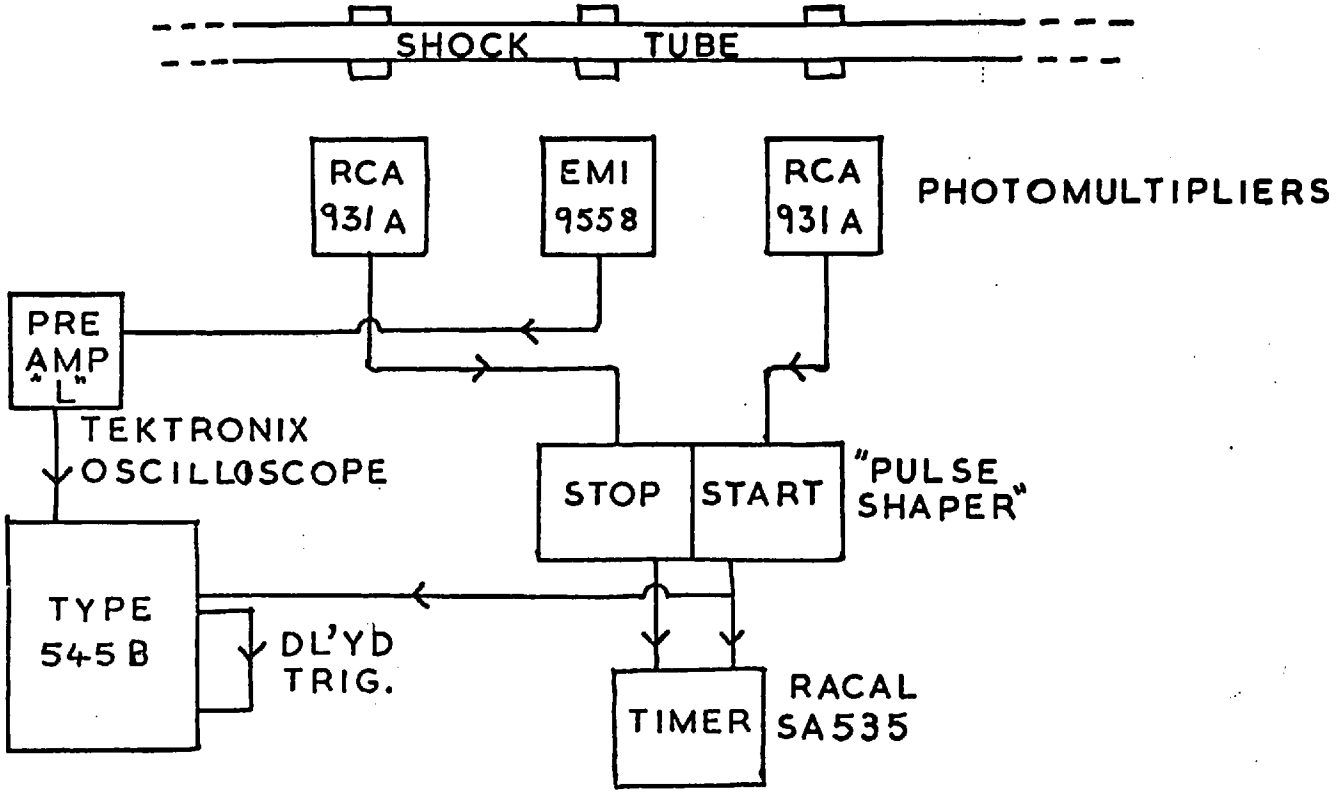

FIG. 2-4 THE SHOCK TUBE ELECTRONICS

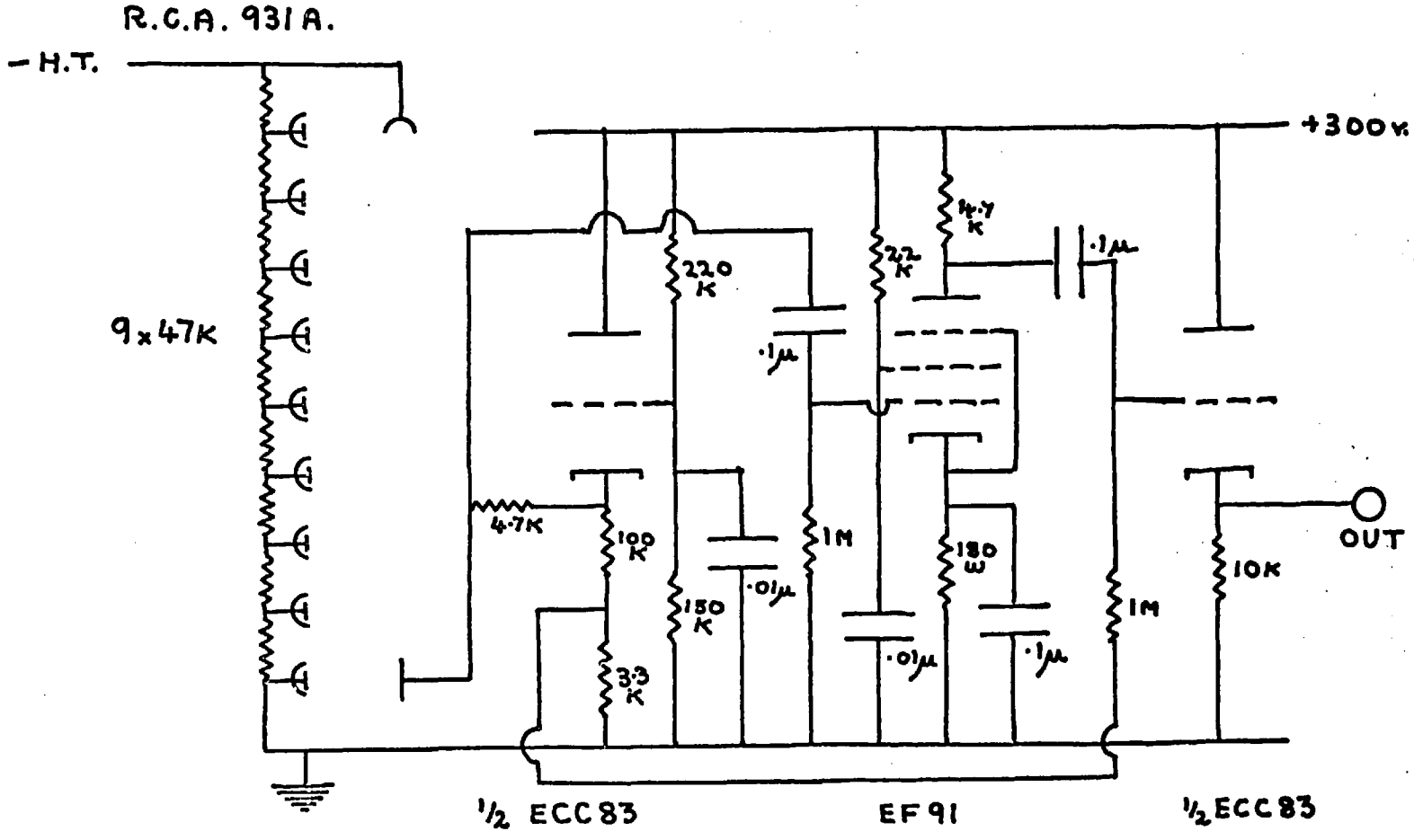

FIG. 2-5 TIMING PHOTOMULTIPLIER CIRCUIT

impedance signals to a pulse shaping/amplifying network. This network was necessary as the emission pulses (either positive or negative in sign) were not of sufficient amplitude to trigger the gates of the chronometer.

2-15) PULSE SHAPER NETWORK. (see fig. 2-6).

The outputs from the start/stop photomultipliers at A and C were fed into identical channels in the pulse shaper. Pulses were amplified by another EF 91 pentode stage, X25 gain. Equal positive and negative pulses were obtained from a phase splitting triode with equal anode and cathode loads. The outputs from these were applied to the grids of a double triode cathode follower with common cathode load, thus producing a positive pulse irrespective of the original polarity.

The signal required to operate the chronometer gate is a pulse of between 8 and 15 volts with a maximum risetime of ·2 μsec. A trigger from the start channel was provided to operate the single sweep on the oscilloscope.

2-16) SIGNAL EQUALISATION.

Owing to the slight variation between slit dimensions, valves and resistors on each channel, equal light intensity did not give equal pulses at the chronometer gates. To eliminate this effect so that the gates trigger at the same point of the emission rise each time, the stage gains were equalised for both channels.

In practice, it was assumed that, to a first approximation, the slit dimensions at A and C were the same. The slits on each channel were illuminated in turn with chopped light of a fixed intensity and the electrical output from the photomultipliers was monitored on the oscilloscope. A

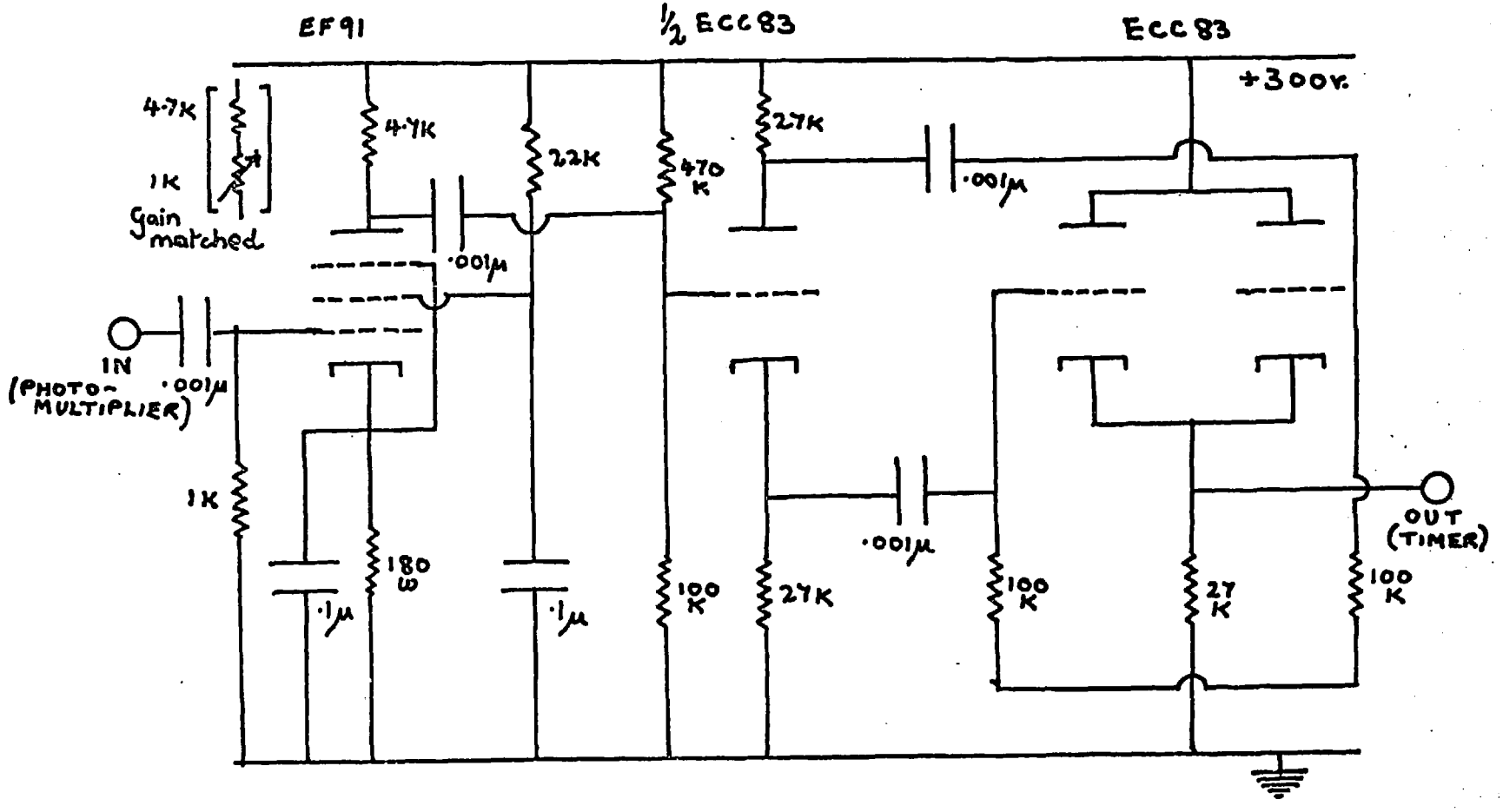

FIG. 2-6 PULSE SHAPING NETWORK
START [STOP] CHANNEL

potentiometer in series with the dynode H.T. supply in one channel was then adjusted until the displayed pulses from each channel were equal.

The pulse shaper network was balanced by altering the gain of the pentode in one channel by inclusion of a potentiometer in series with the EF91 anode. The output obtained by feeding the oscilloscope square wave calibrator into the network was monitored and the potentiometer adjusted until both channels were equalised.

2-17) E.M.I. 9558Q PHOTOMULTIPLIER.

Quantitative measurements were made with an E.M.I. 9558Q photomultiplier. This phototube is fitted with a quartz window and with a tri-alkali cathode. It has a spectral response from 2000 - 8000 Å with a peak at about 4000 Å. The tube, although noisier than the identical tube used by Sheen, has a greater dynode gain. The circuit is shown in fig. (2-7).

The first dynode - cathode voltage was stabilised by two 85A2 neons. The tube was electrostatically screened by metal foil connected via 4 x 5 megohm resistors to the cathode. The anode last dynode voltage was stabilised by a triode cathode follower. The signal from the 4·7K anode load was fed directly to a White cathode follower. This has an output impedance of about 20 ohms, low enough to avoid attenuation of fast pulses by the capacitance to earth introduced by the coaxial cable.

The signal taken from the anode was kept to less than a volt and hence the current drawn was a small fraction of the current down the dynode chain, ensuring linear operation.

2-18) OSCILLOSCOPE.

The 535A Tektronix oscilloscope with type L preamplifier possessed a

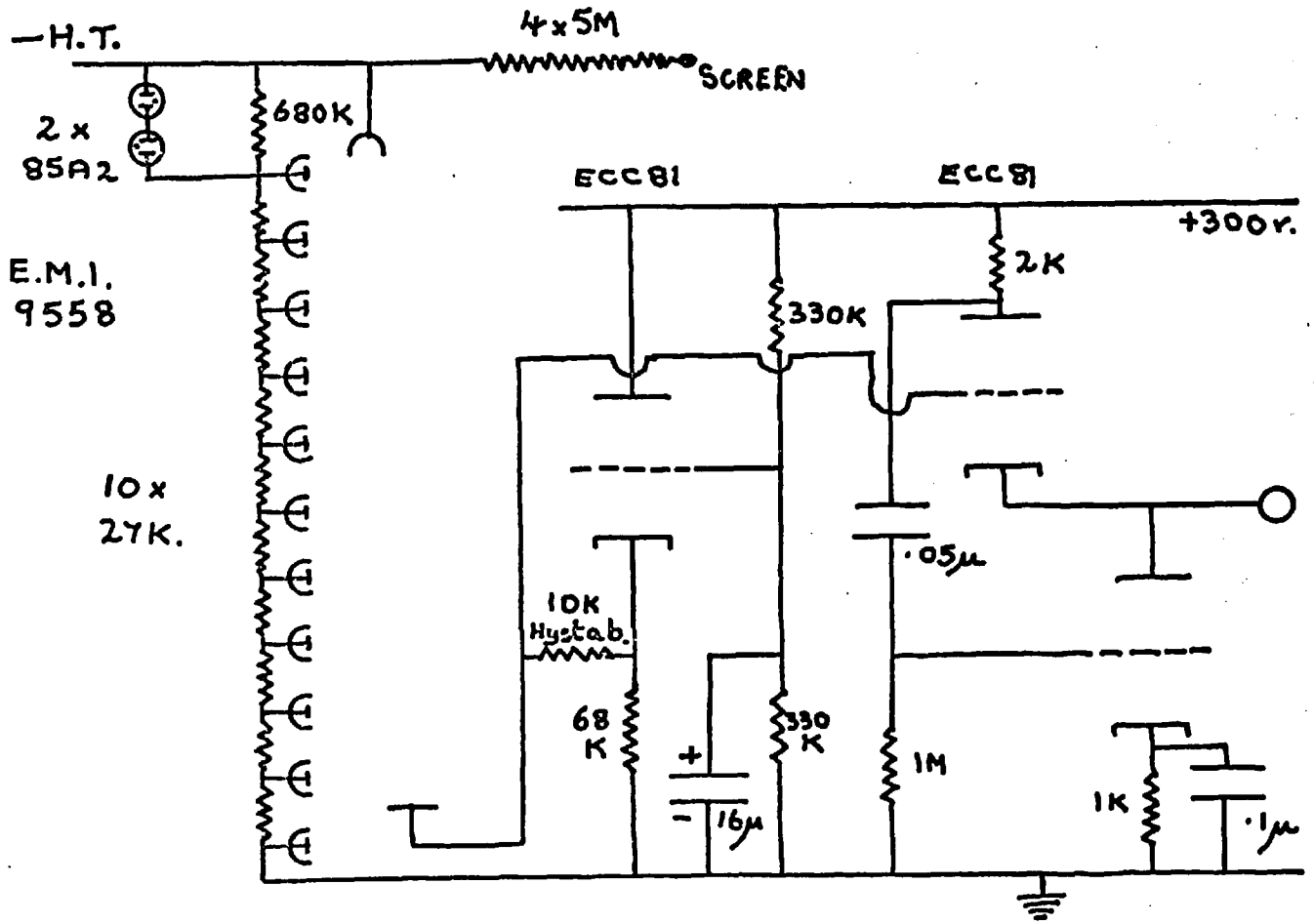

FIG. 2-7 E.M.I. PHOTOMULTIPLIER CIRCUIT

built in delay system suitable for delaying the trace sweep after the input of the trigger signal. This was used in conjunction with a trigger signal from station A to obtain the shock front at a convenient position after the start of a single sweep of the trace. Normally delay times in the order of 100-500 μsec. were used, depending on the estimated shock velocity.

The trace was photographed using a Telford type A oscilloscope camera and Kodak Ortho-Royal sheet film, 5" x 4", speed A.S.A. 400. The film was developed in high contrast Xray developer.

The overall risetime of the photomultiplier-oscilloscope combination was found to be fast compared to the time taken for the shock front to pass the photomultiplier slits and was under 0·5 μsec.

CHAPTER 3.

THE EMISSION TRACER TECHNIQUE.

3-1) INTRODUCTION.

When dilute mixtures of SO_2 in argon are heated by a shock wave, three electronically excited states are populated ($^3B_1$, $^1B_2$ and (?) $^1B_1$). They are depopulated by dissociation, quenching and by radiative transitions. The intensity of the emission at 4360 Å was found to be proportional to the concentration of SO_2 but independent of that of the diluent.

Above 3000^{oK} the dissociation was fast compared to the duration of the experiment. The decay has been used to examine the SO_2 dissociation kinetics (50). Below 2800^{oK} the dissociation was slow and the emission rose at the shock front to a steady level - indicating a constant temperature zone where any chemical relaxation was very slow.

Levitt and Sheen showed that the variation of intensity per unit wavelength interval with temperature is given by:

$$I = I_o[SO_2] \frac{\rho_2}{\rho_1} \cdot \exp\left[\frac{-E_a}{RT}\right] \qquad (3\text{-}1)$$

Here I_o is a constant for the apparatus, independent of pressure, mole fraction of SO_2 and temperature. E_a is the apparent activation energy of the emission. It is an average value which depends on the excitation kinetics for each wavelength, the spectral response of the monochromator - photomultiplier combination and the temperature.

Eqn. (3-1) shows that an "Arrhenius" plot of ln I against reciprocal temperature should be linear, whose slope is defined by $\frac{E_a}{R}$.

In computing the temperature of the shocked gas, the SO_2 was assumed to be fully relaxed in the shock front. This assumption has been discussed

fully elsewhere (47, 48); relaxation measurements of P τ (SO_2 - SO_2) at 293, 375 and 473^{oK} (51, 52) extrapolate to a relaxation time of about 10^{-8}atm.sec. at these higher temperatures. Millikan and White's semi empirical formula, using the lowest vibrational frequency of SO_2, 518 cms^{-1}, gives 4.10^{-8}atm.sec. These times are short compared to the experimental time scale of the work to be described.

When argon is replaced by nitrogen as the diluent and the gas is shocked to about 2500^{oK}, the traces show a rapid rise at the shock front followed by an exponential decay to a steady level. The traces resemble the higher temperature dissociation of SO_2 in argon.

It has been shown that this decay is not due to the dissociation of SO_2 but to the vibrational relaxation of the nitrogen; the emission follows the translational temperature of the nitrogen and not its vibrational energy. This contrasts with the sodium line reversal technique which monitors the latter parameter.

3-2) ANALYSIS OF EMISSION RECORDS.

When nitrogen is shock heated, the translational temperature of the hot gas, T, rises to a peak value T^1 immediately behind the front and then falls to an equilibrium value T^{11} where relaxation is complete. The dependence of the emission at the front, I^1, and at equilibrium, I^{11}, may be obtained by inserting $T = T^1$, T^{11} and $\rho = \rho^1$, ρ^{11} respectively into equation (3-1). The rate of emission decay may be used to obtain vibrational relaxation times.

The intensity I at any point in the relaxation is obtained in terms of I^1 by writing (3-1) in the form:

$$I = I^1 \left(\frac{\rho_2}{\rho_2^1} \right) \cdot \exp \left[- \frac{E_a}{R} \left(\frac{1}{T} - \frac{1}{T^1} \right) \right] \qquad (3\text{-}2)$$

A degree of relaxation, α , is defined such that the effective enthalpy H exhibited by the partly relaxed gas is given by

$$H = \alpha H_r + (1 - \alpha) H_u$$

where H_r, H_u refer to the enthalpy of the relaxed and unrelaxed gas respectively. The instantaneous vibrational energy of the nitrogen E_v is given by:

$$E_v = H - H_u = \alpha (H_r - H_u) \qquad (3\text{-}3)$$

The equilibrium vibrational energy at the translational temperature T is simply

$$E_T = H_r - H_u$$

so that

$$E_T - E_v = (1 - \alpha) (H_r - H_u) \qquad (3\text{-}4)$$

From eqn (1-2), the Landau-Teller equation for vibrational relaxation:

$$- \frac{d E_v}{dt_g} = \frac{E_T - E_v}{\tau} \qquad (3\text{-}5)$$

t_g is gas particle time, τ the relaxation time for the diatom. The instantaneous value of τ at any point of the relaxation α is denoted as τ_α.

By substituting (3-4) into (3-5) and differentiating (3-3):

$$\frac{d E_v}{dt_g} = \frac{(1 - \alpha) (H_r - H_u)}{\tau_\alpha}$$

$$= (H_r - H_u) \frac{d\alpha}{dt_g} + \alpha \frac{d(H_r - H_u)}{dt_g}$$

Since $(H_r - H_u)$ is a single valued function of T and T a function of α :

$$\frac{I-\alpha}{\tau_\alpha} = \frac{d\alpha}{dt_g}\left(1 + \frac{\alpha}{H_r - H_u} \times \frac{d(H_r - H_u)}{d\alpha}\right)$$

$$= \frac{d\alpha}{dt_g}\left(1 + \frac{\alpha T}{H_r - H_u} \times \frac{d(H_r - H_u)}{dT} \cdot \frac{d\ln T}{d\alpha}\right) \quad (3\text{-}6)$$

Consider the last term on the R.H.S. of (3-6). Now:

$$\frac{d\ln(H_r - H_u)}{dt_g} = \frac{T}{(H_r - H_u)} \cdot \frac{d(H_r - H_u)}{dT} \cdot \frac{d\ln T}{dt_g}$$

Since $H_u = \frac{7}{2}RT$, $\frac{dH_r}{dt} = C_p$ where C_p is the specific heat of the relaxed gas at T^{0K}.

$$\frac{d\ln(H_r - H_u)}{dt_g} = \frac{T}{H_r - 3{\cdot}5RT}(C_p - 3{\cdot}R) \cdot \frac{d\ln T}{dt_g}$$

$$= \frac{(C_p - 3{\cdot}5R)}{((H_r/T) - 3{\cdot}5R)} \cdot \frac{d\ln T}{dt_g} \quad (3\text{-}7)$$

Substituting (3-7) into (3-6):

$$\frac{1-\alpha}{\tau_\alpha} = \frac{d\alpha}{dt_g}\left(1 + \frac{\alpha(C_p - 3{\cdot}5R)}{[(H_r/T) - 3{\cdot}5R]} \cdot \frac{d\ln T}{d\alpha}\right) \quad (3\text{-}8)$$

Finally by differentiating (3-2) and substituting into (3-8):

$$\tau_\alpha = \frac{(1-\alpha)\left(\frac{E_a}{RT} \cdot \frac{d\ln T}{d\alpha} - \frac{d\ln\rho}{d\alpha}\right)}{\left(1 + \alpha \cdot \frac{d\ln T}{d\alpha} \frac{(C_p - 3{\cdot}5R)}{((H_r/T) - 3{\cdot}5R)}\right) \cdot \frac{d\ln I}{dt_g}} \quad (3\text{-}9)$$

For ideal inviscid flow behind the shock front, the relationship between the laboratory and gas particle time scales is given by

$$\frac{d\ln I}{dt_1} = \left(\frac{\rho_2}{\rho_1}\right) \frac{d\ln I}{dt_g} \quad (3\text{-}10)$$

From this and equation (3-9), measured values of $\frac{d\ln I}{dt_1}$ (the rate of

emission decay behind the shock front) can be converted to values of τ_α .

3-3) VARIATION OF SO_2 EMISSION WITH TEMPERATURE.

To improve the signal to noise ratio in these experiments, unfiltered radiation from all three excited states of SO_2 was observed. Fig. (3-1) shows oscilloscope traces of SO_2/Ar mixtures shock-heated to various temperatures. At 3355^{oK} dissociation is fast; at 2935^{oK} the induction period for the dissociation may be observed for $\simeq$ 10 μsec.; at 2407^{oK} the dissociation is much slower than the time scale of the photographed oscilloscope trace.

An Arrhenius plot of the logarithm of the unfiltered light intensity behind the front against reciprocal temperature is shown in fig. (3-2). It is linear and the activation energy, E_a, was found to be 88.5 Kcals. mole^{-1}. Fig. (3-2) demonstrates that eqn. (3-1) adequately represents the total response to the unfiltered radiation for the experimental conditions investigated.

3-4) SHOCK IMPERFECTIONS.

Occasionally emission traces showed a slow rising portion which was ascribed to shock attenuation. (Fig. 3-3(a)). From the rate of change of light intensity, the increase in temperature and hence the velocity attenuation may be calculated. This value may be compared to the value calculated from the expected, and observed, delay times for the shock to traverse from timing station A to station B. Both values indicated that attenuation was less than 1%/metre.

At high shocked gas pressures (> latm) the traces often showed irregularities similar to the trace illustrated in fig. (3-3(b)). This was

FIG. 3-1

DISSOCIATION OF SO_2 IN Ar.

(a) C.48 10% SO_2/Ar $T' = 3355^{\circ}K$

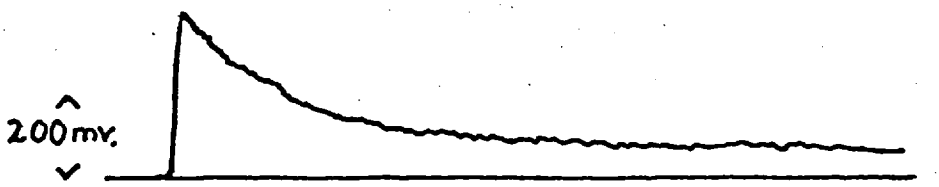

(b) C.54 10% SO_2/Ar $T' = 2935^{\circ}K$

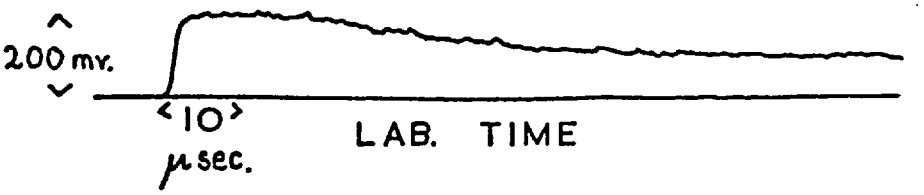

(c) C.212 2% SO_2/Ar $T' = 2407^{\circ}K$

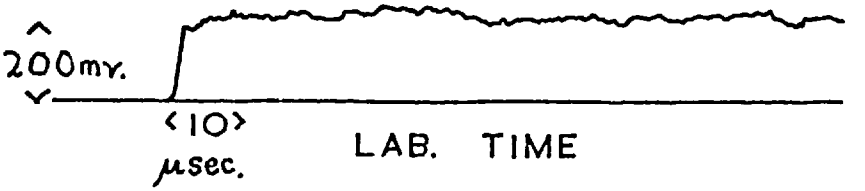

FIG. 3-2

DEPENDENCE OF PEAK LIGHT INTENSITY ON TEMPERATURE — SO_2/Ar.

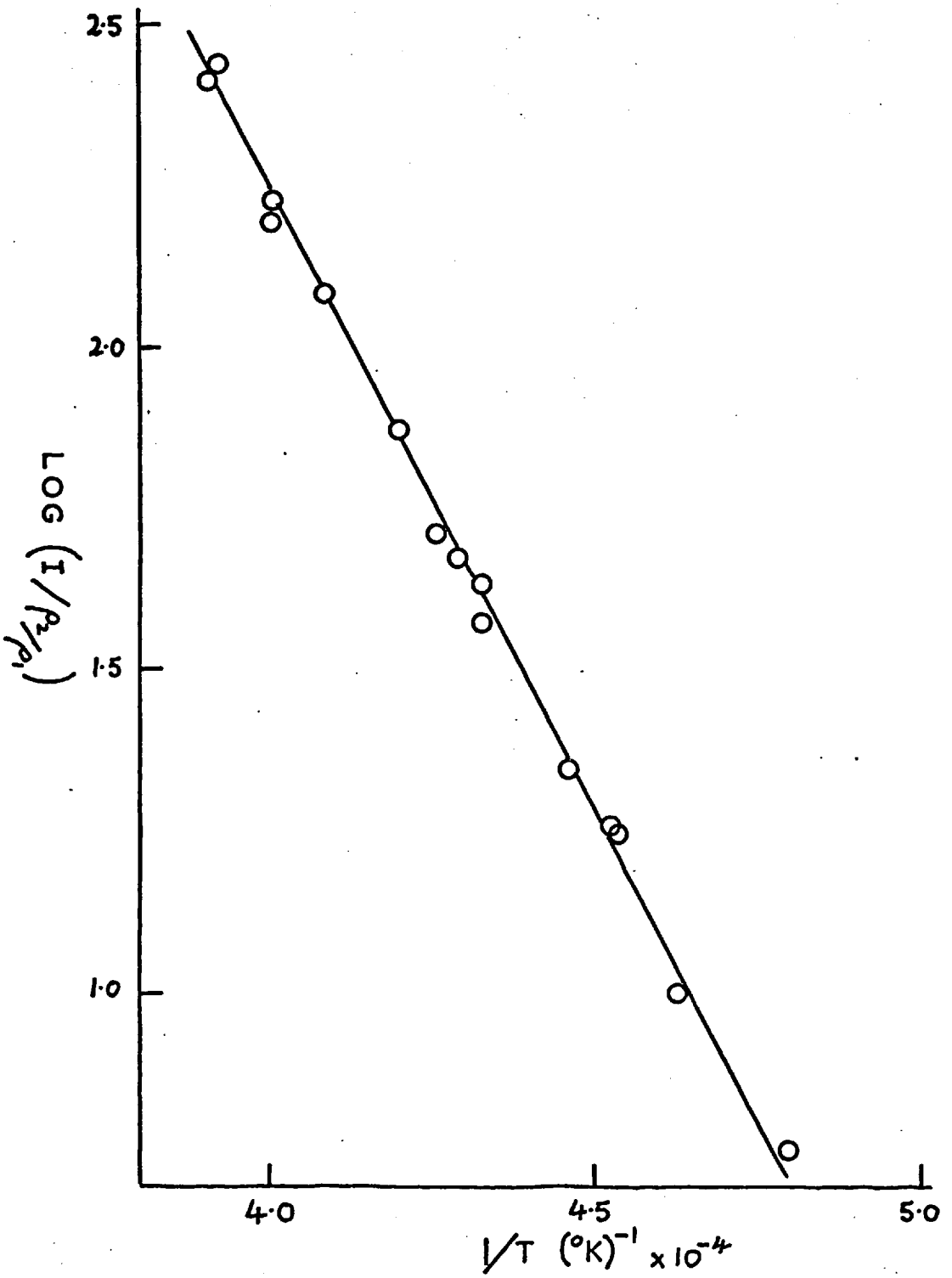

FIG. 3-3

SHOCK DEFECTS

(a) C.215 2% SO_2/Ar P_1 = 15 torr T' = 2468°K

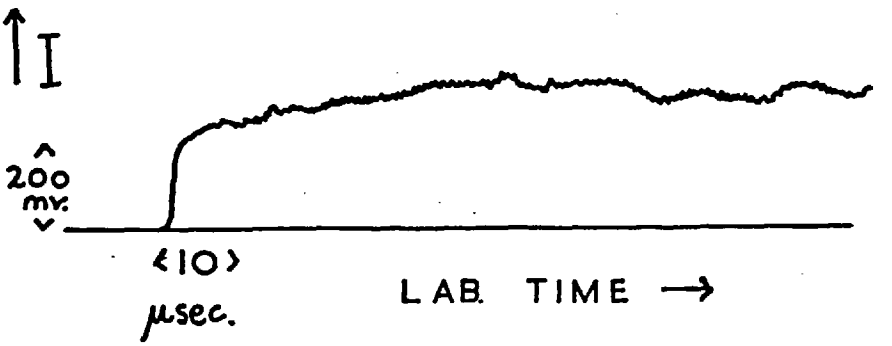

(b) C.75 2% SO_2/Ar P_1 = 21 torr T_1 = 2311°K

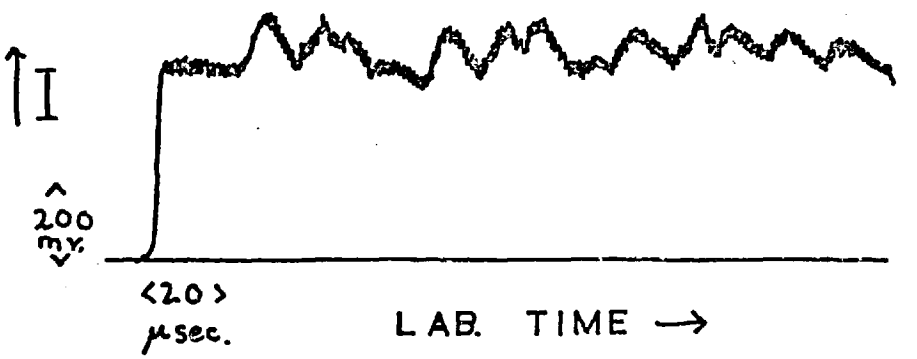

due to sonic irregularities in the gas in the square section shock tube. Normally a pressure region was selected for study where these effects were small.

3-5) LIGHT EMISSION IN SO_2/N_2.

For the N_2 - SO_2 runs, values of the logarithm of the peak light intensity, I^1, plotted against reciprocal temperature, $1/T^1$, always fell within experimental scatter - on the line representing the argon results. The experimental equilibrium intensities, I^{11}, plotted against $1/T^{11}$, either fell on the argon line or were slightly too high. In these instances a true equilibrium intensity was not observed but the traces showed a slow rise which was attributed to attenuation. (Fig. 3-5(a)).

Extrapolation of this slow rising intensity back to the shock front gave values of I^{11} in reasonable agreement with the argon results although the extrapolation was not always very accurate. An example of the corrected traces is given in the form of a log I^{11} vs. $1/T^{11}$ graph in fig. (3-4).

To eliminate changes in intensity due to attenuation from effecting the relaxation calculations, the intensity profile was corrected on the assumption that changes in log I due to flow effects increased linearly with laboratory time behind the front. The procedure is illustrated in fig. (3-5(b)). For each run the final intensity level expected from eqn. (3-2), I^{11}, was calculated using the experimental value of I^1. By comparison to the observed final intensity, the rate of change of intensity due to attenuation $\left(\frac{d\ln I}{dt}\right)_{Attn.}$ could be calculated. The true rate of decay of light intensity due to relaxation is then given by:

$$\left(\frac{d\ln I}{dt}\right)_{Obs.} = \left(\frac{d\ln I}{dt}\right)_{Relaxation} + \left(\frac{d\ln I}{dt}\right)_{Attn.} \qquad (3\text{-}11)$$

FIG. 3-4

INTENSITY / TEMPERATURE PLOT

SO_2/N_2.

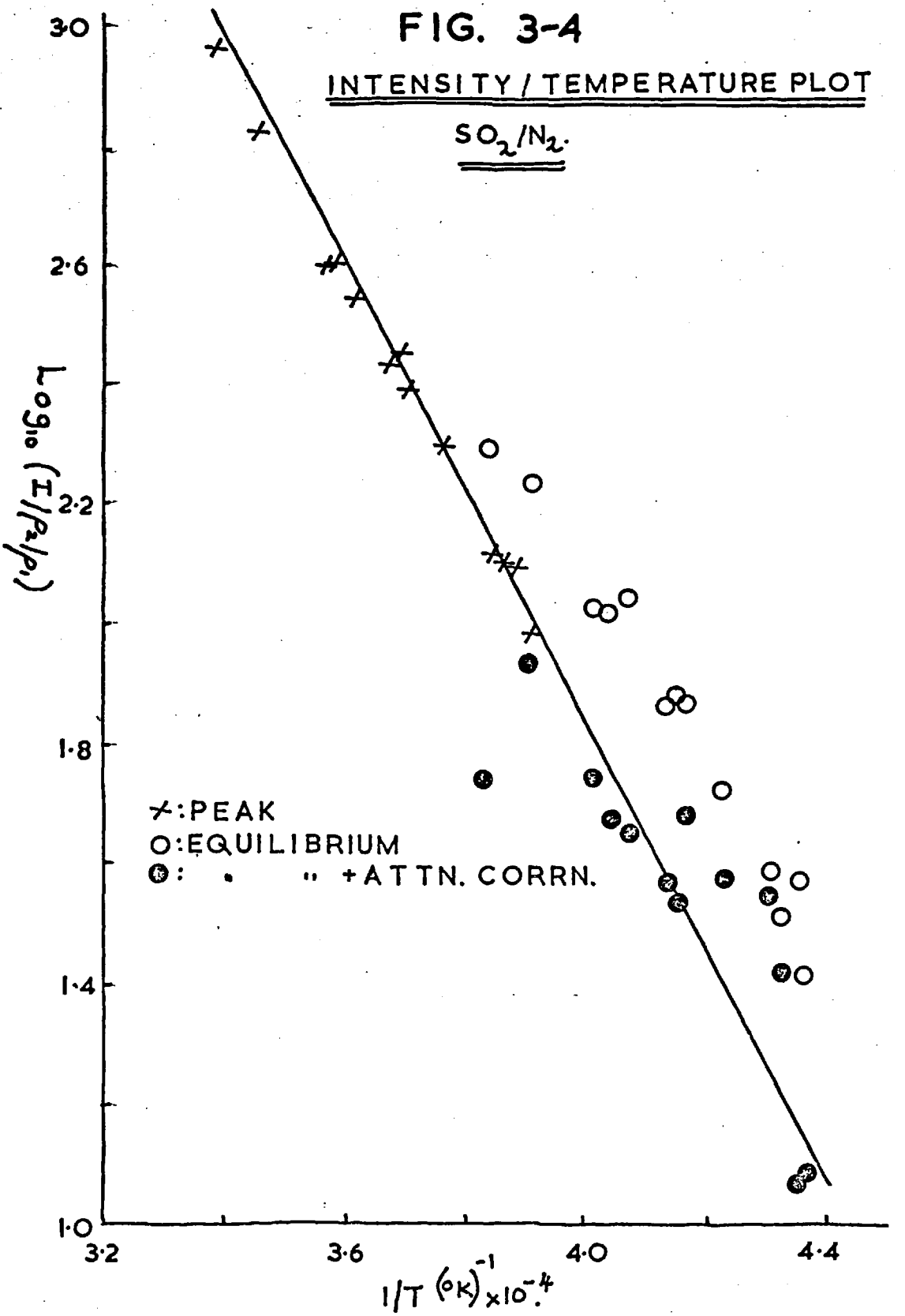

FIG. 3-5

ATTENUATION CORRECTION.

(a) C110. 1%SO_2/N_2. P_1=5 TORR T'= 2894°K

(b) INTERPRETATION OF ATTENUATION.

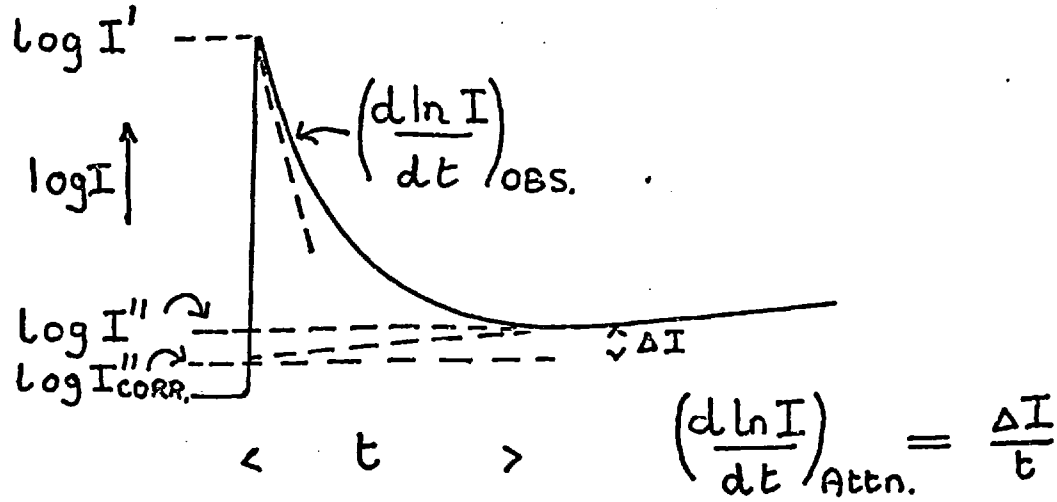

where $\left(\frac{d\ln I}{dt}\right)_{Obs.}$ refers to the measured rate of emission decay as indicated in fig. (3-5).

This procedure has two defects. The assumption that the intensity change due to attenuation is linear, may be false; the choice of the value of t (the time required for the gas to reach its observed equilibrium intensity) is rather arbitrary. Immediately behind the shock front, the attenuation term used in eqn. (3-11) was always small compared to the observed decay due to relaxation and hence these defects will be negligible. As the relaxation proceeds however, the rate of emission decay falls and the attenuation term may contribute a significant error to the calculated relaxation time.

Traces may be analysed in two distinct ways. The emission decay immediately behind the shock front ($\alpha = 0$) can be converted into a value of $P\tau_0$. The temperature dependence of the relaxation and the efficiency of SO_2 as a collision partner may be determined from the $P\tau_0$'s of several runs. Alternatively a single trace may be analysed as $\alpha \rightarrow 1{\cdot}0$ and the variation of $P\tau_\alpha$ with α obtained. As mentioned in the introduction, previous results by Levitt and Sheen showed an apparent decrease in $P\tau_\alpha$ as $\alpha \rightarrow 1{\cdot}0$. This was in contrast to the expected increase. The remainder of this chapter describes further measurements on the variation of $P\tau_\alpha$; chapter 4 describes the results obtained by analysing many traces for values of $P\tau_0$. In chapter 4 it will be shown that the SO_2 tracer has little or no effect on the N_2 relaxation.

3-6 VARIATION OF $P\tau_\alpha$ WITH α.

Traces were analysed as follows:

(i) Equation (3-2) was used to calculate the value of I at $\alpha = 0$, $\cdot1, \ldots$ 1·0 using the experimentally determined intensity at the front I^1, and the temperatures and density ratios obtained from the computer program solution of the hydrodynamic equations.

(ii) A graph of log I against t_1, suitably corrected for attenuation, was plotted. The values of t_1 at which the intensity reached values predicted at $\alpha = \cdot1, 2, \ldots$ 1·0 were noted.

(iii) The gas particle times equivalent to these laboratory times were calculated using an equivalent form of equation (3-10) in integrated form.

$$t_g = t_1 \cdot \int_0^1 \frac{\rho_2}{\rho_1} \cdot d\alpha.$$

The integral was evaluated graphically by the "method of areas" from the computed values of $\frac{\rho_2}{\rho_1}$

(iv) Log I ($\alpha = 0 \ldots 1\cdot0$) was plotted against the calculated gas particle times and $\frac{d\ln I}{dt_g}$ at $\alpha = 0, \cdot1 \ldots 1\cdot0$ evaluated from the slope of the graph.

(v) Substitution into equation (3-9) therefore gave the values of τ_α, hence $P\tau_\alpha$, equivalent to each value of the degree of relaxation α.

3-7) A TYPICAL ANALYSIS.

The differentials $\frac{d\ln T}{d\alpha}$, $\frac{d\ln \rho}{d\alpha}$

for eqn. (3-9) were obtained directly by solving the hydrodynamic equations for the shocked gas at α, $\alpha + \cdot001$ on the computer. Thermodynamic data for the various gases was taken from reference (53). The results of a computation for a shock through 1% SO_2/N_2 at 2·217 mm. μsec.$^{-1}$ are given in

table (3-1).

Table 3-1.

α	T^{oK}	ρ_2/ρ_1	$-\left(\frac{E_a}{RT} \times \frac{d\ln T}{d\alpha} - \frac{d\ln\rho}{d\alpha}\right) = A$	
0	2591	5·39	(17·2 x ·131) - ·169 = 2·08	
1	2314	6·21	(19·2 x ·098) - ·121 = 1·76	
α	$1 + \alpha \frac{d\ln T}{d\alpha}\left(\frac{C_p - 3{\cdot}5R}{(H_r/T)-3{\cdot}5R}\right) = B$			A/B
0	1 + (0 x - ·131 x 1·80) = 1·00			2·08
1	1 + (1 x - ·102 x 1·91) = ·81			2·19

It may be seen from the table that the product A/B involved in the calculation of τ_α viz:

$$\tau_\alpha = (1-\alpha)\ \frac{A}{B}\ \frac{1}{d\ln I/dt_g}$$

varied by 5% in going from $\alpha = 0$ to $\alpha = 1{\cdot}0$. The previous results (47) ignored the variation of the denominator B with α. It was taken as exactly 1·0 and this involved an error of about 10% in the quoted values of $P\tau_\alpha$ at $\alpha = 1{\cdot}0$. The variation of B with α has been taken into account in the results presented here.

Examples of the analyses of traces containing varying amounts of SO_2 and at differing temperatures are shown in fig. (3-6). It may be seen that at longer times behind the shock front $P\tau_\alpha$ decreases in value. In general the value of $P\tau_\alpha$ at $\alpha = 1{\cdot}0$ is almost one half the frontal value $P\tau_0$.

This result contradicts the expected Landau-Teller behaviour. The fall in translational temperature behind the shock front was about 250^{oK} for most of the shock mixtures examined. Chosing Millikan and White's shock to shock temperature dependence of $P\tau$ (eqn. 1-3), this fall in temperature should

FIG. 3-6

VARIATION OF $P\tau$ WITH α.

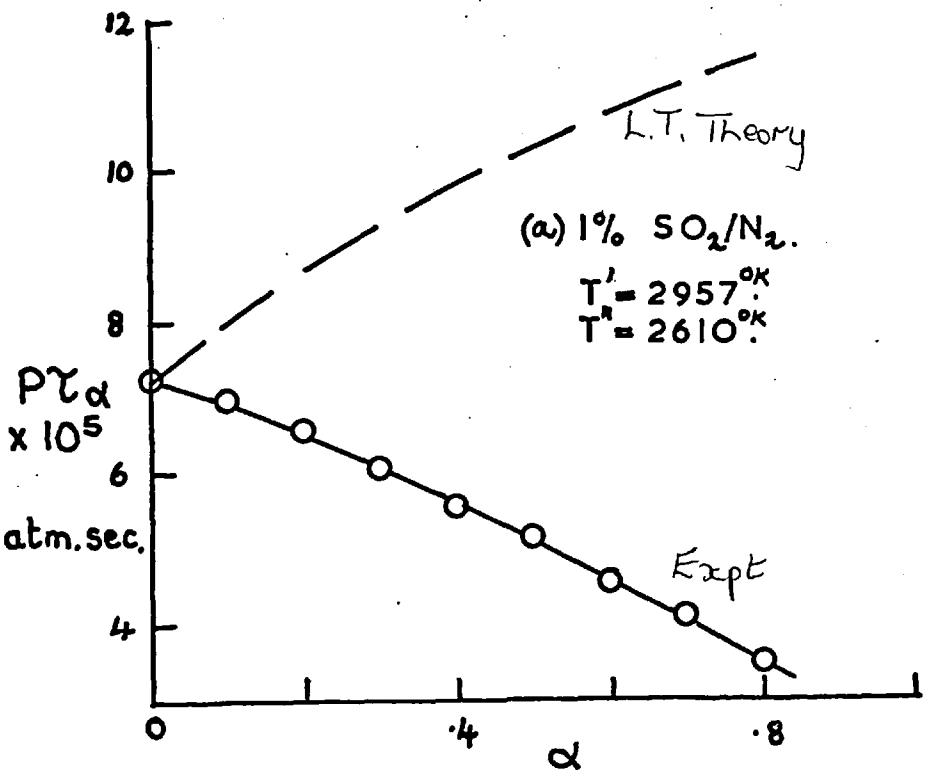

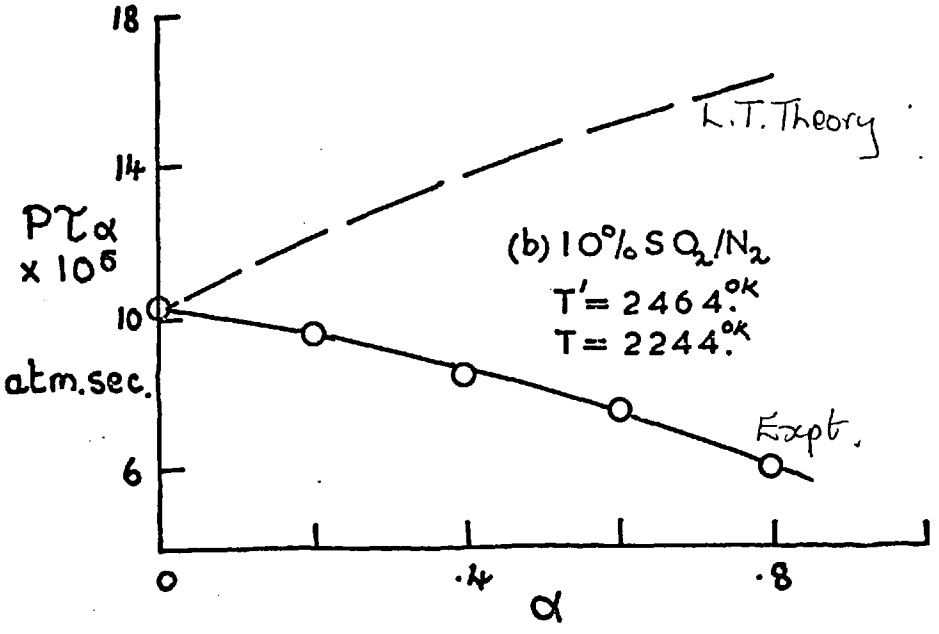

double the observed relaxation time.

3-8) COMPARISON TO OTHER RESULTS.

Vibrational relaxation measurements on nitrogen in a nozzle expansion have been obtained using the sodium line reversal technique (SLR) (54). Relaxation times were also abnormally fast compared to the rates predicted for the local translational temperature. The N_2 produced in such nozzle experiments is vibrationally "hot", translationally "cold". The possibility that these two effects are complimentary must be considered. The rates obtained in these SLR measurements were however about 15 times faster than theory, compared to the doubling in rate observed here.

Holbeche and Wocdley (55) extended the measurements to oxygen and carbon monoxide. The former gas gave relaxation rates slower than predicted, the latter gas conformed to Landau-Teller behaviour.

Bray (56) has given an explanation for these nozzle experiments in terms of anharmonicity. The vibrational levels of an anharmonic oscillator converge as the vibrational "ladder" is climbed; the (T-V) energy transfer rates therefore increase due to the decrease in the size of the vibrational quanta. Combining this with the rapid near resonant (V-V) energy transfer processes between adjacent vibrational levels, Bray showed that abnormally fast relaxation rates will be observed in nozzle expansions. Unfortunately the theory is complex and requires a differential equation for each vibrational level. The solution of the fifty or so equations required for nitrogen is impossible without precise data on all the parameters involved. The theory, however, does not explain the slower relaxation rate observed in oxygen.

Despite Russo's (57) conclusion that impurities do not appreciably effect these nozzle relaxation rates, recent evidence (58) has suggested that minute traces of impurities e.g. H atoms significantly reduce these relaxation times.

Until recently other workers had observed similar fast relaxation rates in various gases behind incident shock waves. Both Blackman's (59) work on nitrogen relaxation and Johannesen et al.'s (60, 61) work on carbon dioxide shows a fall in $P\tau_\alpha$ as $\alpha \rightarrow 1{\cdot}0$ although not to the same extent as ours. Both these groups of workers used interferometric methods of measurement and assumed an exponential change in the density gradient with a time constant equal to the vibrational relaxation time.

Simpson et al. (62) have shown this assumption to be incorrect. By analysing the density change using a curve fitting procedure they have obtained results consistent with Landau-Teller theory. Simpson (63) has recently confirmed this result for CO_2 using a laser schlieren technique.

Bristow (64) has also attempted to explain the effect behind incident shocks in nitrogen and carbon dioxide in terms of anharmonicity. By taking Nikitin's model of an anharmonic oscillator and by selecting suitable factors, the decrease in relaxation times can to some extent be accounted for. There seems to be no evidence however that in our case anharmonic effects are as large as suggested. Bray's more detailed theory suggests the anharmonic effect to be very small behind incident shocks at our temperatures.

It is now clear that gases show the same temperature dependence during a single relaxation behind a shock wave as they do on a "shock for shock" basis. Simpson's work on CO_2 has already been mentioned. Kiefer and Lutz (65)

have measured relaxation times in oxygen using the laser schlieren technique. Their results indicate that no large decrease in relaxation times take place.

Probably the most striking demonstration has been the measurement by Appleton (66) on the relaxation of nitrogen using U/V absorption spectroscopy. By monitoring the population of the $\simeq$ 10th. vibrational level, Appleton showed that below 5,500^{oK} nitrogen relaxed, up to at least this 10th level, via near Boltzmann distributions governed by a single time dependent vibrational temperature.

Above 5,500^{oK} the results indicate that the instantaneous vibrational relaxation time was dependent on the degree of relaxation. Bray (56) considers this last phenomenon to be an anharmonic effect. It has been pointed out, however, that it could also be due to the onset of ionisation: the prescence of even small numbers of electrons would enhance the relaxation rate (67).

These results obtained by other workers do not explain the curvature of the $P\tau_{\alpha}/\alpha$ plots that have been obtained using the emission tracer technique except to indicate that the effect is probably a function of the method of measurement. The decrease in relaxation times as $\alpha \rightarrow 1{\cdot}0$ was found to be neither a function of SO_2 concentration nor temperature. The range of pressure over which the shocked gas could be examined at a particular temperature was too small to enable any detailed examination of pressure variation to be made.

3-9) DISSOCIATION.

Apart from a fall in light intensity due to the decreasing temperature resulting from dissociation, the dissociation products themselves could

accelerate relaxation. However it can be shown that quite considerable concentrations of dissociation products would be needed before any decrease in relaxation time could be observed. In fact the temperature drop due to dissociation would have a much greater effect on the intensity level than any change in the rate of relaxation: these effects are not observed (see above).

The absence of any dependence of the relaxation time on SO_2 concentration also seems to rule out dissociation as being the likely answer.

3-10) FLOW EFFECTS.

As the results described throughout this thesis were conducted in a small, square section shock tube operated at reasonably low pressures ($P_1 \simeq$ 5-10 torr.), the effect of boundary layers in the tube must be considered. It has been known for some time that observed test-times in shock tubes obtained under these conditions are much shorter than times predicted from ideal theory (37 p.72).

This phenomenon has been described in terms of boundary layer formation behind the shock front; a cold layer of gas builds up adjacent to the shock tube walls and the mass flow into this layer attenuates the shock front. The particles further back in the gas flow accelerate because the area presented to them by the boundary layer/shock tube cross section decreases. The overall effect is for the shock front to decelerate and the contact surface to accelerate until a "steady-state" is reached. Both discontinuities then continue down the tube at a fixed distance apart. The phenomenon is illustrated in fig. (3-7). Much of the original work on this effect was performed by Mirels; the equilibrium distance between shock and contact

FIG. 3-7
BOUNDARY LAYER PHENOMENA.

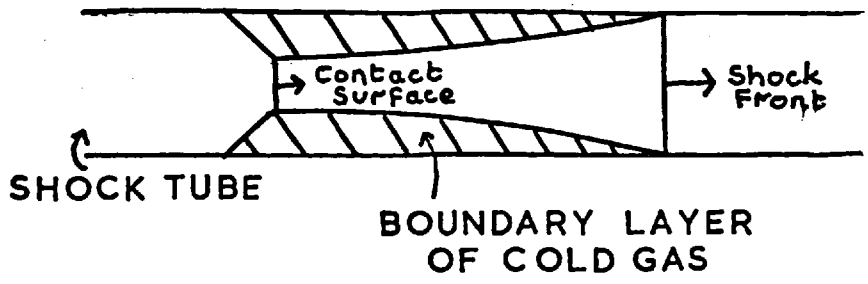

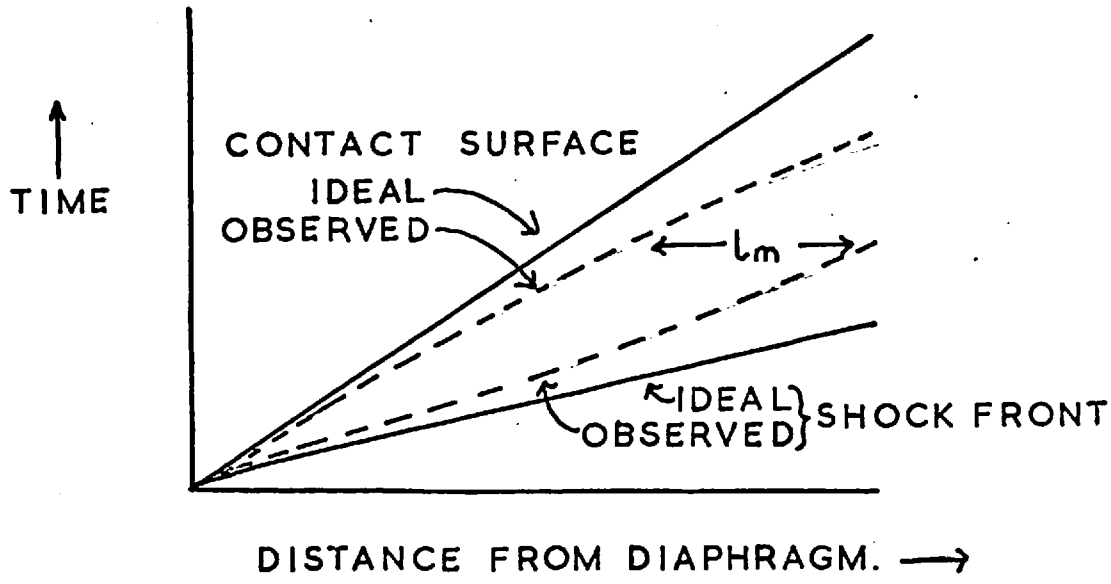

surface is sometimes referred to as the "Mirels length".

The main effect that these flow disturbances have on any kinetic measurements made far behind the shock front, is to upset the time scale of the experiment. Processes will appear to take place much faster than expected. To a lesser extent the shocked gas temperature, pressure and density increase over their theoretical values. Flow effects could therefore account for the apparent decrease in $P\tau_{\alpha}$ with α .

Photographing the light intensity on a slower oscilloscope time base enables the emission to be traced from shock front to contact surface; an estimate of the experimental test-times can be made. A calculation of the ideal test times (i.e. in the absence of boundary layer effects) shows that they are considerably longer than the observed values.

Recently two papers have been published (68, 69) indicating how the shocked gas parameters may be corrected for these flow effects. Mirels expanded his boundary layer theory and presented tables of the variation of shocked gas pressure, density and temperature as a function of a parameter l/l_m . l_m is the Mirels length and l the distance from the shock front to the point at which measurement is being taken. Hobson et al. (70) confirmed Mirels theory experimentally by tracking slugs of ionised gas behind shocks in argon. They also interpreted Mirels equations and calculated the correction factor to the gas particle time.

The method used to apply flow corrections in the Author's shock tube is given in Appendix 1. The Mirels length was assumed to be equal to the length of hot flow actually observed. For a relaxation run, log I at $\alpha = 0$ .... 1·0 was replotted against the longer, corrected gas particle times.

The slopes $\left(\frac{d\ln I}{dt_g}\right)_{CORR.}$ were calculated and the effect on the relaxation is shown in fig. (3-8). It may be seen that the recalculated relaxation times show the temperature dependence expected for Landau-Teller behaviour more closely.

The flow correction is not strictly exact for our conditions - the theory was developed for a non-relaxing gas in a round section shock tube. Hobson's correction for gas particle time is strictly exact only when the gas has reached its steady state condition l_m.

At the observation point, for a nitrogen relaxation at 5 torr. pressure, $U = 2{\cdot}36$ mm.μsec.$^{-1}$, the ideal inviscid test time should be 200μsec. The observed test time is 85 μsec.; Mirels theory predicts 95μsec. Mirels also predicts that the test time t_m equivalent to l_m ($t_m \simeq l_m/U$) should be 280μsec. under these conditions. In other words at the point of observation the test time has already been halved from its ideal value but the gas has not yet reached its steady state condition.

For the run illustrated (fig. 3-8) the "l_m" used in the flow correction was calculated from the shorter, observed test time 85μsec. If the longer l_m - calculated from Mirels theory (280μsec.) - is used, the traces remain undercorrected.

Working backwards from Landau-Teller theory (using Millikan and White's semi empirical formula to obtain the temperature dependence), the flow correction required to reproduce this theory may be established. This procedure is illustrated in fig. (3-9) by depicting Hobson's test time vs. $1/l_m$ correction. The full line has been taken from Hobson's paper; the flow correction required to reproduce the theory corresponds to the shorter

FIG. 3-8

FLOW CORRECTED ANALYSIS OF FIG. 3-6(a)

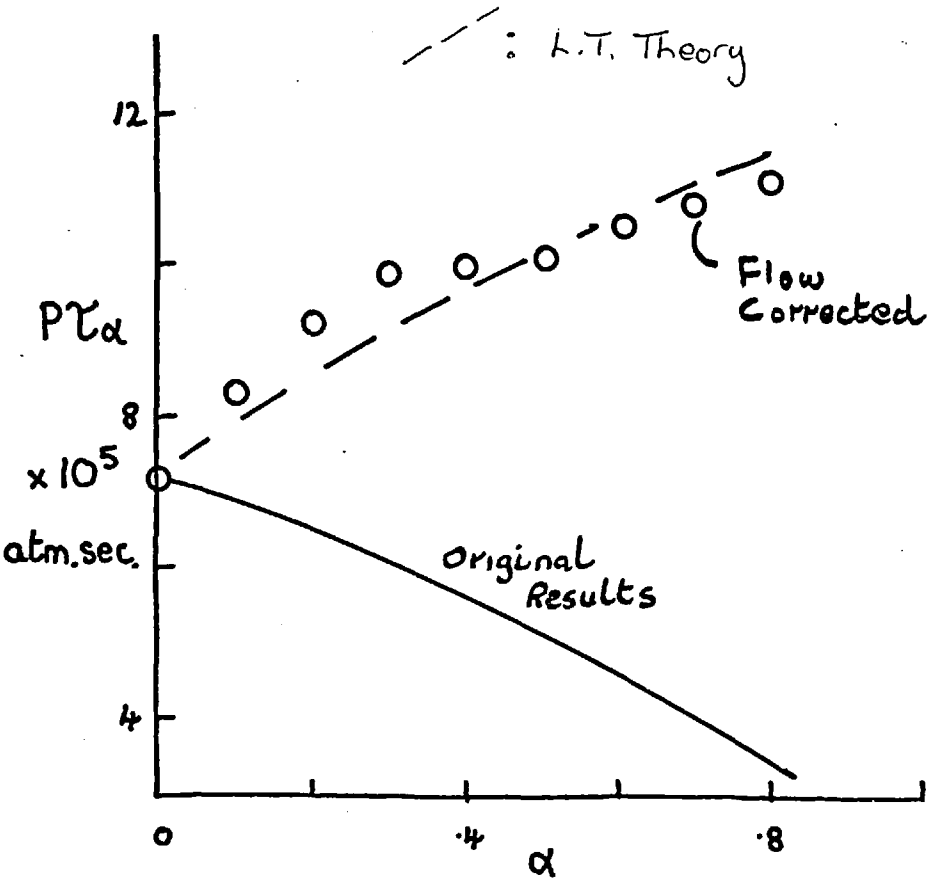

FIG. 3-9

FLOW CORRECTION TO THE PARTICLE TIME OF FLIGHT.

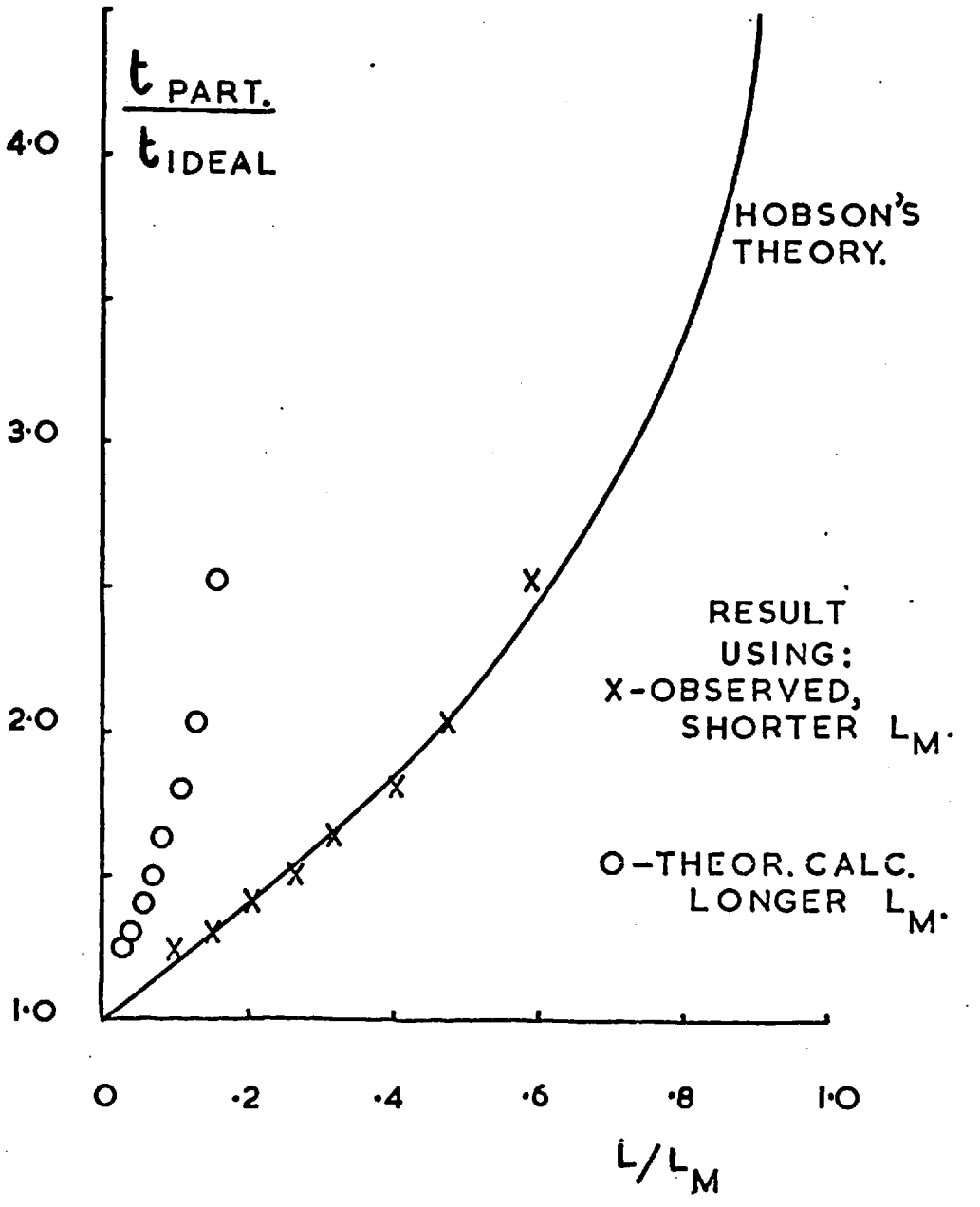

test time, 85 μsec. It may be seen that the correction predicted by the longer test time 280 μsec. does not follow the theory. Hobson has also found that the gas flow, when limiting conditions have not been reached, is better described by the theory using the observed hot flow length rather than the calculated Mirels length for l_m.

A further test was employed to demonstrate that the anomalous results are due to flow effects. Observations were made on the relaxation of nitrogen accelerated by the addition of a small quantity of helium. The helium - nitrogen reduced mass is 3·5 a.m.u. and T-V energy transfer is very efficient (see Chapter 4). Under these conditions, relaxation is complete in under 20 μsec. and any flow correction to the relaxation rate is small. The correction increases rapidly at increasing times behind the front.

The result of an analysis of a run containing 1% SO_2/10% He/20% Ar/69% N_2 is shown in fig. (3-10). The argon was added to make the average molecular weight of the mixture approximately that of a 1% SO_2/N_2 mixture. The gas was therefore "acoustically matched" with the SO_2/N_2 mixture so the gas flow should be similar in the two mixtures.

Although the temperature drop in this four gas system was less than with 1% SO_2/N_2 (only 69% of the gas was relaxing c.f. 99%), the observed relaxation time increases with α and is in much better agreement with Landau-Teller theory.

One anomaly does arise from this last measurement. It has been shown that the original results reproduced the theory provided that the shorter, observed, test time was used in the flow correction. If this shorter value is used to

FIG. 3-10

RELAXATION ANALYSIS FOR C.473. 1%SO_2/10%He/20%Ar/69%N_2.

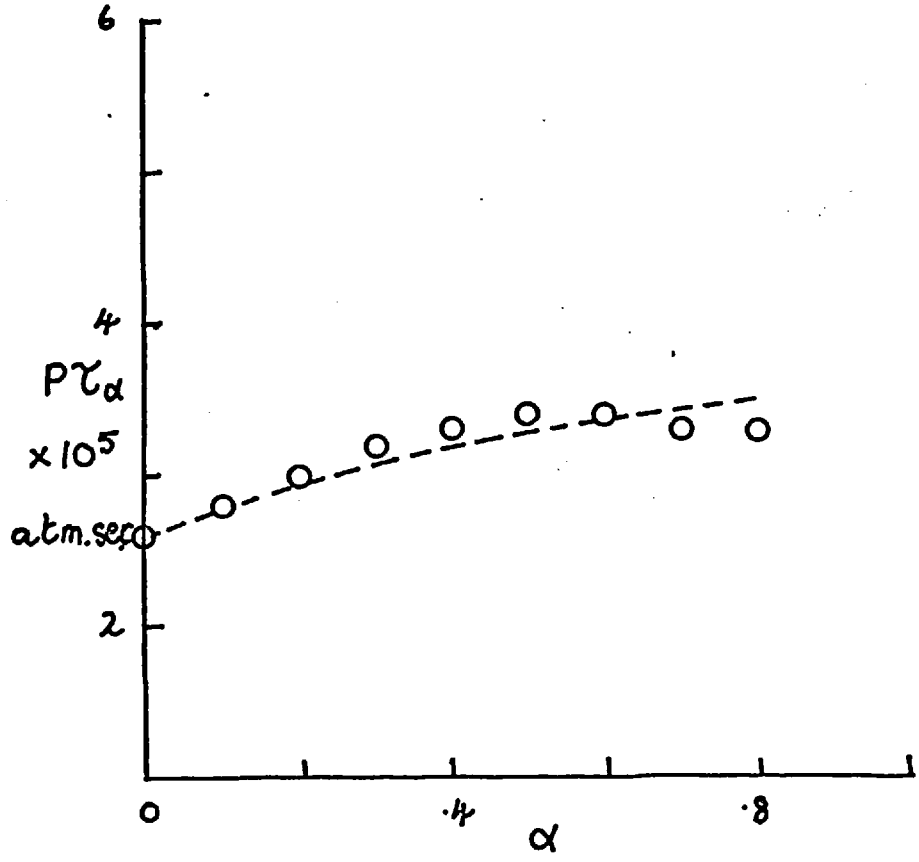

---- : THEORETICAL DEPENDENCE

o : OBSERVED " "

calculate the small flow correction still remaining in the four gas system then the relaxation times become somewhat over corrected. The correction that must be applied to reproduce Landau-Teller behaviour is now nearer the long "steady state" value.

Various explanations may be offered for the difference between this correction and that for the SO_2/N_2 mixtures: the discrepancy between "round-tube" and "square-tube" theory; the effect of relaxation on the boundary layer formation. It is possible that the flow changes from laminar to turbulent at some point between the shock front and contact surface.

As a check that the gas flow was being correctly predicted by Mirels theory, one further test was employed. Aided by an extra photomultiplier and a dual channel oscilloscope preamplifier (Tektronix type 1A1), test times were observed at all three stations. The light emission from 10% SO_2/N_2 was used; the results are summarised in Table 3-2. These enable an x-t diagram (c.f fig. 3-7) to be constructed and this is shown in fig. (3-11). To obtain the diagram, shock attenuation has been assumed to be 1%/metre at the three stations.

TABLE 3-2.

Test times for 10% SO_2/N_2 , $P_1 = 8$ torr., $T^1 = 2475^{oK}$.

Observation Station	Ideal	Mirels	Observed
		Test times in μsec.	
A	155	105	85
B	200	125	105
C	245	155	135

Table 3-2 and fig. (3-11) demonstrate that although Mirels theory is not exact, it gives a reasonable description of the flow profile in this shock tube.

FIG. 3-11

"x-t" DIAGRAM FOR 10% SO_2/N_2.

$T_1' = 2475^{\circ}K$ $P_1 = 8$ TORR

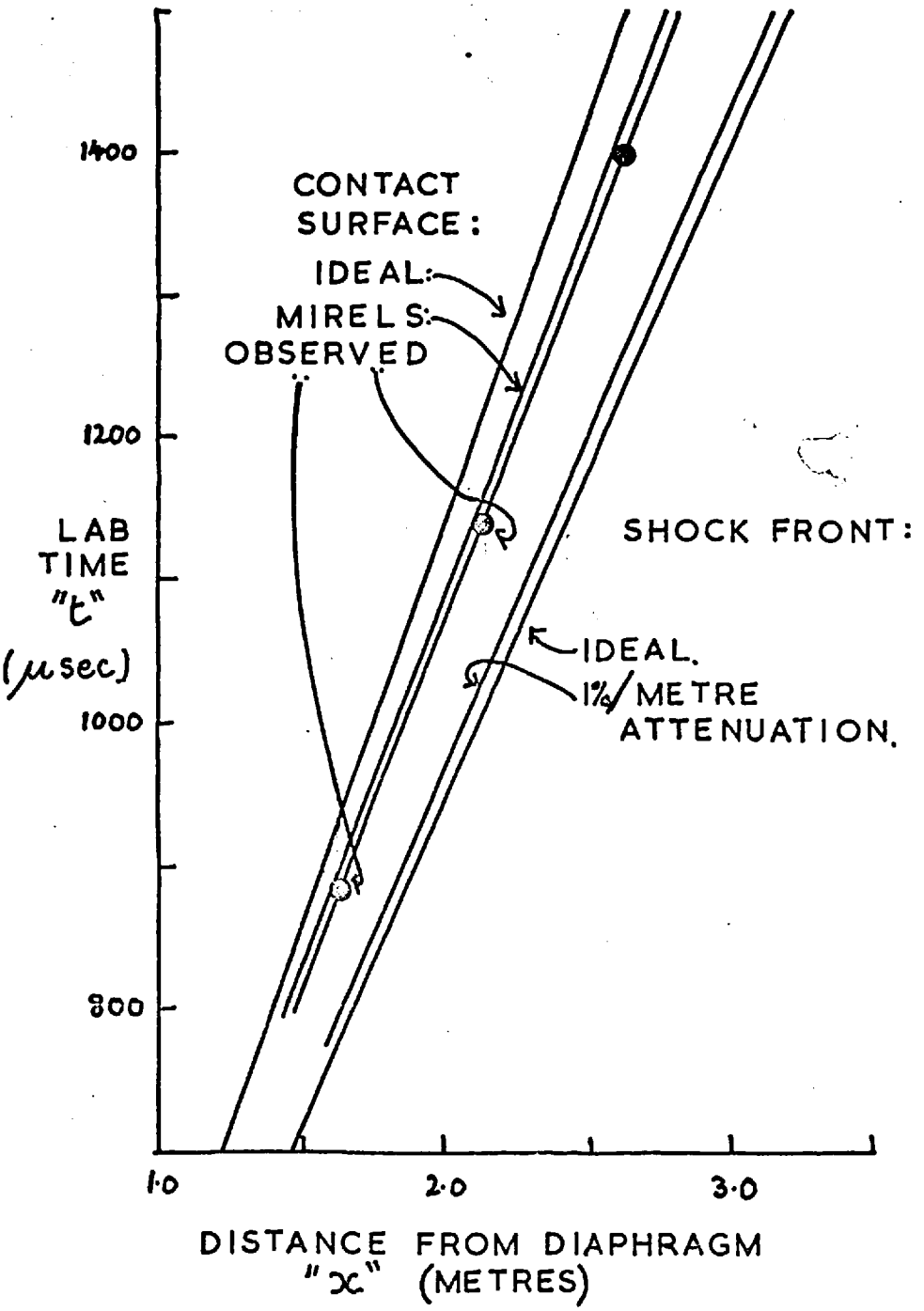

3-11) ELECTRONIC RELAXATION.

Before the final work on flow effects was completed, it was considered possible that the electronic excitation kinetics of the SO_2 were complex at intermediate vibrational temperatures.

Sheen (48) observed a finite risetime for the emission from SO_2 - Ar mixtures; the risetimes were different for transitions from the three excited states of SO_2. These results were interpreted to yield values of the collisional efficiencies of electronic relaxation; i.e. electronic relaxation times were calculated for these three states. Sheen suggested that the electronic relaxation might interfere with measurements of vibrational relaxation in nitrogen; incomplete electronic relaxation would lead to a diminution of light emission and hence an apparent decrease in the instantaneous vibrational relaxation time.

All these electronic relaxation times were obtained in separate experiments. No results were obtained from the simultaneous monitoring of emission at more than one wavelength. Examination of Sheen's oscilloscope traces shows that these risetimes were not reproduceable. These experiments were therefore repeated, this time simultaneously monitoring emission at 4360 and 3650 Å using two interference filter/photomultiplier combinations.

Mixtures of 10% SO_2/Ar and 2% SO_2/Ar were shocked under the conditions observed by Sheen. None of the runs performed showed a significant discrepancy between the risetimes at the two wavelengths. On some traces a slight identical delay was observed; it was not reproduceable. It was concluded that both this effect, and that observed by Sheen, was due solely to shock defects in the hot gas.

It is considered that the anomalously fast relaxation rates observed behind the shock front were due to boundary layer effects. When these are corrected according to current theory, the relaxation times show the same temperature dependence during a single relaxation as is observed from shock to shock. This result agrees with those found by other workers.

The result also shows that the population of excited states of SO_2 is controlled purely by the translational temperature of the N_2 diluent. This is true not merely immediately behind the front where the vibrational temperature is low, but also at higher vibrational temperatures between the front and equilibrium.

CHAPTER 4.

VIBRATIONAL RELAXATION OF NITROGEN WITH VARIOUS COLLISION PARTNERS.

4-1) INTRODUCTION.

The results in this chapter were obtained from analyses of the emission decay just behind the shock front. Under these conditions $\alpha \simeq 0$ and equation (3-9) may be rewritten:

$$P\tau_o = \frac{P\left(\frac{E_a}{RT} \cdot \frac{d\ln T}{d\alpha} - \frac{d\ln \rho}{d\alpha}\right)}{\frac{d\ln I}{dt_g}} \qquad (4\text{-}1)$$

where the differentials are computed at exactly $\alpha = 0$ and

$$\text{gas time, } t_g, = \left(\frac{\rho_2}{\rho_1}\right)_{\alpha=0} \times \text{lab. time, } t_1 .$$

The calculation of several relaxation times at $\alpha = 0$, each corresponding to a temperature T^1, enables the temperature variation of relaxation times to be determined.

4-2) VIBRATIONAL RELAXATION IN GAS MIXTURES.

The emission tracer method of measuring relaxation times requires the presence of a small amount of SO_2; it is relevant at this stage to discuss the effect of foreign gases on the nitrogen relaxation.

If nitrogen is mixed with a monatomic gas M e.g. argon, then there are two collisional processes (both T-V) whereby energy transfer can proceed:

$$N_2\,(\nu = 1) + N_2\,(\nu = 0) \underset{k_{01}}{\overset{k_{10}}{\rightleftharpoons}} N_2\,(\nu = 0) + N_2\,(\nu = 0) \qquad (4\text{-}2)$$

$$N_2\,(\nu = 1) + M \underset{k_{02}}{\overset{k_{20}}{\rightleftharpoons}} N_2\,(\nu = 0) + M \qquad (4\text{-}3)$$

Since (4-2), (4-3) have different probabilities of energy transfer, the observed relaxation rate τ will be given by:

$$\frac{1}{\tau} = \frac{m}{\tau(N_2\text{-}M)} + \frac{1-m}{\tau(N_2 - N_2)} \qquad (4\text{-}4)$$

or in more general terms

$$\frac{1}{\tau} = \sum_i \frac{m_i}{\tau(N_2\text{-}M_i)} \qquad (4\text{-}5)$$

where m_i is the mole fraction of component M_i. $P\tau(N_2 - M_i)$ is the relaxation time of nitrogen dilute in component M_i. (4-4) may be re-arranged:

$$\frac{1}{P\tau} = m \cdot \left(\frac{1}{P\tau(N_2\text{-}M)} - \frac{1}{P\tau(N_2\text{-}N_2)} \right) + \frac{1}{P\tau(N_2\text{-}N_2)} \qquad (4\text{-}6)$$

A plot of $1/P\tau$ against m at a particular temperature should be linear. Measuring the observed relaxation time of nitrogen at various concentrations of M enables an accurate determination of the rate of both (4-2) and (4-3) to be obtained from the slope and intercept of the plot of (4-6).

If M is diatomic or polyatomic and hence has internal modes which can themselves relax, further processes must be considered:

$$N_2\,(\nu = 1) + M\,(\nu = n\text{-}x) \underset{k_{03}}{\overset{k_{30}}{\rightleftharpoons}} N_2\,(\nu = 0) + M\,(\nu = n)$$

$$x = 1, 2 \ldots . n. \qquad (4\text{-}7)$$

$$M\,(\nu = 1) + M\,(\nu = 0) \underset{k_{04}}{\overset{k_{40}}{\rightleftharpoons}} M\,(\nu = 0) + M\,(\nu = 0) \qquad (4\text{-}8)$$

$$M\,(\nu = 1) + N_2\,(\nu = 0) \underset{k_{05}}{\overset{k_{50}}{\rightleftharpoons}} M\,(\nu = 0) + N_2\,(\nu = 0) \qquad (4\text{-}9)$$

(4-7) is an example of a resonant or near-resonant vibration-vibration (V-V) transfer process. (4-8) and (4-9) are the (T-V) processes for relaxation of the added gas M. If (4-7) is very slow or does not occur, then two distinct relaxation times will exist in the gas mixture - one for nitrogen,

the other for M. There is no cross coupling of vibrational energy between N_2 and M; equation (4-4) will still be valid.

The presence of a fast (V-V) process (4-7) complicates the analysis. Camac, Taylor and Feinberg (43) overcame the problem by simultaneously monitoring the rate of relaxation of both N_2 and M. By defining a parameter α^1, the ratio of the fraction of vibrational energy in N_2 to that in M, the relaxation time for (4-7) could be defined:

$$P\tau(N_2 - M)_V = (1 - m_{N_2}) \left[\left(\frac{1 - e^{-\theta_{N_2}}}{1 - e^{-\theta_M}} \right) - (1 - \alpha^1) \right] . P\tau \quad (4\text{-}10)$$

where $\theta = \frac{h\nu}{kT}$

At exact resonance $\theta_{N_2} = \theta_M$ and (4-10) simplifies to:

$$P\tau(N_2 - M)_V = \alpha^1 m_{N_2} \; . \; P\tau$$

In this thesis a different approach has been adopted. It is based on Tuesday and Boudart's scheme relating the observed $P\tau$ to the rates of (4-2) (4-3) (4-7) (4-9). This equation has been quoted by Herzveld and Litovitz (15, eqn. 40-12):

$$\frac{1}{\tau} = (1-M)\, k_{10} + M k_{20} + \frac{M k_{30}\, k_{50} + M^2 (k_{40} - k_{50}) . k_{30}}{(1-M)k_{03} + ((1-M)\, k_{50} + M k_{40})} \quad (4\text{-}11)$$

where $\tau_{ox} = 1/k_{ox}$. M is the mole fraction of component M.

Put $k_{50} = x k_{40}$ in (4-11), remembering that $\frac{k_{03}}{k_{30}} = \exp - (\theta_{N_2} - \theta_M) = K_3$

$$\frac{1}{\tau} = \frac{1}{(1-K_1)} \left[\frac{1 - M}{\tau(N_2 - N_2)_T} + \frac{M}{\tau(N_2 - M)_T} \right] + \frac{Mx + M^2(1-x)}{(1-K_4)(1-M)K_3 \tau(M-M) + \tau_{50}(x - M(x-1))} \quad (4\text{-}12)$$

$K_1 = e^{-\frac{h\nu}{kT}}$. $K_4 = e^{-\frac{h\nu_M}{kT}}$. The subscripts T, V on the relaxation times $\tau(N_2-M)$ refer specifically to the rate of the (T-V) or (V-V) process respectively.

If x and the variables $\tau(N_2\text{-}N_2)$, $\tau(N_2\text{-}M)_T$, $\tau(M\text{-}M)$ are known, the value of the relaxation time $\tau(N_2\text{-}M)_V$ may be calculated. The values chosen for x, $\tau(M\text{-}M)$ etc. will be discussed for each collision partner below.

Two special cases arise from equation (4-12):

(1) When

$$(K_4)(1\text{-}M)\, K_3 \tau(M\text{-}M) \ll \tau(N_2\text{-}M)_V \cdot (x\text{-}M(x\text{-}1))$$

i.e. when the relaxation of pure M is very fast, eqn. (4-12) simplifies to eqn. (4-4) where

$$\frac{1}{P\tau(N_2\text{-}M)} = \frac{1}{P\tau(N_2\text{-}M)_T} + \frac{1}{P\tau(N_2\text{-}M)_V} \qquad (4\text{-}13)$$

Under this circumstance the use of (4-4) is justified; the relative contributions to the observed relaxation time from the (T-V) and (V-V) processes may be calculated from (4-13).

(2) Under certain conditions (4-12) imposes a quadratic dependence of M on $\frac{1}{P\tau}$. When the (V-V) process (4-7) is very fast, the vibrational energy of M and N_2 will be kept in equilibrium. The total system will relax through the fastest of the four (T-V) processes. If this is process (4-8):

$$M^* + M \rightarrow M + M$$

then the observed relaxation time is quadratically dependent on M. This has been fully discussed by Lambert (7) in his review article.

4-3) VIBRATIONAL RELAXATION OF NITROGEN - SULPHUR DIOXIDE MIXTURES.

Relaxation times for 1% SO_2/N_2 were determined over the temperature range 2900-1900^{oK}. The upper limit is determined by the onset of the SO_2 dissociation during the time of measurement and the lower limit by the drop in emission intensity; this reduces the signal to noise ratio and also makes it difficult to obtain reliable pulses from the timing photomultipliers.

The relaxation times, calculated using (4-1) and corrected for attenuation (Chapter 3) are plotted against $(T^1)^{-1/3}$ in fig. (4-1). The line represents extensive results obtained by Millikan and White (71); the results are also shown on a diminished scale fig. (4-2) for comparison to nitrogen relaxation times obtained by other workers over a wider temperature range. (66, 72, 73).

To determine the effect of SO_2 on the observed relaxation times, the variation of $P\tau$ ($= P\tau_0$) with mole fraction of SO_2 was determined at 2500^{oK}. For each mixture (m_{SO_2} = ·01, ·05, ·10, ·15) $P\tau$ was measured over a narrow range of shock strengths; a plot of $\log_{10} P\tau$ against $(T^1)^{-1/3}$ was interpolated to give values of $P\tau$ at exactly $T^1 = 2500^{oK}$. The results are presented in fig. (4-3). No attempt was made to check the pressure scaling in detail; however no systematic variation of $P\tau$ was observed over a twofold range of total pressure. Interpolated results are given in table 4-1 and the plot of equation (4-6) is shown in fig. (4-4). From the intercept and slope:

$$\left.\begin{aligned} P\tau\,(N_2\text{-}N_2) &= 1{\cdot}9.\ 10^{-4}\ \text{atm.sec.} \\ P\tau\,(N_2\text{-}SO_2) &= 2{\cdot}9.\ 10^{-5}\ \text{atm.sec.} \end{aligned}\right\} \quad \text{at } 2500^{oK}$$

Table 4-1.

Interpolated results, N_2-SO_2 relaxation times, 2500^{oK}

m_{SO_2}	$P\tau$, atm.sec.
·01	$1{\cdot}82.\ 10^{-4}$
·05	$1{\cdot}41.\ 10^{-4}$
·10	$1{\cdot}26.\ 10^{-4}$
·15	$1{\cdot}02.\ 10^{-4}$

Levitt and Sheen (47) presented the temperature dependence of their results as a plot of $\log_{10} P\tau$ vs. $T_m^{-1/3}$ where T_m was the mean of T^1

FIG. 4-1

VIBRATIONAL RELAXATION TIMES

1% $S O_2/N_2$

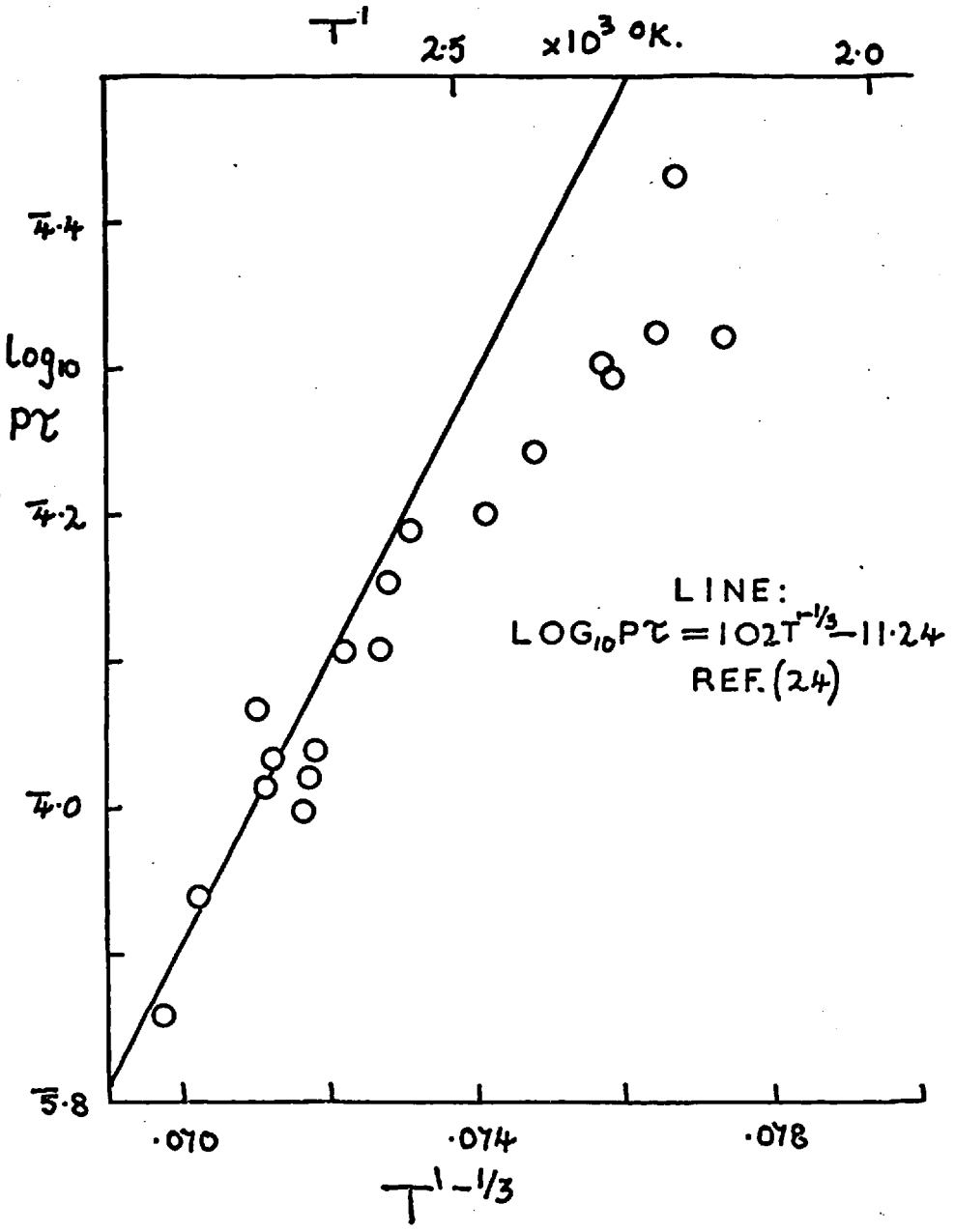

FIG. 4-2

VIBRATIONAL RELAXATION TIMES.
NITROGEN.

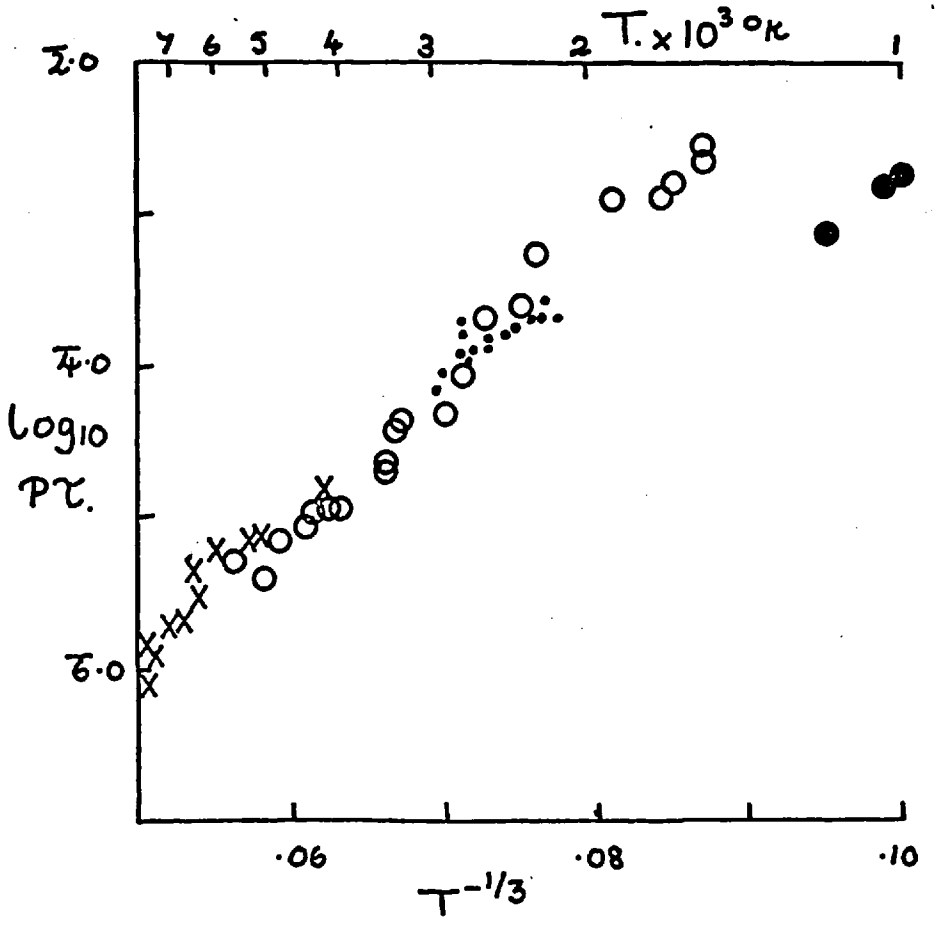

X APPLETON REF. (66)
O MILLIKAN & WHITE (Y2)
• SELF - 1% SO_2/N_2
● LUKASIK & YOUNG (Y3)

FIG. 4-3

OBSERVED RELAXATION TIMES.

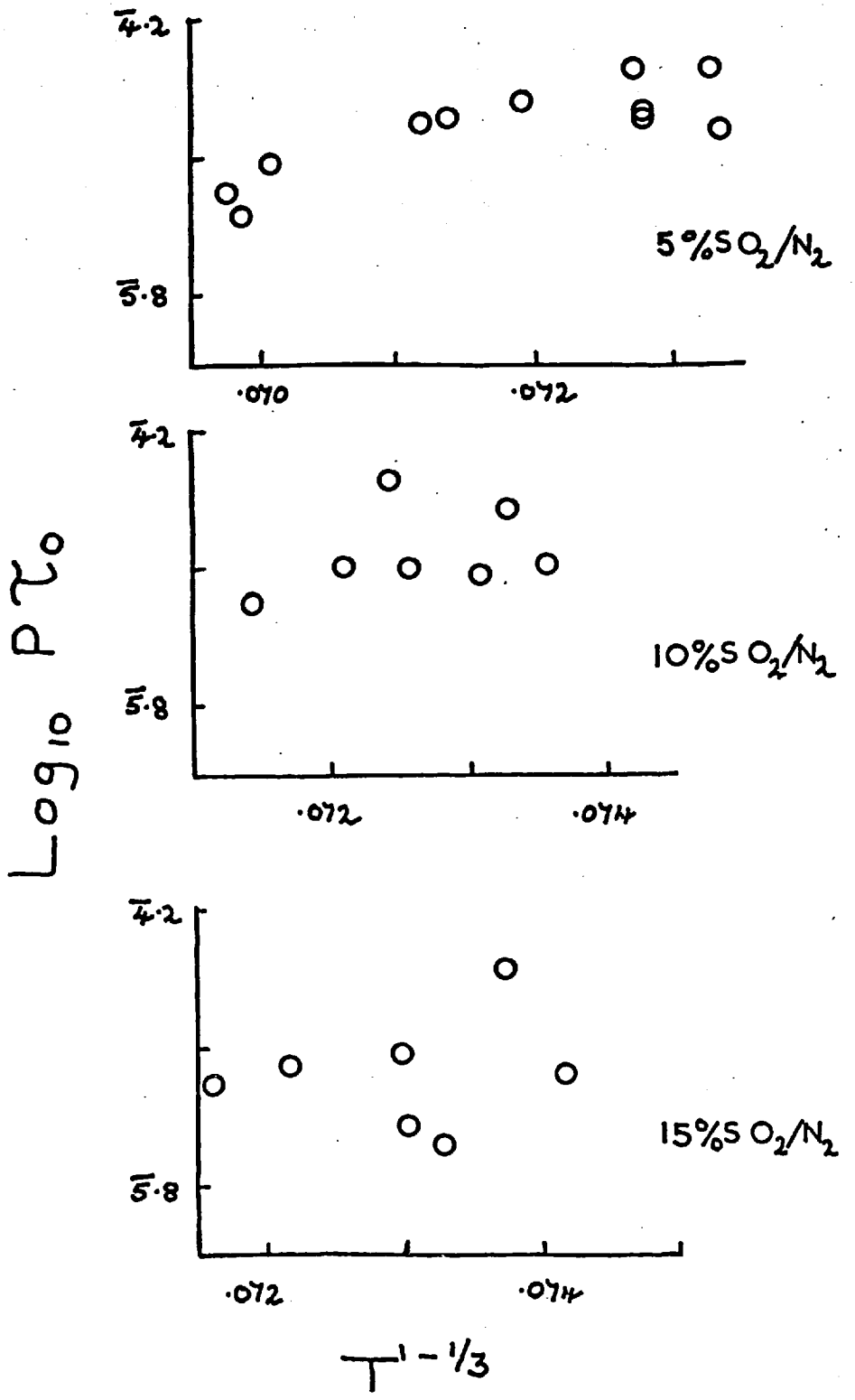

FIG. 4-4
PLOT OF EQN.4-6 FOR N_2–SO_2

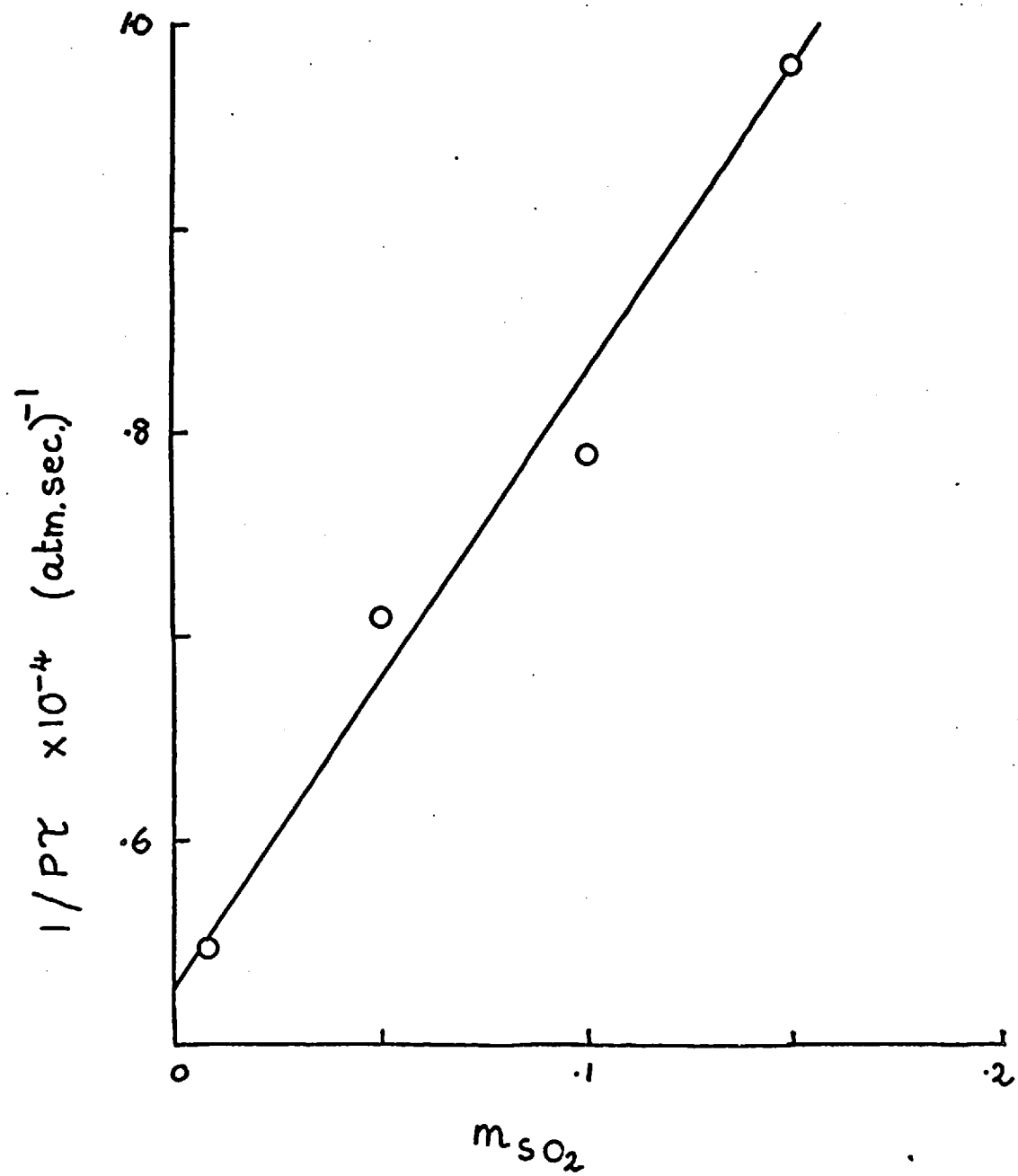

and T^{11}. This mean temperature was selected to compare to the results of other workers who had determined relaxation times averaged over the whole relaxation process. This comparison is not strictly correct; the results presented here are plotted against the true instantaneous translational temperature: here the frontal temperature T^{1}.

The result for $P\tau\ (N_2\text{-}N_2)$ may be compared with that obtained by Millikan and White for nitrogen. (71, 72). A shock with $T^{1} = 2500^{oK}$ behind the front corresponds to a mean temperature $T_m = 2370^{oK}$. At this value of T_m, Millikan and White find $P\tau = 2{\cdot}6.\ 10^{-4}$ atm.sec. This is an average value obtained over the first $(1 - {}^{1}/_{e})$th. of the relaxation and therefore corresponds to about $\alpha = {\cdot}3$ or $T = 2420^{oK}$. From the temperature dependence they observed from shock to shock, the corresponding value at exactly 2500^{oK} would be $2{\cdot}2.\ 10^{-4}$ atm.sec.- some 15% higher than the result found here. The agreement is well within the combined experimental errors and those involved in making the comparison.

4-4) EXTENSION OF RELAXATION TIMES TO LOWER TEMPERATURES.

Below 2400^{oK} the relaxation times for 1% SO_2/N_2 deviate from the plot expected for pure nitrogen (fig. 4-1). To ascertain that this was a real effect and not due to impurities in the gas, the results were repeated using 10% SO_2/N_2. The results were extended to as low a temperature as possible - 1700^{oK}.

The relaxation times, indicated in fig. (4-5), show that as the temperature decreases so the temperature dependence of the relaxation times becomes less steep. The ratio of relaxation times with and without the addition of a small amount of SO_2 increases with a decrease in temperature.

FIG. 4-5

10% SO_2/N_2 RELAXATION TIMES

(1650 - 2900°K)

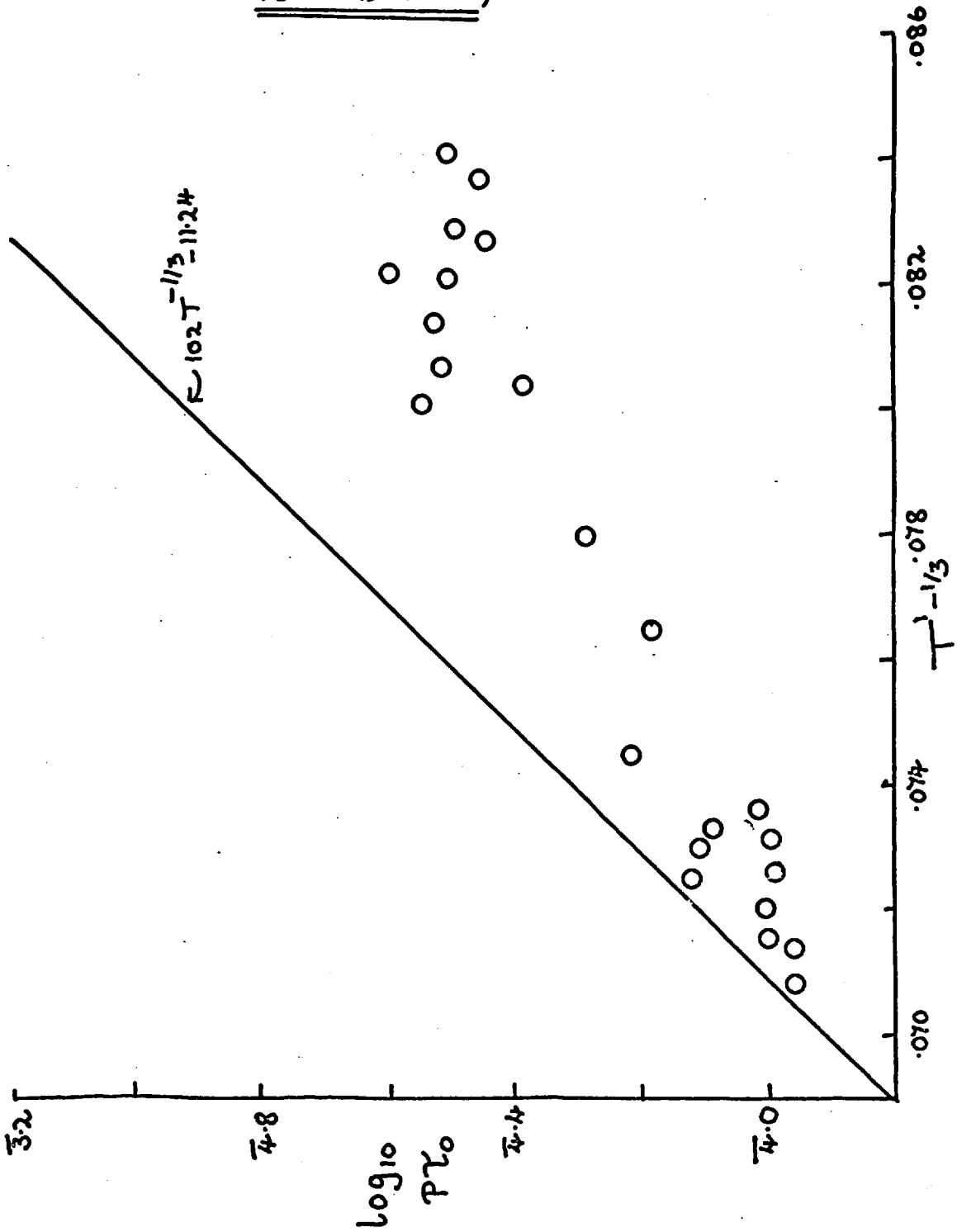

4-5) COMPARISON TO THE RESULTS OF LEVITT AND SHEEN (47).

A few runs were performed on 1% SO_2/N_2 using the emission isolated by a 4360 Å interference filter. The results were found to be indistinguishable from the unfiltered radiation results presented in fig. (4-1). Previous relaxation times obtained by Levitt and Sheen (47) using filtered emission from 2% and 10% SO_2/N_2 mixtures were also in line with the results which have been presented here. At no stage in this work could any difference be detected between the filtered and unfiltered emission results. This suggests that all three excited states of SO_2 "follow" the translational temperature of the relaxing gas.

4-6) VIBRATIONAL RELAXATION WITH FURTHER COLLISION PARTNERS.

The vibrational relaxation of nitrogen with various collision partners was investigated using the emission tracer method. This technique is well suited to obtaining a consistent set of measurements with various collision partners at a single temperature. It is less suited to measuring the temperature variation of relaxation times.

A standard procedure was adopted for measuring these collision partner effects. Sufficient concentration of the gas, M, was added to a 1% SO_2/N_2 mixture to alter the observed relaxation rate by at least a factor of two. For the more efficient collision partners examined e.g. H_2, only a few per cent. concentration of M was added. For Ar and Kr as much as 60-70% was required and the resultant relaxation times were not so accurate (only 29% of the gas is relaxing).

As with the SO_2/N_2 mixtures previously described, the relaxation time at 2500^{oK} was obtained from an interpolated plot of $\log_{10} P\tau$ versus

$\left(T^1\right)^{-1/3}$ over a narrow range of shock strengths. For the more important collision partners, further results were obtained at various mole fractions of the added gas; $P\tau\ (N_2\text{-}M)$ was obtained from a plot of $1/P\tau$ versus mole fraction of M. Otherwise $P\tau\ (N_2\text{-}M)$ was calculated directly from equation (4-6): the correction for the 1% of SO_2 added was always small.

Measurements were possible only when the added gas satisfied certain conditions. Firstly it must not dissociate appreciably during the time required for the measurement. It must not emit radiation comparable to the tracer. The molecule must also be chemically inert with respect to both SO_2 and N_2 during the measurement. To supplement literature information on these subjects, the intensity of the emission plateaux of $SO_2/Ar/M$ mixtures were observed to be level, indicating ~~slow~~ no chemical reaction. The intensities of these plateaux were compared to the SO_2/Ar results to indicate that no emission from the molecule M was observed.

The peak emission, I^1, from the $SO_2/N_2/M$ mixtures was also compared to the results obtained for SO_2/N_2.

4-7) RESULTS - RARE GASES.

Relaxation times were measured in the presence of He, Ar and Kr. The mixtures contained 4%, 70% and 60% added gas respectively. Values of $\log_{10} P\tau$ are plotted against $\left(T^1\right)^{-1/3}$ in fig. (4-6).

Using eqn. (4-6):

$$\left.\begin{aligned} P\tau\ (N_2 - He) &= 4{\cdot}5.\ 10^{-6}\ \text{atm.sec.} \\ P\tau\ (N_2 - Ar) &= 4{\cdot}8.\ 10^{-4}\ \text{atm.sec.} \\ P\tau\ (N_2 - Kr) &= 9{\cdot}4.\ 10^{-4}\ \text{atm.sec.} \end{aligned}\right\} \quad 2500^{\circ}K$$

FIG. 4-6
RELAXATION TIMES
$1\%SO_2/N_2$ + He, Kr, Ar.

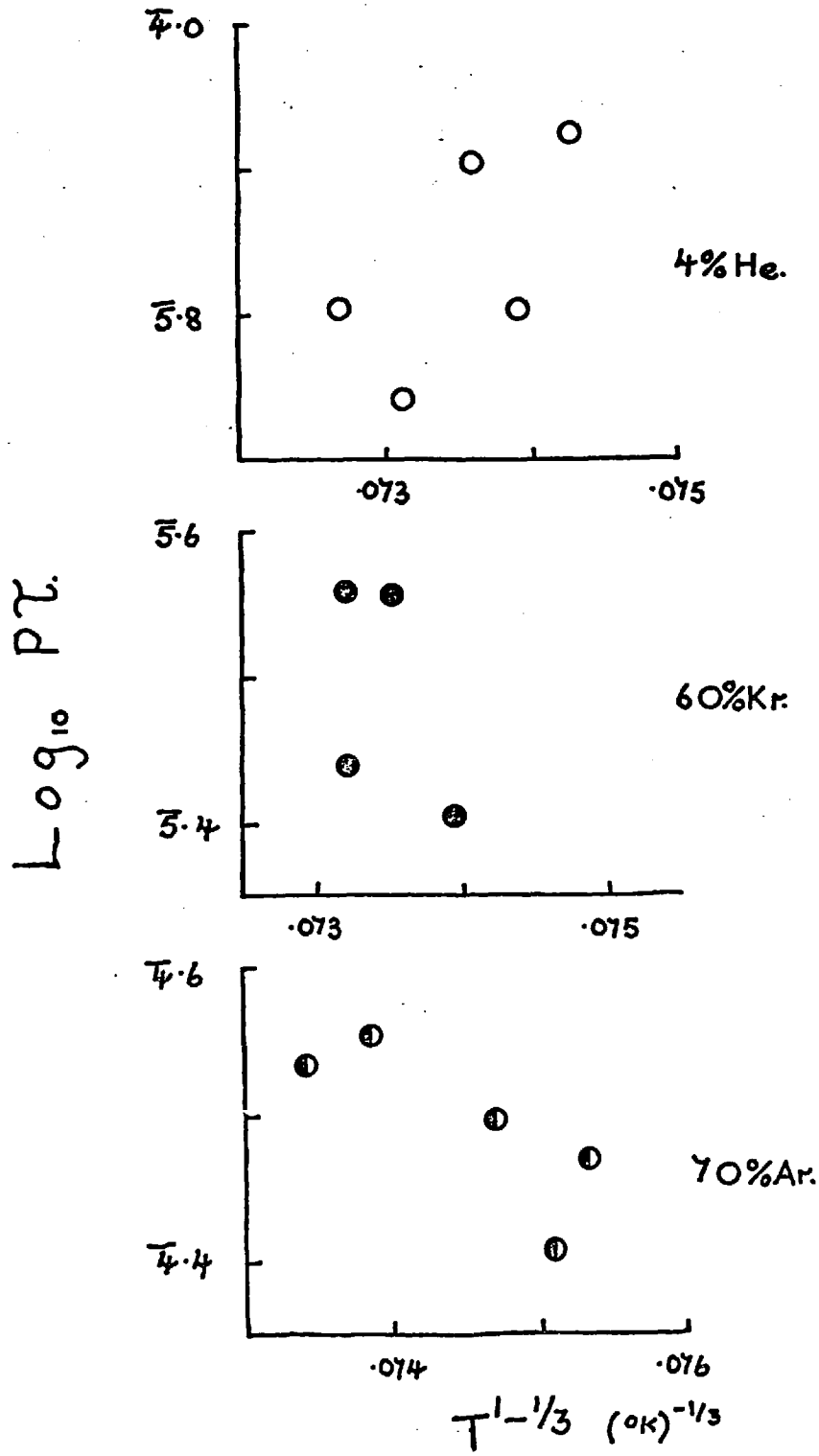

4-8) RESULTS-DIATOMIC GASES.

H_2, D_2, O_2, HCl and DCl were examined as collision partners. For H_2 and D_2, the traces in argon gave the correct steady intensity level for about 50 μsec. whereafter the emission rose rapidly off the top of the oscilliscope trace. Similar effects were observed in H_2 and D_2 / N_2 mixtures at the completion of relaxation. The phenomenon may well be due to an exothermic reaction between H_2 and SO_2.

Dissociation of oxygen is slow at 2500^{oK}; no Schumann-Runge emission was observed.

The dissociation of HCl has been measured by Jacobs (74). From both his I.R. emission photographs and dissociation rate constants, it is clear that the dissociation is several orders of magnitude slower than the relaxation process at 2500^{oK}.

The relaxation results are shown in fig. (4-7) and (4-8). Fig. (4-9) shows $1/P\tau$ against m_{H_2} for the concentrations measured (1%, 3%, 6% H_2). The slope of the plot gives

$$P\tau\ (N_2 - H_2) = 1{\cdot}3.\ 10^{-6} \text{ atm.sec. at } 2500^{oK}$$

Relaxation times in 4% D_2 and 5% O_2 gave, using eqn. (4-6):

$$\left.\begin{aligned} P\tau\ (N_2 - D_2) &= 4{\cdot}1.\ 10^{-6} \text{ atm.sec.} \\ P\tau\ (N_2 - O_2) &= 1{\cdot}2.10^{-5} \text{ atm.sec.} \end{aligned}\right\} \quad 2500^{oK}$$

Concentrations of 3% and 5% HCl were used. Fig. (4-9) also gives the plot of $1/P\tau$ versus m_{HCl}.

$$P\tau\ (N_2 - HCl) = 3{\cdot}7.\ 10^{-6} \text{ atm.sec. at } 2500^{oK}$$

For DCl (5%), equation (4-6) gives

$$P\tau\ (N_2 - DCl) = 3{\cdot}7.\ 10^{-6} \text{ atm.sec. at } 2500^{oK}$$

FIG. 4-7

RELAXATION TIMES

$1\%SO_2/N_2 + H_2, D_2$.

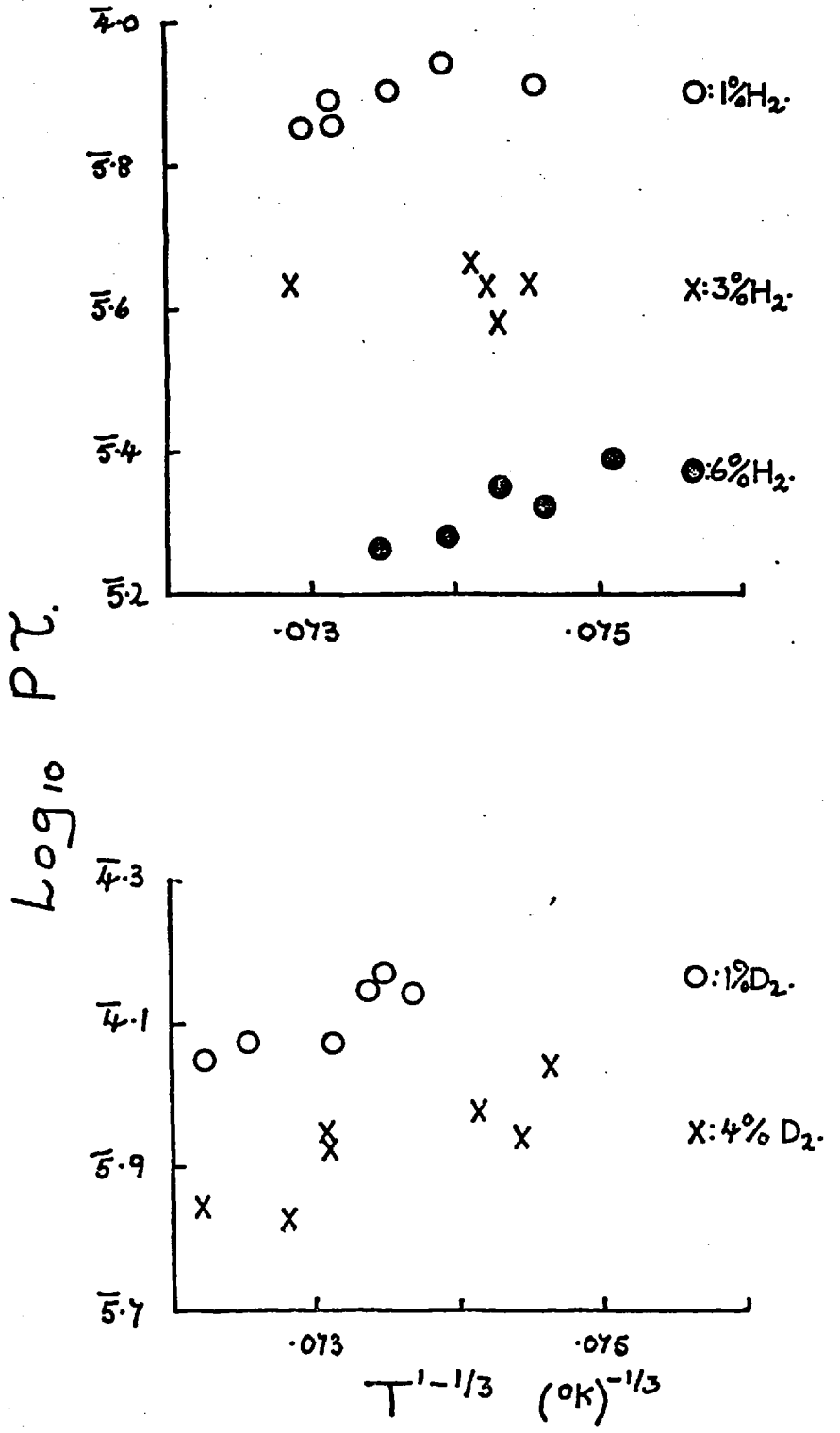

FIG. 4-8

RELAXATION TIMES

1% SO_2/N_2 + O_2, HCl, DCl.

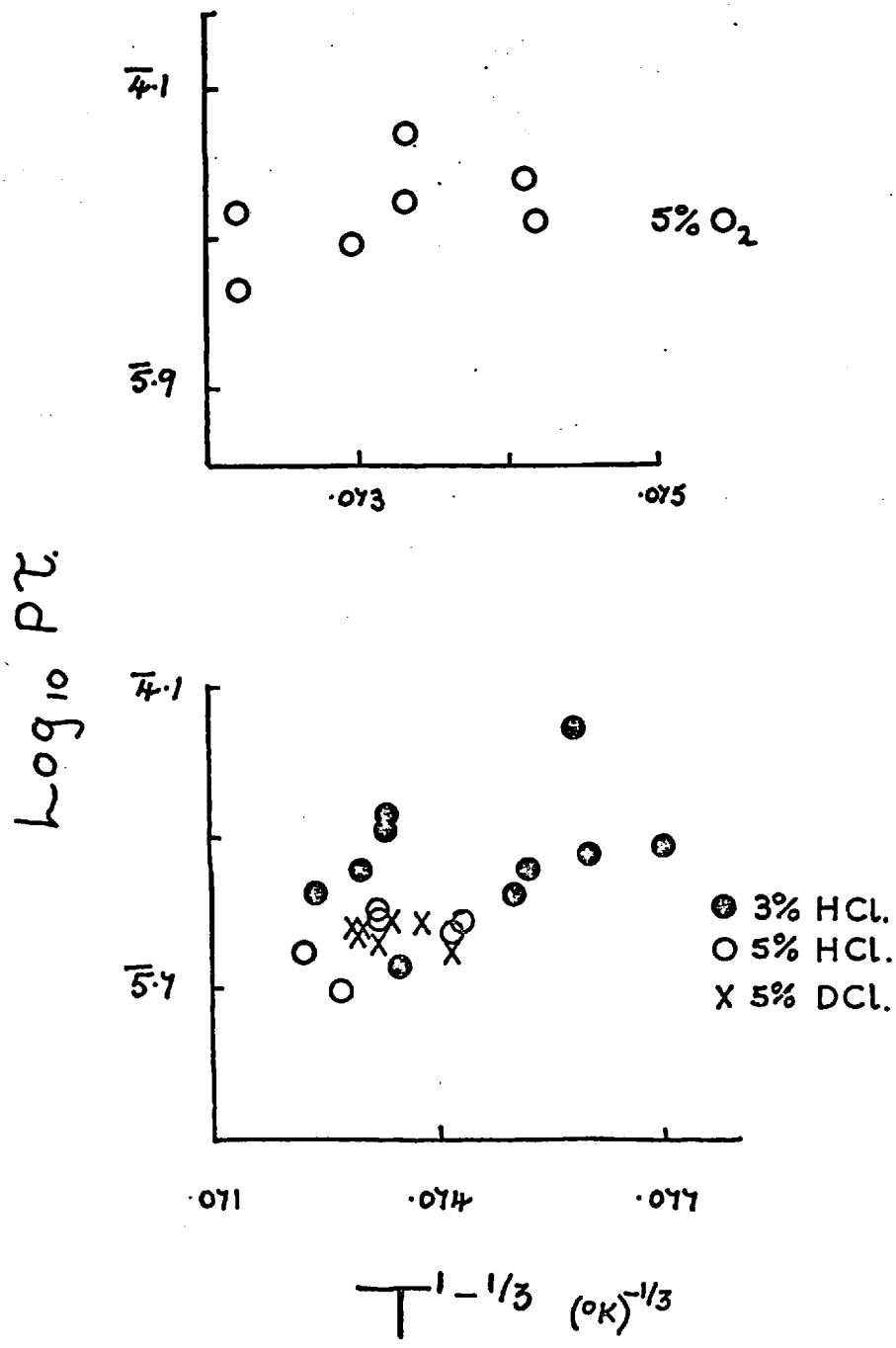

FIG. 4-9

PLOT OF EQN. 4-6.

1% SO_2/N_2 + H_2, HCl, DCl.

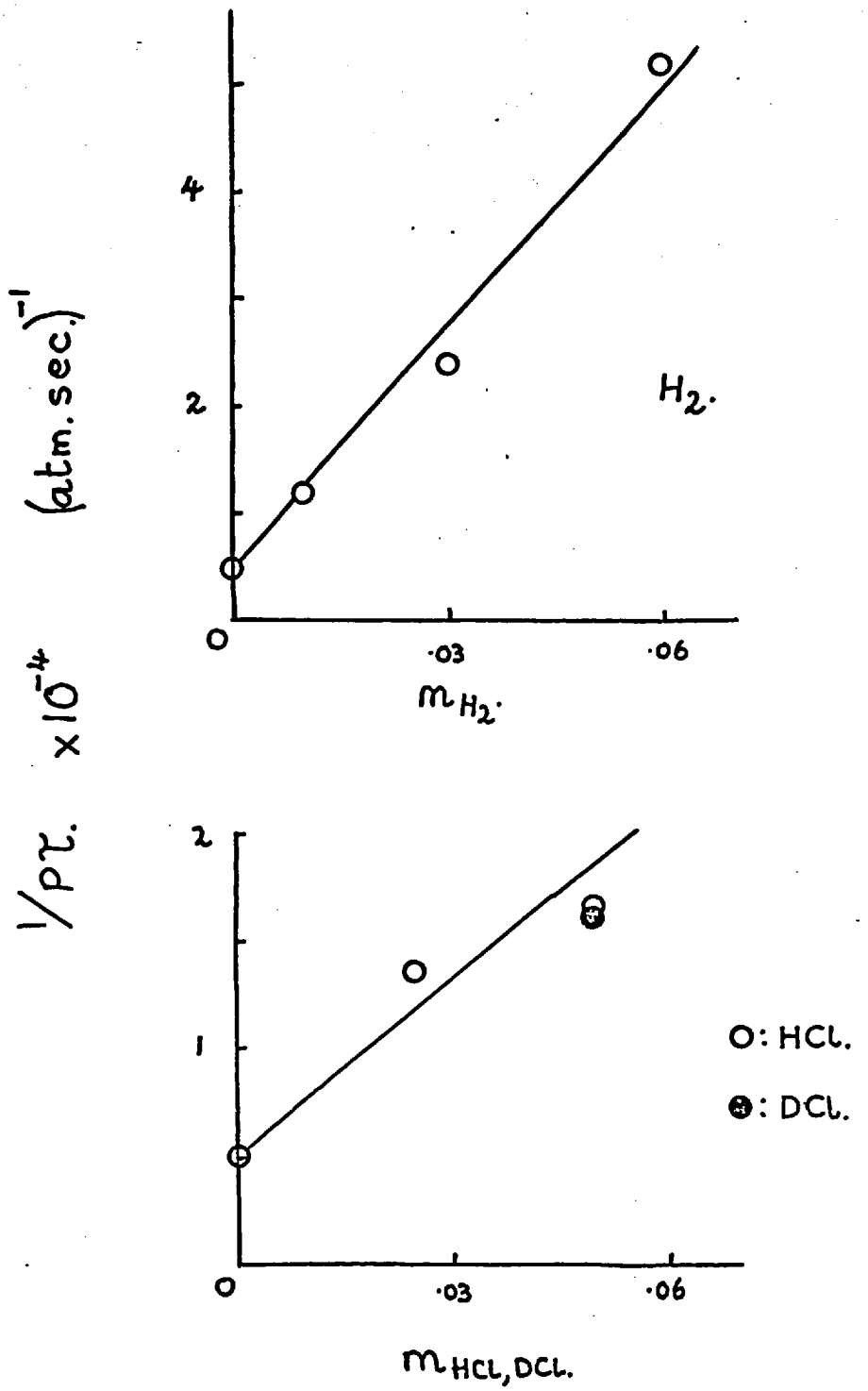

The question of isotopic exchange in the DCl mixtures (DCl $\longleftrightarrow$ HCl) was examined using I.R. spectrophotometric analysis. Previous attempts to investigate the exchange using a mass spectrometer were unsuccessful. The DCl prepared from either the $D_2O/Si\ Cl_4$ or $D_2SO_4/NaCl$ contained about 30% HCl immediately after preparation; on storage in a bulb this concentration did not increase appreciably. The shock tube was flushed with a few torr of DCl; a further sample was left there for two minutes and then analysed. The HCl concentration was found to be about 50%. Thus the proportion of HCl in the shocked gas lay between 30 and 50%, probably nearer the former. There is very little difference between the HCl and DCl results; as we can be certain that the values of $P\tau$ do not differ by more than 30%, there can be little difference between the efficiencies of HCl and DCl in relaxing nitrogen.

4-9) RESULTS - POLYATOMIC GASES.

Traces of SO_2/Ar containing 5% NH_3 showed considerable emission over and above the SO_2 radiation. Both Jacobs (75) and Bradley et al. (76) have examined the pyrolysis and oxidation of NH_3 in the shock tube. It is clear that the surplus emission is a function of the NH_3 and stems from the radicals formed during the NH_3 dissociation. No relaxation measurements were possible.

Measurements were made in gas mixtures containing H_2O and D_2O. Water is easily absorbed on the surface of reaction vessels etc. and consistent results were difficult to obtain. The shock tube was flushed with test gas prior to firing; results were obtained at several concentrations of added gas (2,3,5,10% H_2O; 3,5,10% D_2O). The plot of $1/P\tau$ versus $m_{H_2O,\ D_2O}$ is given in fig. (4-10). The observed relaxation times in H_2O and D_2O were

FIG. 4-10

PLOT OF EQN. 4-6.

1% SO_2/N_2 + H_2O, D_2O.

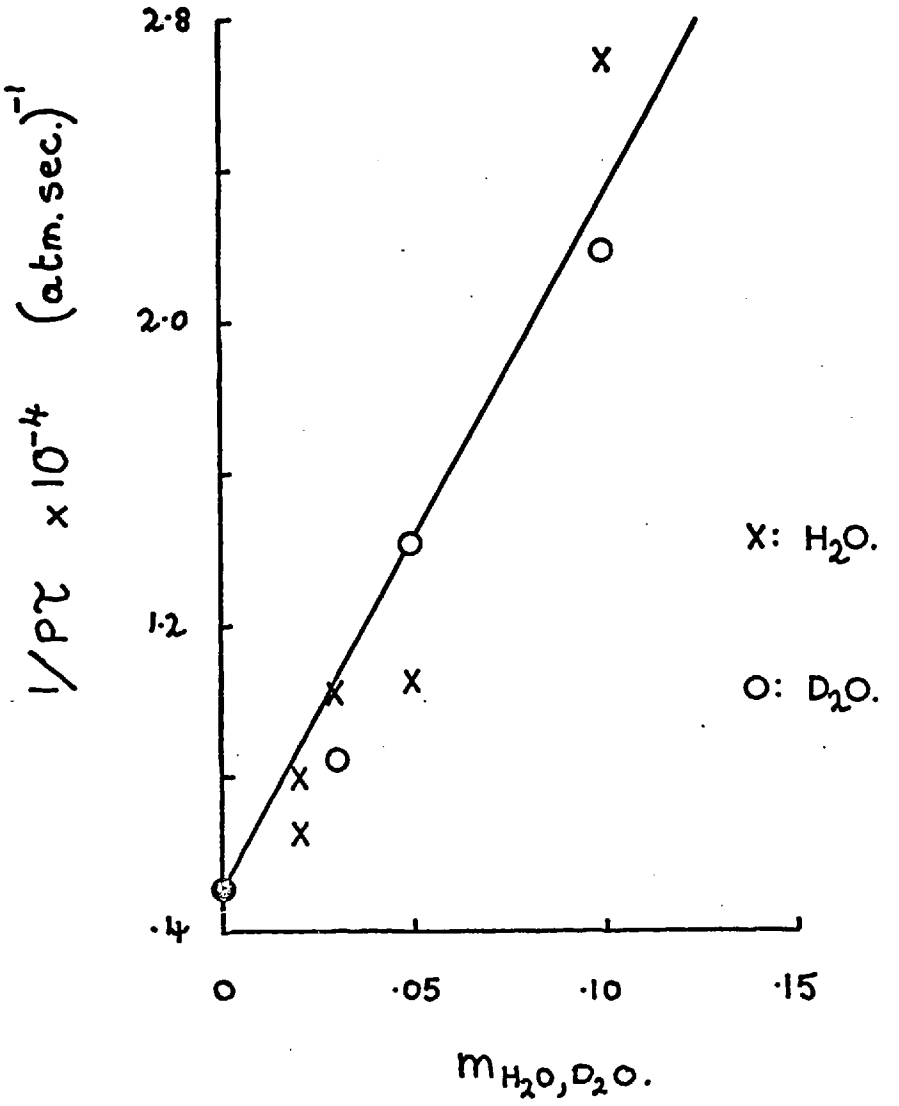

almost identical within experimental error.

$$\left.\begin{array}{l} P\,\tau\,(N_2 - H_2O) \\ P\,\tau\,(N_2 - D_2O) \end{array}\right\} = 6.10^{-6} \text{ atm.sec. at } 2500^{oK}$$

The question of isotopic exchange in the D_2O mixture must be considered; it is a topic that cannot easily be checked experimentally. If, at the time of firing the shock, 75% of the deuterium had exchanged to give H_2O, unless

$$\frac{P\,\tau\,(N_2 - H_2O)}{P\,\tau\,(N_2 - D_2O)} \ll \text{ or } \gg 1$$

very little difference will be observed between the H_2O/D_2O results. Although the flushing technique should have saturated the walls with D_2O, the safest interpretation is to say that $P\,\tau\,(N_2 - D_2O)$ cannot be different from $P\,\tau\,(N_2 - H_2O)$ by more than a factor of two.

Examples of oscilloscope traces of SO_2/Ar. containing a few per cent methane are given in fig. (4-11). Above 2400^{oK} the emission rose sharply at the shock front to a steady level but showed a further rise soon after. At lower temperatures, below 2400^{oK}, the onset of this surplus emission is delayed by a few tens of microseconds.

From an examination of the rate of pyrolysis of methane (77, 78, 79), it is evident that this secondary emission arises from the dissociation products C_2, CH etc. The literature values for the dissociation rate constant are not consistent. From our point of view, the most pessimistic half life for the methane dissociation is about 25 μ sec. gas time at 2200^{oK}. Other rate constants suggest over double this time.

Relaxation of nitrogen containing 5% CH_4 was completed in 5 μsec. lab.

FIG. 4-11

EMISSION TRACES IN MIXTURES CONTAINING METHANE.

(a) 1%SO_2/5%CH_4/Ar.

(i) C282. $T' = 2465^{\circ}K$.

(ii) C286. $T' = 2122^{\circ}K$.

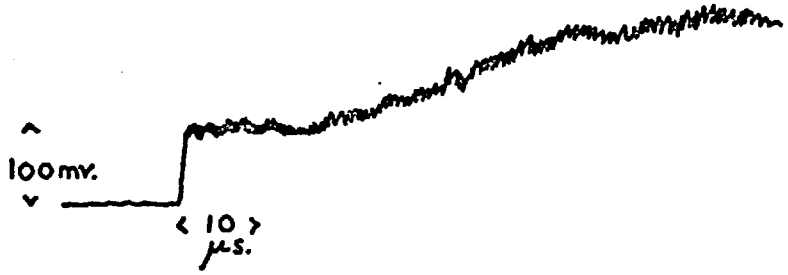

(b) 1%SO_2/5%CH_4/N_2

C.299 $T' = 2203^{\circ}K$.

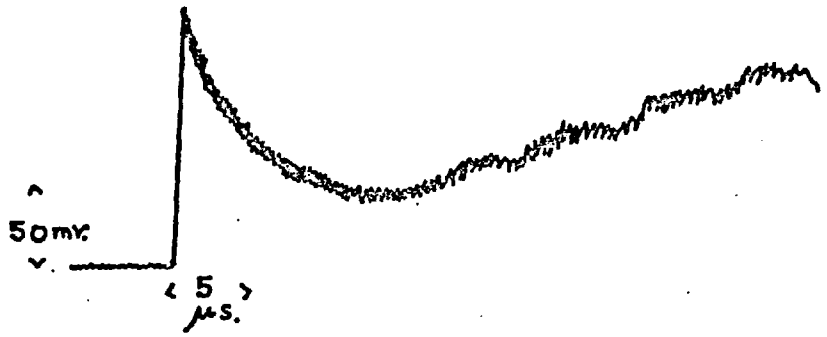

time; a measurement of the initial relaxation rate could be determined from the first 2-3 μsec. It is considered unlikely that dissociation effects the results to any extent provided measurements are taken at $T^1 < 2300^{oK}$. The results have hence been interpolated at $T^1 = 2250^{oK}$.

Fig. (4-12) depicts the measured relaxation times for 1% and 5% CH_4; 4·5% CD_4. These results give:

$$\left.\begin{aligned} P\,\tau\,(N_2 - CH_4) &= 1{\cdot}0.\ 10^{-6}\ \text{atm.sec.} \\ P\,\tau\,(N_2 - CD_4) &= 8.\ 10^{-7}\ \text{atm.sec.} \end{aligned}\right\} \quad \text{at } 2250^{oK}$$

It seems unlikely that the CD_4 exchanges isotopically within the time of measurement, although no tests were undertaken to confirm this. The ratio $P\tau\,(N_2 - CH_4) : P\tau\,(N_2 - CD_4) = 1{\cdot}25 : 1$ should therefore be correct within the other experimental errors.

4-10) EXPERIMENTAL ERRORS.

The major source of error associated with the emission tracer method is the interpretation of the emission decay just behind the shock front. This was not always well defined - especially on traces having low signal to noise ratios or shock defects. As relaxation proceeds, the attenuation correction becomes a significant part of the rate of emission decay . Just behind the shock front, however, this correction is always less than 10% of the rate of decay due to relaxation and was usually negligible compared to other errors.

The shocked gas temperature was defined by the shock velocity to $\pm 25^{oK}$. The pressure of the test gas was known to better than $\pm$ 2%. The amounts of impurities in the gas mixtures (determined mass spectrally) were too small at these high temperatures to have any significant effect. Flushing the shock tube with test gas prior to firing made little or no difference

FIG. 4-12

RELAXATION TIMES

$1\%\ SO_2/N_2 + CH_4, CD_4$.

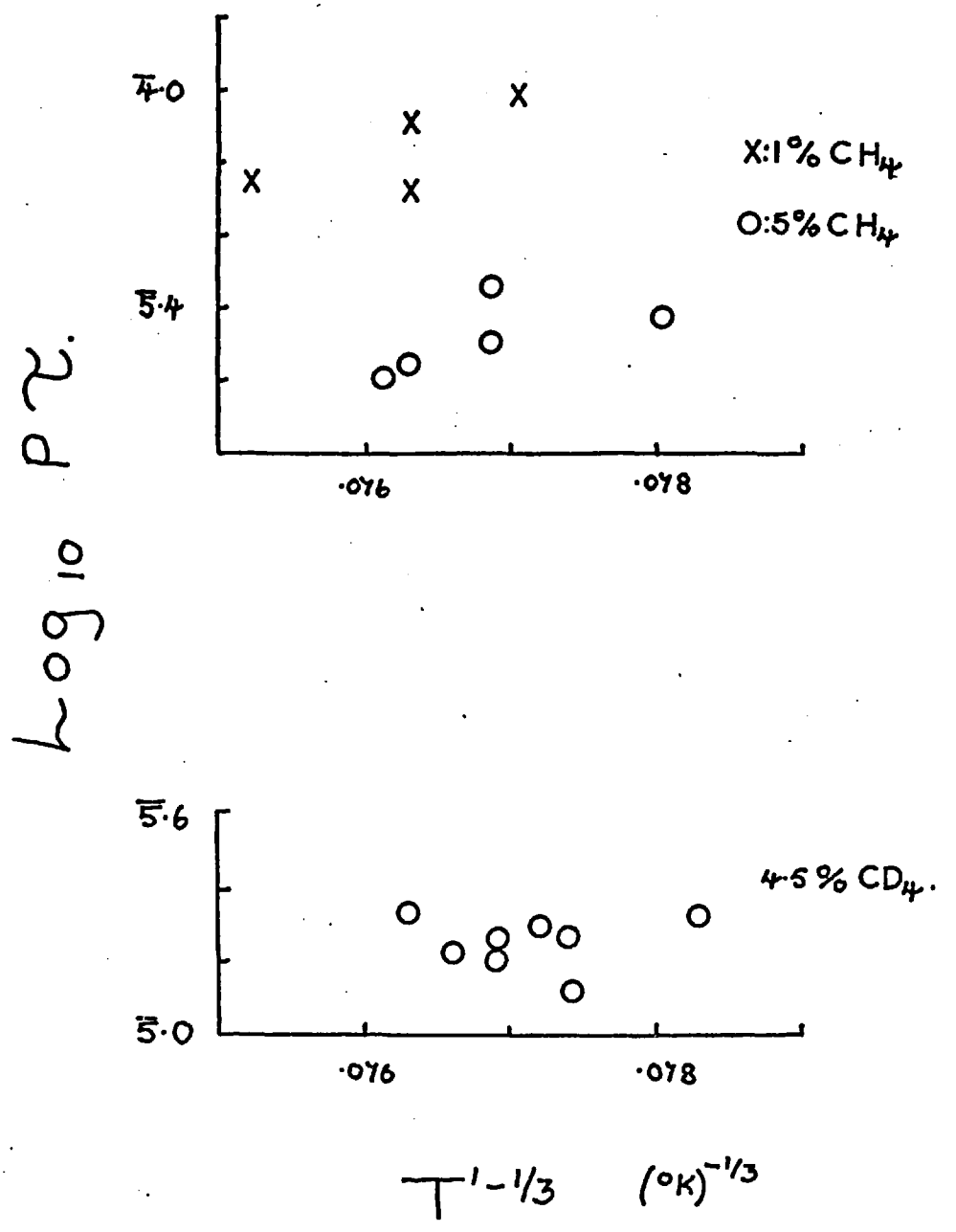

except in the presence of polar gases. The total random error for any individual relaxation time on the interpolation plot was about $\pm$ 25%. The interpolation of many relaxation times decreases the random errors by at least a factor of two.

4-11) COMPARISON TO THE RESULTS OF OTHER WORKERS.

White has been active in the field of nitrogen relaxation - collision partner effects. His results (published since the beginning of this work) were mainly obtained using shock tube interferometry. At 2500^{oK} Millikan and White (72) found $P\tau\ (N_2 - O_2) = 1{\cdot}4.\ 10^{-5}$ atm.sec. compared to the value of $1{\cdot}2.\ 10^{-5}$ atm.sec. obtained here. Both these results were obtained using eqn. (4-6) and require modification (see below). White (80) determined $P\tau\ (N_2 - H_2) = 1{\cdot}0.\ 10^{-6}$ atm.sec. at 2500^{oK} (c.f. $1{\cdot}3.\ 10^{-6}$ atm.sec.). More recently values of $P\tau\ (N_2 - CH_4) = 9.\ 10^{-7}$ atm.sec. at 2250^{oK} (c.f. $1{\cdot}0.\ 10^{-6}$ atm.sec.) and $P\tau\ (N_2 - He) = 2.\ 10^{-6}$ atm.sec. at 2500^{oK} (c.f. $4{\cdot}5.\ 10^{-6}$ atm.sec.) have been published (81).

White's result for helium is a factor of two less than the result quoted here, but the other result $P\tau\ (N_2 - CH_4)$ agrees well. White also extended his $N_2 - CH_4$ measurements to 2700^{oK}. However at this temperature it seems certain that CH_4 dissociates rapidly: both the endothermic dissociation and the effect of dissociation products on the relaxation process will effect the apparent values of $P\tau$.

Gaydon and Hurle (42) measured relaxation times in 2% H_2O/N_2 mixtures using the sodium line reversal technique. They found that the presence of 2% H_2O halved the relaxation time of pure nitrogen at 2500^{oK}. This result indicates a slightly higher efficiency for water as a collision

partner than obtained here.

4-12) DERIVATION OF THE RESULTS.

As discussed in this Chapter, section 2, under certain circumstances equation (4-6) is invalid; the more complex equation (4-12) which includes the cross coupling of vibrational energy through a (V-V) process must be used. All the results have initially been calculated using (4-6) and these suffice for a comparison to the results where this equation is definitely valid e.g. N_2 with N_2, He, Ar, Kr. Results for each molecule will then be discussed individually. Table 4-2 summarises all the relaxation times calculated using eqn. (4-6).

Table 4-2.

M.	$\underline{P}\tau$ (N_2 - M) at 2500^{oK} (eqn. 4-6) $P\tau$ (N_2 - M) atm.sec.
N_2	$1{\cdot}9.\ 10^{-4}$
SO_2	$2{\cdot}9.\ 10^{-5}$
Ar	$4{\cdot}8.\ 10^{-4}$
Kr	$9{\cdot}4.\ 10^{-4}$
He	$4{\cdot}5.\ 10^{-6}$
H_2	$1{\cdot}3.\ 10^{-6}$
D_2	$4{\cdot}1.\ 10^{-6}$
O_2	$1{\cdot}2.\ 10^{-5}$
HCl	$4{\cdot}0.\ 10^{-6}$
DCl	$4{\cdot}0.\ 10^{-6}$
H_2O	$6.\ 10^{-6}$
D_2O	$6.\ 10^{-6}$
CH_4 *	$1.0.\ 10^{-6}$
CD_4 *	$8.\ 10^{-7}$

* at 2250^{oK}

4-13) CORRELATION OF RELAXATION TIMES WITH MILLIKAN AND WHITE'S FORMULA.

The most convenient correlation for vibrational relaxation times of diatomic molecules where the relaxation is predominantly T-V is due to Millikan and White (MW). Their semi-empirical formula, Chapter 1 sect. 4, may be written:

$$\log_{10} P\tau = A\,(T^{-1/3} - \cdot 015\mu^{1/4}) - B$$

where $A = C\,\theta^{4/3}\mu^{m}$. $B = 8\cdot 0$.

and $C = 5.10^{-4}$ for $m = \frac{1}{2}$.

MW determined m experimentally by plotting log A against $\log\mu$ for various collision partners relaxing CO and O_2. The first value reported was $m = \cdot 55 \pm \cdot 05$ (24); a revised value of $m = \cdot 42$ has appeared for CO (82).

Values of A may be calculated from the results in table 4-2. MW determined A and B independently; here their value of B has been used in calculating the values of A. The plot of log A against $\log\mu$ is shown in fig. (4-13). The gases relaxing nitrogen by only a T-V process will lie on a straight line whose gradient will define m. The collision partners whose relaxation times with nitrogen include other processes (V-V, R-V etc.) will lie below this line.

From fig. (4-13) it may be seen that the points describing H_2, D_2, He, N_2, Ar and Kr are collinear. The slope of fig. (4-13) gives the value of $m = \cdot 46 \pm \cdot 01$. Since this shows that N_2, H_2, D_2 all behave as a monatomic gas in the relaxation of nitrogen then

$$P\tau\,(N_2 - N_2)_T \ll P\tau\,(N_2 - N_2)_R$$

$$P\tau\,(N_2 - D_2)_T \ll P\tau\,(N_2 - D_2)_{V\,\&\,R}$$

$$P\tau\,(N_2 - H_2)_T \ll P\tau\,(N_2 - H_2)_{V\,\&\,R}$$

FIG. 4-13

MILLIKAN & WHITE CORRELATION FOR N_2-M VIBRATIONAL RELAXATION.

2500°K

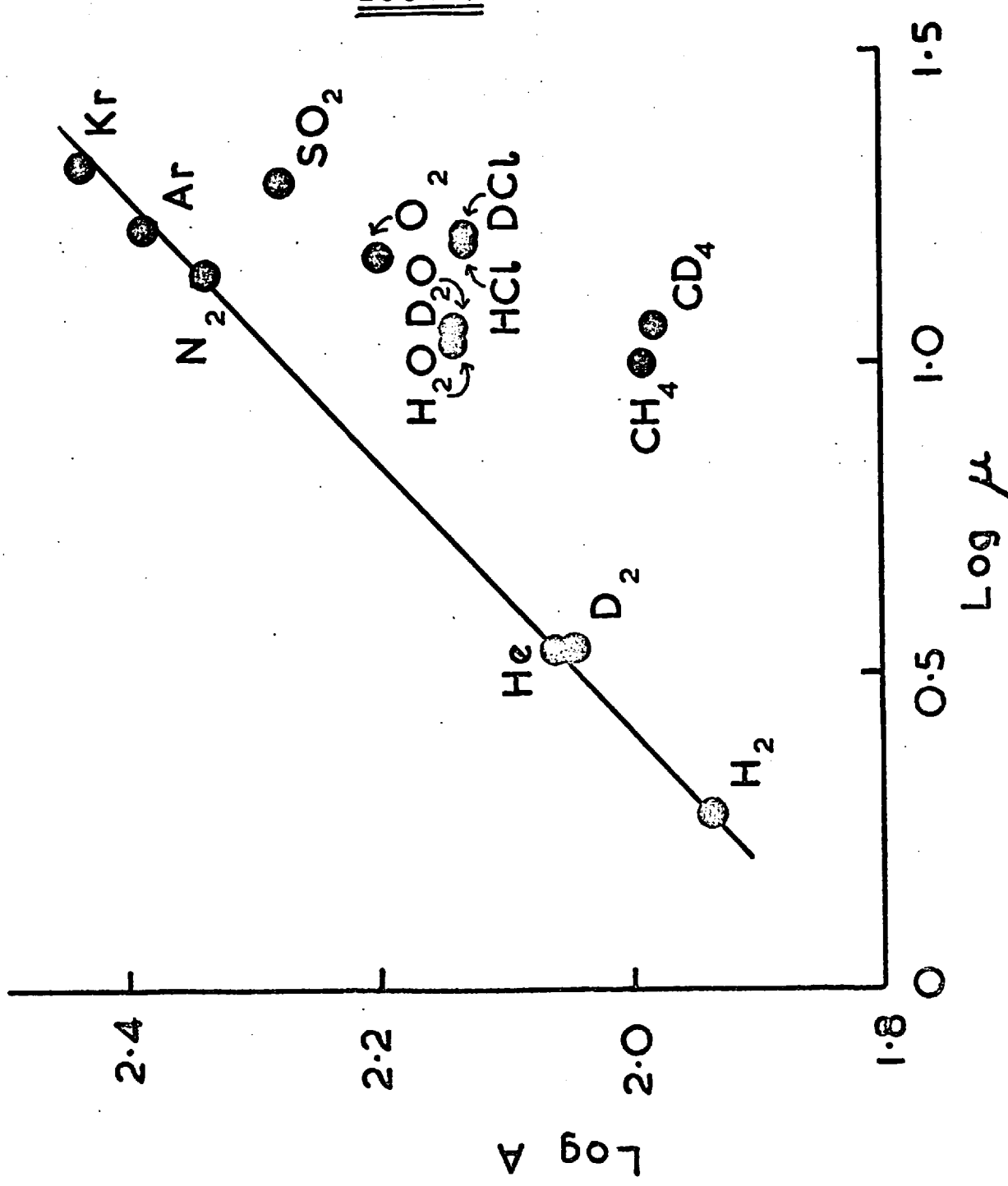

These results are in agreement with the collision partner effects described by MW for CO and O_2 with one minor exception.

White (83) has measured relaxation times in D_2/CO mixtures using both I.R. emission and shock interferometry. From 940 - 1600^{oK} the I.R. emission measurements produced relaxation times in accord with the MW formula i.e. $P\tau\ (CO - D_2) \simeq P\tau\ (CO - He)$ as $\mu(CO - D_2) = \mu(CO - He)$. From 1600 - 2800^{oK} interferometry was used as the method of measurement. In these results the temperature dependence of the relaxation times increased. White interpreted this in terms of a V-V process between the D_2 and CO. There does, however, seem to be a discrepancy between the two methods of measurement and possibly the explanation lies here, not in a V-V process.

Cary (84) measured $P\tau\ (N_2 - Ar)$, $P\tau\ (N_2 - Ne)$ at temperatures in excess of 3500^{oK}. Both relaxation times conformed with the MW formula at these temperatures.

4-14) COMPARISON OF RELAXATION TIMES TO T-V THEORY.

The collision partners exhibiting only T-V energy transfer may be further compared to theory. The theoretical expression developed by SSH (Chapter 1 sect.2) has been successful in predicting relaxation times of many molecules. Boade (85) has pointed out that the theory can be used to predict the variation of the relaxation time of molecule A by collision partner B with the nature of B:

$$\tau\ (A\text{-}B) \cdot (r_c^{AB})^2 \cdot \mu^{5/3} \cdot (S_{AB})^{7/3} \cdot \exp\left(\frac{\varepsilon_{AB}}{k\,T}\right) = K_A \exp 1{\cdot}5 \left(\frac{f_A}{T}\right)^{1/3} \cdot \mu^{1/3} \cdot (S_{AB})^{2/3} \qquad (4\text{-}14)$$

Here r_c^{AB} is the minimum separation of two molecules approaching one another with the relative velocity most likely to result in energy transfer.

s_{AB} is the interaction range of the repulsive potential, ε_{AB} is the intermolecular potential well depth. K_A only depends on the nature of A and $f_A = 16\,\pi^4 \cdot (\nu^A_m)^2 / R$ where ν^A_m is the vibrational frequency of A.

Using the Lennard-Jones potential parameter r_0^{AB} for r_c^{AB}, a plot of:

$\log_{10} (\tau (A\text{-}B)(r_0^{AB})^2 \cdot \mu^{5/3} (s_{AB})^{7/3} \cdot \exp(\varepsilon_{AB}/kT))$ against $\mu^{1/3}(s_{AB})^{2/3}$

should be linear, with slope $1{\cdot}5 \left\{\frac{f_A}{T}\right\}^{1/3}$

In fig. (4-14) the results for N_2 from table 4-2 and the results for CO and O_2 obtained by MW (24, 82, 86) are shown. The necessary parameters were taken from Hirshfelder, Curtiss and Bird (87). Within experimental scatter the points lie on reasonable straight lines. The best test of eqn. (4-14) is the value of the slopes from fig. (4-14) compared to the theoretical value, $1{\cdot}5 \cdot \left(\frac{f_A}{T}\right)^{1/3}$ [Table 4-3] .

Table 4-3.

Comparison of results to theory, Boade's eqn.

	N_2	CO	O_2
expt. :	$2{\cdot}0.\ 10^6$	$1{\cdot}7.\ 10^6$	$1{\cdot}7.\ 10^6$
theor. :	$2{\cdot}3.\ 10^6$	$2{\cdot}1.\ 10^6$	$2{\cdot}3.\ 10^6$

For N_2, CO and probably also for O_2 the agreement is within the combined uncertainty of experiment and of the parameters used for the correlation.

The variation of $P\tau$ with temperature as predicted by SSH theory can also be tested. By including the temperature dependent terms in K_A, the ratio of the relaxation times $P\tau_1$, $P\tau_2$ at temperatures T_1, T_2 is given by :

FIG. 4-14

BOADE CORRELATION FOR N_2 CO, O_2 WITH VARIOUS COLLISION PARTNERS.

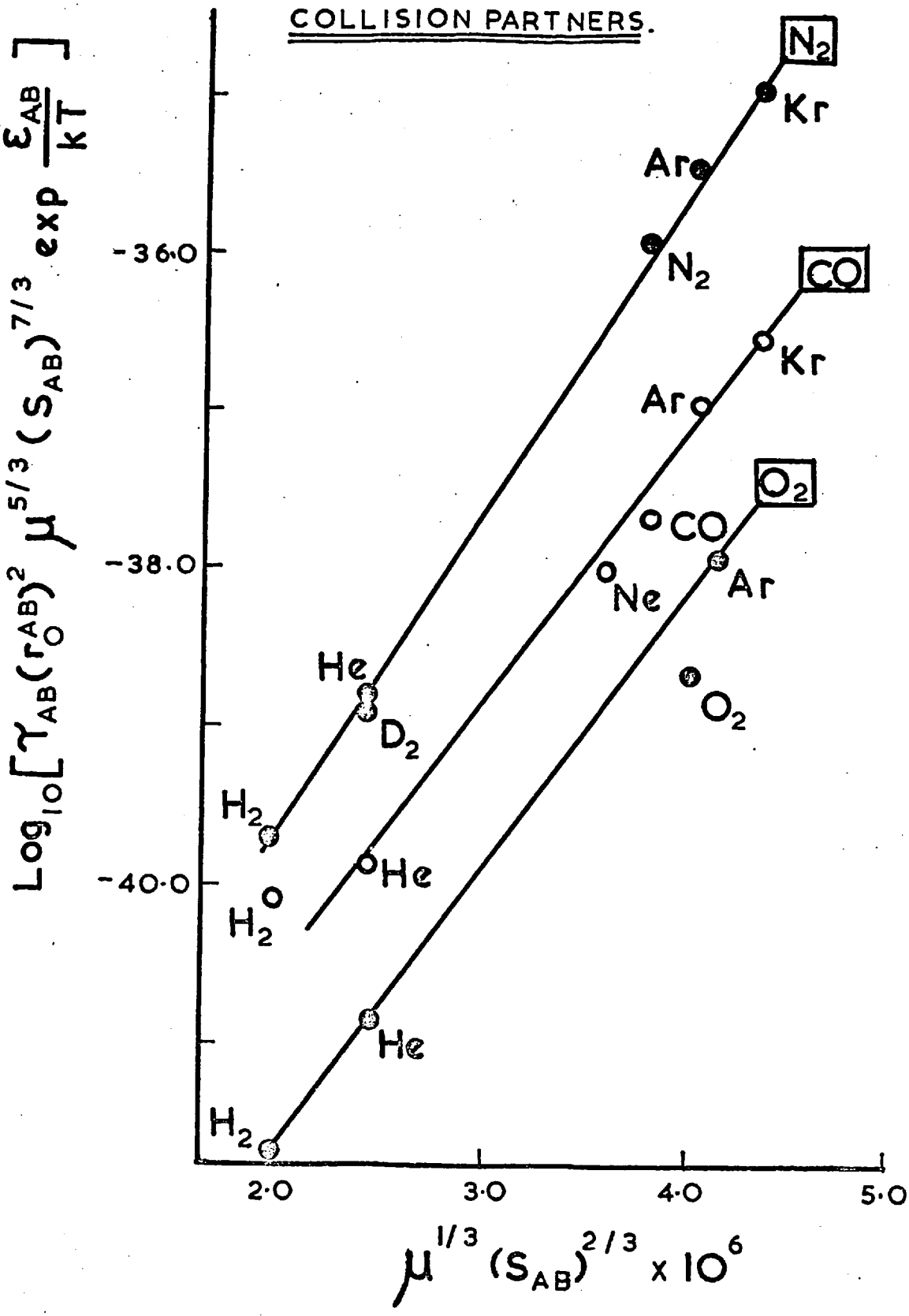

$$\log(P\tau_1/P\tau_2) = K_1 (T_1^{-1/3} - T_2^{-1/3}) - K_2(T_1^{-1} - T_2^{-1}) + \log(T_1/T_2)^{1/6} \quad (4\text{-}15)$$

where

$$K_1 = \cdot 6514 \cdot f_A^{1/3} \cdot \mu^{1/3} \cdot s_{AB}^{2/3} \quad (4\text{-}16)$$

$$K_2 = (\cdot 4343/k)\,(h\nu_m^A/2 + \varepsilon_{AB})$$

First the ratio of the values of $P\tau$ at 1950°K and 3650°K are compared (1) from the experimental values found by MW and (2) predicted by equation (4-15). The term in K_1 is dominant in the r.h.s. of (4-15). The values of K_1 can be compared (1) by substituting the experimental values at the two temperatures into (4-15) and (2) from (4-16). This is a more useful comparison for different molecules. The results for pure N_2, CO, O_2 and for O_2 dilute in Ar are given in table 4-4.

Table 4-4.

Temperature dependence of relaxation times: theory and experiment.

	$P\tau$, 1950°K / $P\tau$, 3650°K		Value of K_1	
	(1) expt.	(2) theor.	(1) expt.	(2) theor.
N_2	27	30	111	114
CO	15	33	93	115
O_2	6·6	15	66	90
O_2 - Ar	11	17	81	93

For pure N_2, SSH theory gives a good description of the experimental temperature dependence. For CO and O_2 in Ar, the agreement is less good. The value of K_1 is, of course, sensitive to the values of s_{AB}, r_0^{AB} etc. selected for the comparison.

The agreement for O_2 is worse still and it seems that $O_2 - O_2$ collisions are abnormally effective. The MW semi-empirical formula also

predicts too low a probability for $O_2 - O_2$ collisions if the $O_2 - Ar$ prediction is assumed to be correct (24). Nikitin (88) has suggested that the relaxation rate is increased by rotational energy transfer. Kiefer and Lutz (35) have shown that the relaxation of O_2 by O atoms is accelerated by chemical interaction. Perhaps this is a possible explanation for the $O_2 - O_2$ case. Further work will be required before this problem can be fully resolved.

4-15) COMPARISON OF RELAXATION TIMES TO (V-V) THEORY.

The collision partners O_2, SO_2, H_2O/D_2O, HCl/DCl, CH_4 and CD_4 all lie below the line in fig. (4-13) given by the MW empirical formula. Processes other than T-V transfer must be included to describe the transfer of vibrational energy from these molecules to the nitrogen. All these gases have their own vibrational and rotational modes and an obvious explanation is that V-V or R-V energy transfer enhances the observed rate of vibrational relaxation.

Fig. (4-13) may be used as a basis for estimating, to a first approximation, the T-V relaxation rates for these collision partners with nitrogen. Using equation (4-12) or its shortened form (4-6) + (4-13), the rates of energy transfer between the internal modes of the collision partner with nitrogen may be obtained.

4-15-1) RELAXATION OF NITROGEN BY SULPHUR DIOXIDE.

The value of $P \tau (N_2 - SO_2)$ at 2500^{oK} confirms Levitt and Sheen's preliminary work on the efficiency of SO_2 as a collision partner. SO_2 is indeed more efficient than would be expected for a heavy molecule. The reduced mass of $SO_2 - N_2$ is 19·5 a.m.u. compared to the 14 a.m.u. for

$N_2 - N_2$ collisions. Applying the equations:

$$P_{01} = \left[Z(P\tau(N_2\text{-}SO_2))\left(1 - e^{-\frac{h\nu}{kT}}\right)\right]^{-1}$$

$$Z = n\sigma_{AB}^2 \left(\frac{8\pi kT}{\mu}\right)^{\frac{1}{2}}$$

as described in Chapter 1. (n - no. of molecules per cc. σ_{AB} = collision diameter for $N_2 - SO_2$ (81)).

$$\left.\begin{aligned} P_{01}(N_2 - N_2) &= 2{\cdot}8.\ 10^{-6} \\ P_{01}(N_2 - SO_2) &= 1{\cdot}9.\ 10^{-5} \end{aligned}\right\} \quad \text{at } 2500^{oK}$$

and hence a sulphur dioxide molecule is about seven times as efficient in transfering energy into the vibrations of a nitrogen molecule as a nitrogen molecule itself.

Chemical affinity between the colliding molecules seems most unlikely. There is no reasonable chemical explanation for affinity between sulphur dioxide or the other collision partners and nitrogen at 2500^{oK}.

At least one low moment of inertia must exist in SO_2 for its rotational modes to be coupled to the vibrational relaxation of nitrogen. This would enable the higher peripheral velocity to effect the translational impact of the SO_2 and N_2 molecules. This cannot be so; all three moments of inertia of SO_2 are relatively high. Furthermore a calculation of R-V energy transfer rates based on Bradley-Moore's theory (32) gives a probability of energy transfer two orders of magnitude lower than the observed value.

Although all three normal vibrational modes of SO_2 - 519, 1152, 1362 cms.$^{-1}$ - are well outside the close or exact resonance range w.r.t. nitrogen, a single quantum near-resonant V-V transfer is possible through the ν_3 mode of SO_2:

$$SO_2\ (0,0,n.) + N_2\ (0) \rightarrow SO_2\ (0,0,n\text{-}1.) + N_2\ (1) + \Delta E = 995\ \text{cms.}^{-1}$$

The energy gap, ΔE, for the V-V process is 995 cms.$^{-1}$ This is the excess energy which would have to be dissipated as translational energy during the vibrational quantum transfer.

A double quantum jump is also a possibility through the SO_2 (ν_1) mode. Doubling the wave number for this mode gives only 54 cms.$^{-1}$ as the energy gap ΔE.

$$SO_2 (n,0,0) + N_2 (0) \longrightarrow SO_2 (n-2, 0,0) + N_2(1) + \Delta E = 54 \text{ cms.}^{-1}$$

A single quantum resonance energy transfer of $\Delta E = 54$ cms.$^{-1}$ (= 150 cals. mole^{-1}) would be very fast. Callear (6) has shown that as expected from SSH theory, the probability of V-V energy transfer is proportional to $e^{-\Delta E/RT}$. The probability of double quantum jumps is much less (23); unfortunately SSH theory has not yet been successfully applied to multiple quantum jumps.

Modica and LaGraff (89) have postulated double quantum jumps as an explanation for the high efficiency CF_2 has in transfering vibrational energy to nitrogen. The CF_2 radical is in many respects similar to SO_2 and has vibrational frequencies of 667, 1162, 1440 cms.$^{-1}$.

Experimental and theoretical results show that the temperature dependence of a V-V process is less than the corresponding T-V process. The effect of this is to make V-V transfer more important at low temperatures. At higher temperatures the T-V processes can become as fast as, and may even exceed, the rate of the V-V processes.

Considering that V-V transfer occurs between SO_2 and N_2, the low temperature "tail off" of the relaxation times in fig. (4-5) is not surprising. It is simply due to an increased contribution from the V-V

process to the observed relaxation time. At 2500^{oK}, 10% SO_2 lowers the relaxation time of pure nitrogen by a factor of 1·5. At 1800^{oK} this factor has increased to 3·3.

The relaxation time for the V-V process may be calculated using eqn. (4-12) derived in section 2. By analysing the 10% SO_2/N_2 results at 1800^{oK} ($P\tau\ (N_2 - 10\%\ SO_2) = 3{\cdot}5.\ 10^{-4}$ atm.sec.) and the 15% SO_2/N_2 results at 2500^{oK} (Table 4-1), the temperature dependence of this V-V process may be calculated. An estimate of $P\tau\ (N_2 - SO_2)_T$ was made using Millikan and White's semi empirical formula. $P\tau\ (SO_2 - SO_2)$ was extrapolated from Lambert and Salter's (51) results at lower temperatures. Although a value for "x" in eqn. (4-12):

$$x = \frac{P\tau\ (SO_2 - SO_2)}{P\tau\ (SO_2 - N_2)}$$

was taken as ·5, it was found that the special condition (1) for eqn. (4-12) held so that it reduced to eqn. (4-13).

$P\tau\ (N_2 - SO_2)_V$ is thus independent of x.

Table 4-5 gives the results of the analysis.

Table 4-5.

Parameters for calculation of $P\ (N_2-SO_2)_V$

T	$P\tau\ (N_2-N_2)$	$P\tau\ (N_2-SO_2)_T$	$P\tau\ (SO_2-SO_2)$	x	K	$P\tau\ (N_2-SO_2)_V$
1800	$1{\cdot}3.\ 10^{-3}$	$4{\cdot}8.\ 10^{-3}$	$1{\cdot}3.\ 10^{-8}$	·5	·96	$5{\cdot}0.\ 10^{-5}$
2500	$1{\cdot}9.\ 10^{-4}$	$7{\cdot}1.\ 10^{-4}$	$1{\cdot}10^{-8}$	·5	·97	$4{\cdot}3.\ 10^{-5}$

(Relaxation times in atm.sec.)

The temperature dependence of the various relaxation processes in N_2 - SO_2 mixtures is given in fig. (4-15). The upper dashed line represents

FIG. 4-15

ESTIMATE OF THE VARIOUS RELAXATION RATES IN N_2-SO_2 MIXTURES.

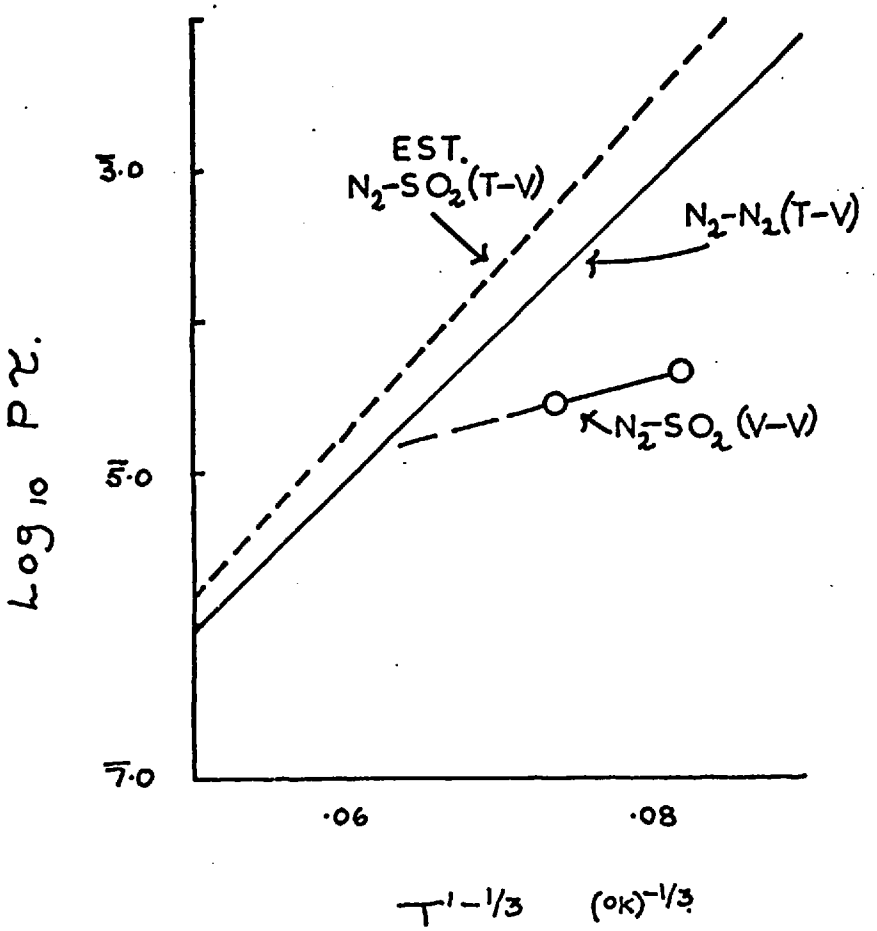

the $N_2 - SO_2$ relaxation time for the T-V process (MW). The lower line of lesser slope represents the $N_2 - SO_2$ V-V process. Obviously this slope is not well defined - the temperature range over which it was determined is only 700^{oK}. Fig. (4-15) does however represent a rough indication of the relative rates of the T-V and V-V processes.

The relaxation times for all the other collision partners have been analysed to obtain $P\tau\ (N_2 - M)_V$ using (4-12). All these V-V rates will then be correlated using current V-V theory. It is unnecessary to invoke (R-V) energy transfer processes to describe vibrational relaxation in these gas mixtures.

4-15-2) RELAXATION OF NITROGEN BY OXYGEN.

The vibrational relaxation of pure oxygen has been measured by several workers (see 86). Millikan and White (72) have discussed the possible value of $P\tau\ (O_2 - N_2)_T$; hence their value of

$$x = \frac{P\tau\ (O_2 - O_2)}{P\tau\ (O_2 - N_2)} = 1{\cdot}2 \text{ at } 2500^{oK}$$

is probably quite accurate. Eqn. (4-12) predicts $P\tau\ (N_2 - O_2)_V$ to be $1{\cdot}55.\ 10^{-5}$ atm.sec. Using $Z = 2{\cdot}3.\ 10^9$ collisions per second and

$$P\ (\overset{10}{N_2} - \underset{01}{O_2}) = \frac{1}{ZP\tau\ (N_2-O_2)_V}$$

$$P\ (\overset{10}{N_2} - \underset{01}{O_2}) = 2{\cdot}8.\ 10^{-5}$$

This result is in general agreement with the result obtained by Taylor, Camac and Feinberg (43). [Note. The probability $P\ (\overset{10}{N_2} - \underset{01}{O_2})$ quoted in ref.43 is incorrect. It should be multiplied by a factor, 2, giving $\simeq\ 9.\ 10^{-5}$]. White (105) has obtained $P(\overset{10}{N_2}-\underset{01}{O_2}) = 1{\cdot}8.10^{-5}$ at 2500^{oK}.

The effect of x on $P\tau\ (N_2 - O_2)_V$ may be examined. If x = •5 and not 1•2; substitution into (4-12) gives $P\tau\ (N_2 - O_2)_V = 2{\cdot}1.\ 10^{-5}$ atm.sec., some 25% higher than the value calculated with x = 1•2.

A previously reported value of $P\tau\ (N_2 - O_2)_V$ - Colgan and Levitt (90) - is incorrect. The justification for the use of eqn. 6. ref. (90) should read (90, p.2902):

$$P\tau\ (O_2 - O_2) \ll m_{O_2} \cdot P\tau\ (N_2 - O_2)$$

not

$$P\tau\ (O_2 - O_2) \ll P\tau\ (N_2 - O_2).$$

4-15-3) RELAXATION OF NITROGEN BY WATER/HEAVY WATER.

Relaxation of pure water is very fast. The results of Tuesday and Boudart (see 15), $O_2 - H_2O$ mixtures, give a value of $1{\cdot}42.\ 10^{-9}$ atm.sec. at room temperature. Huber and Kantrowitz (91) obtained values slightly longer than this. The value $P\tau\ (H_2O - H_2O)$ has been taken as 1.10^{-9} atm.sec. at 2500°K. The reason for the high probability of vibrational excitation during $H_2O - H_2O$ collisions - hydrogen bonding (?) - probably cannot be extended to $H_2O - N_2$ collisions, so x should be small, say •01.

Detailed analysis shows however, that as with the $N_2 - SO_2$ case, the simplified eqn. (4-13) may be used and $P\tau\ (N_2 - H_2O)_V$ is independent of x. Thence:

$$P\tau\ (N_2 - H_2O)_V = 5.\ 10^{-6} \text{ atm.sec.}$$

$$Z = 2{\cdot}2\ 10^{9} \text{ collisions sec.}^{-1}.$$

and $\left.\begin{matrix} P\ (N_2 - H_2O)_{oi}^{io} \\ P\ (N_2 - D_2O)_{oi}^{io} \end{matrix}\right\}$ 9.10^{-5} at 2500°K

4-15-4) RELAXATION OF NITROGEN WITH HYDROGEN AND DEUTERIUM CHLORIDES.

Both Borrell (92) and Ferguson and Read (29) have measured $P\tau$ (HCl-HCl). At 2500^{oK} this is about 4.10^{-6} atm.sec. This value is at least an order of magnitude shorter than relaxation times predicted by SSH theory for a T-V process. Both sets of workers consider the relaxation to be enhanced by R-V transfer.

If the rate of HCl-HCl relaxation is thus enhanced by R-V processes, it seems likely that the relaxation of HCl by N_2 would have a lower collision probability than HCl by HCl. This suggests a value for x less than unity, say ·1 or ·01.

If x = ·1 then equation (4-12) gives:

$$P\tau\ (N_2 - HCl)_V = 1{\cdot}8.10^{-5} \text{ atm.sec. at } 2500^{oK}.$$

and with $Z = 2{\cdot}1.10^{9}$ collisions. $sec.^{-1}$

$$P\ (\overset{10}{N_2} - \underset{01}{HCl}) = 3.10^{-5}.$$

If x = ·01 then

$$P\tau\ (N_2 - HCl)_V = 4.10^{-6} \text{ atm.sec.}$$

$$P\ (\overset{10}{N_2} - \underset{01}{HCl}) = 1{\cdot}3.10^{-4}.$$

Unfortunately not enough experimental evidence exists enabling us to select the value of x that exactly defines $P(\overset{10}{N_2} - \underset{01}{HCl})$. It will be shown however that the result using x = ·01 is in better agreement with the (V-V) results of other collision partners than that with x = ·1. This observation (making nitrogen a very inefficient collision partner for HCl relaxation) supports the conclusion that HCl relaxation is enhanced by R-V transfer. On T-V theory, since $\mu(N_2\text{-HCl}) < \mu$ (HCl-HCl), x would be about 1·5.

The uncertainty in the parameters precludes any conclusion being drawn on the possibility of (R-V) transfer enhancing the N_2-HCl relaxation.

4-15-5) RELAXATION OF NITROGEN WITH METHANE.

Parker and Swope (93) have measured the relaxation of CH_4 by N_2, Ar, Ne, Kr at room temperature. The rare gases were about $^1/_{10}$th as effective as the parent molecule as collision partners; surprisingly N_2 was still less effective ($\simeq ^1/_{20}$). Richards and Sigafoos (94) measured CH_4 and CH_4-Ar relaxation times up to 1600^{oK} using shock tube U/V absorption spectroscopy. Extrapolation of their results to 2250^{oK} gives $P\tau(CH_4 - CH_4)$ as $5.\ 10^{-9}$ atm.sec. and $x = \cdot 15$ for argon. $x\ (N_2)$ has therefore been taken as $\cdot 1$ at this temperature. Equation (4-12) again reduces to the simpler (4-13) under these conditions and $P\tau\ (N_2 - CH_4)_V$ is independent of x.

$$P\tau\ (N_2 - CH_4)_V = 1\cdot 0.\ 10^{-6} \text{ atm.sec.}$$

$$Z = 3\cdot 0.\ 10^{9} \text{ collisions sec.}^{-1}$$

and $$P\ (N_2 - CH_4)_{o1}^{10} = 3.\ 10^{-4} \text{ at } 2250^{oK}$$

4-15-6) RELAXATION OF NITROGEN WITH TETRADEUTERO METHANE.

At room temperature $P\tau\ (CD_4 - CD_4) = 4\ P\tau\ (CH_4 - CH_4)$ (4) ; using this figure at 2250^{oK} with the methane data, $x = \cdot 1$,

$$P\tau\ (N_2 - CD_4)_V = 8\cdot 2.\ 10^{-7} \text{ atm.sec.}$$

and $$P\ (N_2 - CD_4)_{o1}^{10} = 4.\ 10^{-4}$$

The value of $P\tau\ (CD_4 - CD_4)$ is too high to allow eqn. (4-12) to be simplified to (4-13). The value of $P\tau\ (N_2 - CD_4)_V$ is hence dependent on x. However when $x = \cdot 5$, $P\tau\ (N_2 - CD_4)_V = 9\cdot 4.\ 10^{-7}$ atm.sec and $x = \cdot 01$, $P\tau\ (N_2 - CD_4)_V = 6\cdot 4.\ 10^{-7}$ atm. sec. The value of $P\tau\ (N_2 - CD_4)_V$ is thus not very sensitive to the value chosen for x.

4-15-7) COMPARISON OF THE CALCULATIONS TO (V-V) THEORY.

Formal calculations of V-V energy transfer probabilities are complex. SSH theory has been modified by Tanczos (22) and Stretton (23) and may be applied to nitrogen-polyatom collisions. To obtain an estimate of the observed relaxation time, the calculation must be performed for each vibrational mode of the polyatom. Close multiple quantum jumps must also be considered. For example, in N_2 - CH_4 collisions the following modes must be taken into account:

Mode	degeneracy	ν cms.$^{-1}$	Δ E cms.$^{-1}$
ν_1	1	2916	+ 558
ν_2	2	1535	- 824
ν_3	3	3019	+ 661
ν_4	3	1306	+ 254 (double jump)

Unless the calculation shows one mode to predominate, the observed relaxation time is related to the sum of the probabilities for these four processes. These lengthy calculations require the assistance of a complicated computer program, not only for the probability determination but also for the initial calculation of the interaction parameters such as the characteristic length L.

A rough estimate of V-V relaxation rates may be obtained from Rapp's (26, 27) theory of vibrational energy transfer. This theory is less sophisticated than SSH theory and in consequence is less useful in making detailed comparisons of V-V processes. The theory states that the probability, $P_{10 \rightarrow 01}$, for the process

$$A\ (\nu = 1) + B(\nu = 0) \rightarrow A\ (\nu = 0) + B\ (\nu = 1)$$

may be written

$$P_{10 \rightarrow 01} \simeq 3{\cdot}7.\ 10^{-6}\ T.\ \mathrm{sech}^2 \left(\frac{{\cdot}174 \Delta E}{T^{\frac{1}{2}}} \right)$$

This equation is supposed to hold for simple diatomic molecules - N_2, CO, O_2, NO etc. At 2500^{oK}, $P_{10 \rightarrow 01}$ may be expressed as a function of Δ E. (Fig. (4-16)). Also plotted are the (V-V) probabilities obtained in this thesis as well as data on N_2 - CO_2, CO - NO and N_2 - NO taken from ref.(43). The CH_4/CD_4 results have not been corrected from2250^{oK} to 2500^{oK}; if corrected they would lie slightly higher on the graph.

Millikan and White (95) have shown that N_2/CO mixtures are always in vibrational equilibrium at high temperatures. They considered that the V-V process responsible for this phenomenon had a very high probability. The accuracy of their results is not sufficient to permit an exact calculation of $P\left(\overset{10}{N_2} - \underset{01}{CO}\right)$, but it must be about 10^{-2} at 2500^{oK}, in line with fig.(4-16).

White (96) measured relaxation times in O_2 - CH_4, C_2H_4, C_2H_2 mixtures. At 1000^{oK} estimates of $P\left(\overset{10}{O_2} - \underset{01}{C_xH_y}\right)$ may be obtained. Using eqn. (4-12) for O_2 - CH_4 gives $P\left(\overset{10}{O_2} - \underset{01}{CH_4}\right) \simeq 6.\ 10^{-3}$. As expected this is slightly lower than the points at 2500^{oK} on fig. (4-16). Estimates for the ethylene and acetylene mixtures are more difficult; not enough data exists for the calculation of the relevant variables in eqn. (4-12). A simple analysis may be performed by assuming the relaxation of the hydrocarbons to be complete during the relaxation of the oxygen in the mixture i.e.

$$P\,\tau\,(C_xH_y - C_xH_y) \ll P\,\tau\,(O_2 - C_xH_y)_V$$

When calculated under these conditions,

$$P\left(\overset{10}{O_2} - \underset{01}{CH_4}\right) \simeq P\left(\overset{10}{O_2} - \underset{01}{C_2H_4}\right) \simeq 2{\cdot}5\ P\left(\overset{10}{O_2} - \underset{01}{C_2H_2}\right).$$

As $\Delta E\,(O_2 - CH_4) = 46\ \mathrm{cms.}^{-1}$, $\Delta E\,(O_2 - C_2H_4) = 43\ \mathrm{cms.}^{-1}$

FIG. 4-16

(V-V) PROBABILITIES AT 2500°K

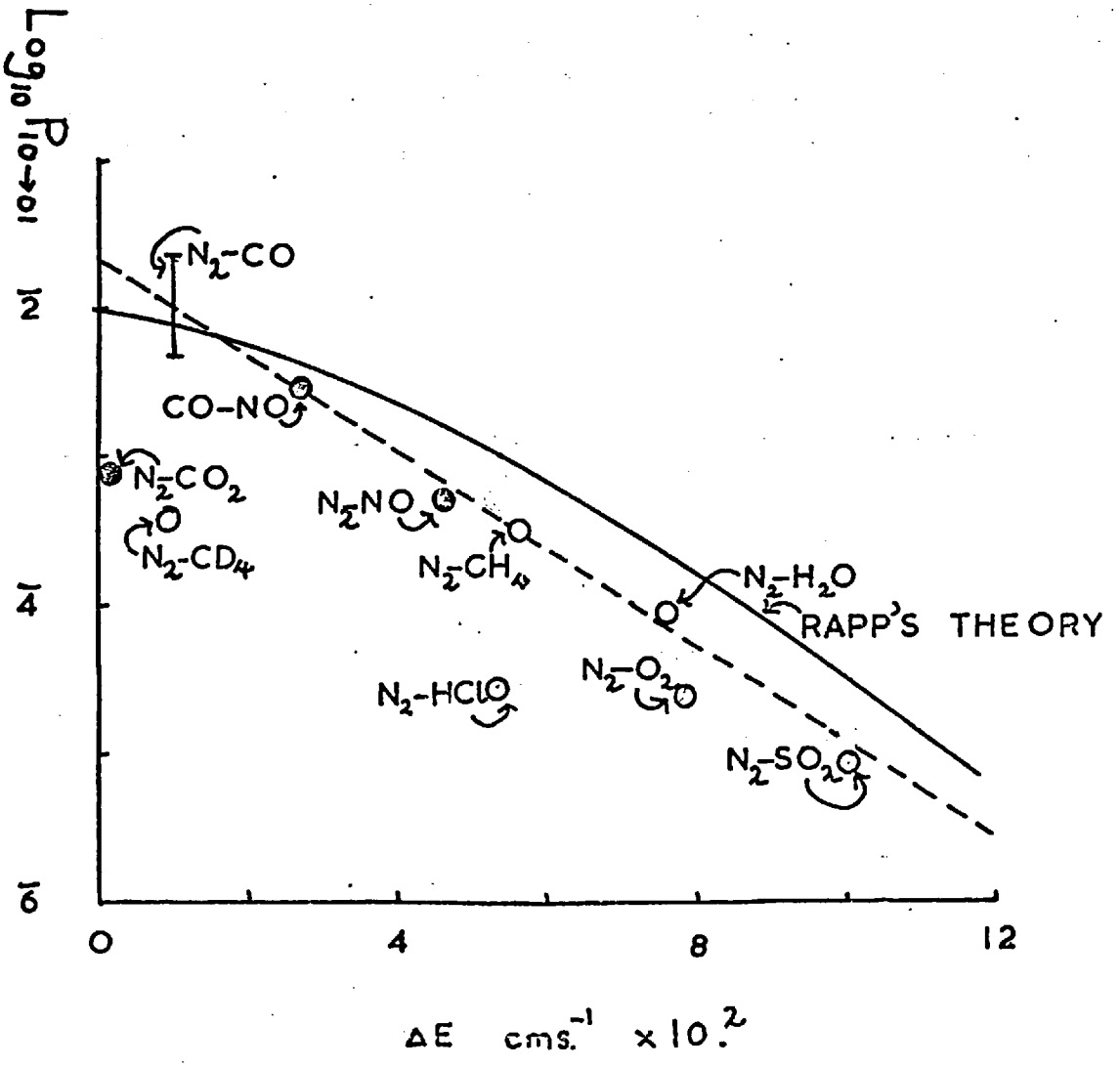

● FROM REF. (43)

O THIS WORK

I REF. (95)

and $\Delta E\ (O_2 - C_2H_2) = 393$ cms.$^{-1}$

these results are in accord with fig. (4-16).

Fig. (4-16) shows that Rapp's theory gives a reasonable account of the variation of $\log P_{10 \rightarrow 01}$ with the ΔE found experimentally. The theory does not describe the points of closest resonance ($N_2 - CO_2$, $N_2 - CD_4$) and the exact magnitudes of the other observed probabilities are roughly a factor of two too low.

On a steric basis one would expect the polyatomic partners to have higher probabilities than the diatomics. This is indeed observed for H_2O and CH_4, but the difference is only of the order of the scatter in the plot. As the temperature is increased, so the steric differences between these collision partners should become less marked.

To a first approximation the $N_2 - SO_2$ point lies on an extrapolation of the line from the other collision partners. This suggests that the single quantum transfer with $\Delta E = 997$ cms.$^{-1}$ is responsible for the V-V process. Any contribution from the double quantum jump must therefore be much smaller than from the single jump.

Both the CO_2 and CD_4 collision partners lie well below the line describing the other results. SSH theory breaks down at closest resonance. Mahan (97) has shown that the V-V probability of I.R. active molecules is enhanced at exact resonance by dipole-dipole interactions. Sharma and Brau (98) have pointed out that the long range attractive forces between the CO_2 dipole and the N_2 quadrupole accelerate vibrational energy transfer. Indeed these forces predict a negative temperature dependance for the vibrational transfer probability below 1000^{oK} and this has been observed

experimentally (98, 99).

This theory cannot account for the $N_2 - CD_4$ case since CD_4 has no dipole moment. Jones, Lambert and Stretton (100) carried out SSH calculations on $CO - CH_4/CD_4$ collision probabilities at room temperature. An extrapolation of their calculations to higher temperatures indicates that the $CO - CD_4$ collisions should be much more efficient than $CO - CH_4$ collisions in transfering vibrational energy. The $N_2 - CD_4$ case remains unexplained.

Both Callear, Williams (34) and Yardley, Bradley-Moore (101) have analysed vibrational relaxation times at room temperature with a plot similar to fig. (4-16). The latter workers consider the plot of $\log P_{10 \rightarrow 01}$ against ΔE to be markedly curved at low values of ΔE rather than linear. This is based on the low temperature result for $N_2 - CO_2$ ($\Delta E = 16$ cms.$^{-1}$); however an explanation for this in terms of dipole-quadrupole interactions has been discussed above.

Fig. (4-17) shows both the high (2500^{oK}) and low (300^{oK}) temperature results. Also included are calculations from both SSH and Rapp theories. The theories, though reasonable, do not predict the exact magnitudes of these V-V probabilities. The linearity of the points on fig. (4-17) when $\Delta E > 200$ cms.$^{-1}$ and their apparent convergence at $\Delta E = 0$, $\log P_{10 \rightarrow 01} \simeq 2.3$, suggests a possible method for calculating these probabilities empirically.

Consider fig. (4-17) as :

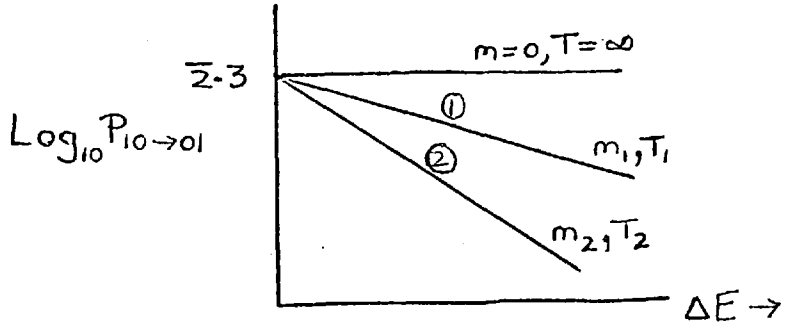

FIG. 4-17

COMPARISON OF (V-V) PROBABILITIES: 2500°K & 300°K

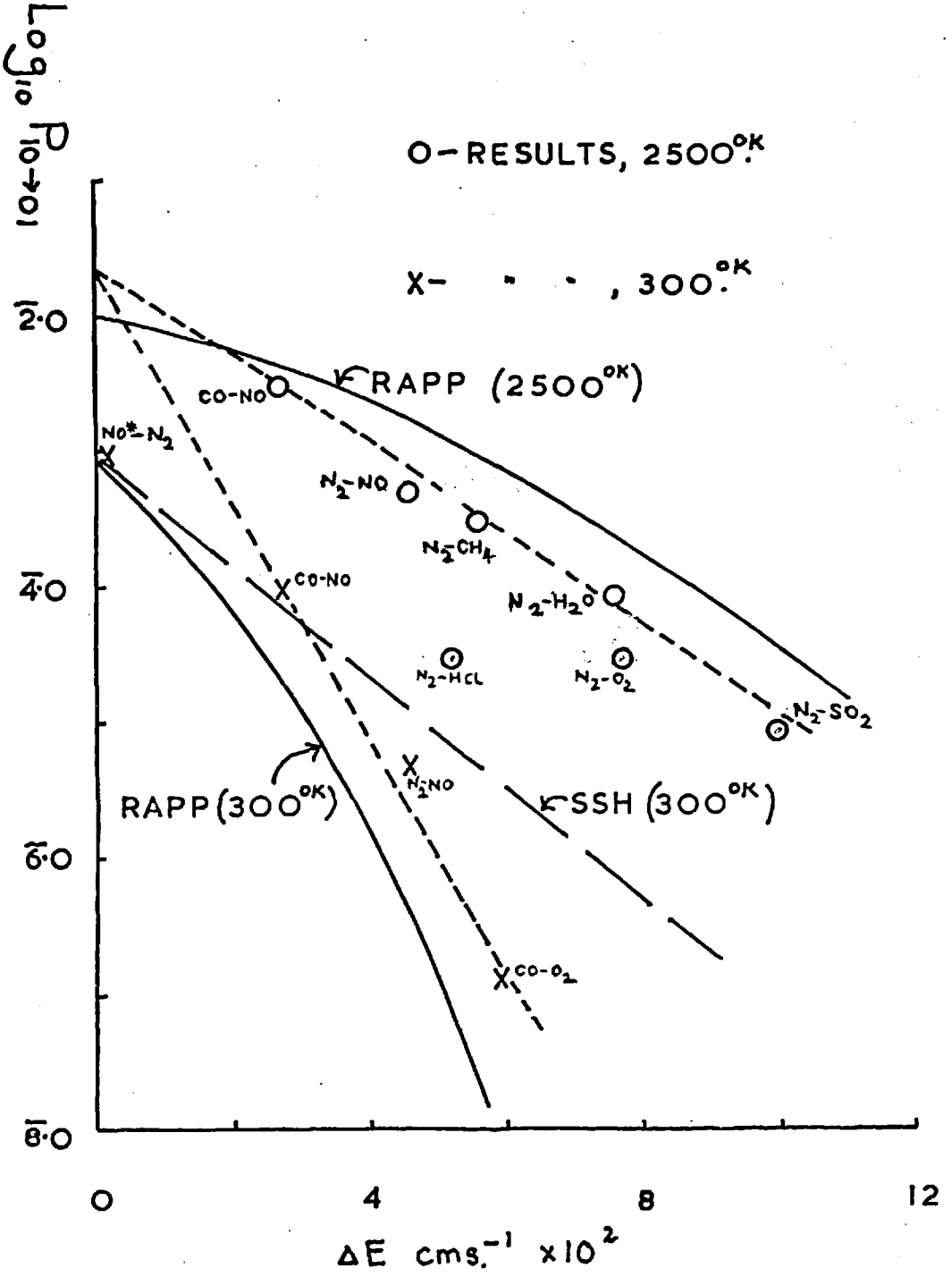

Let $\log P_{10\rightarrow 01} = \log P_0 + m.\Delta E$

where $\log P_0 = \bar{2}\cdot 3 = -1\cdot 7$

and let m_1 and m_2 the gradient of lines 1 and 2 be of the form

$$m = \frac{k}{T^x} + c$$

where k, x and c are constants to be determined from m = o, $T = \infty$ and from Fig. (4-17).

Under these conditions

$$-\log_{10} P_{10\rightarrow 01} \simeq 0.10 \left(\frac{\Delta E}{T^{1/2.3}} \right) + 1\cdot 7 \qquad (4\text{-}17)$$

Equation (4-17) must only be considered as approximate. It does not include any mass terms and it has been derived from the minimum of data. The equation correctly predicts the (V-V) probabilities at 300^{oK} and 2500^{oK} but for the $P\ (^{10}_{01}N_2 - SO_2)$ result of section 15-1 at 1800^{oK} it is a factor of two too low.

The probabilities derived from eqn. (4-12) depend on the knowledge of several factors. The possibility of the incorrect selection of "x" has been discussed for each case; however the literature values for $P\,\tau\,(M\text{-}M)$ have been accepted as accurate. Should these values be incorrect, the conclusions drawn in each case could be invalid. This is especially true of the conclusions for the N_2 - HCl case. Should further evidence show that Borrell's (92) $P\,\tau\,(HCl\text{-}HCl)$ result to be invalid, the conclusions of section 4-15-4 will need re-examination.

4-16) CONCLUSION.

It seems unlikely that rotational effects are important in the

relaxation of N_2 - HCl, CH_4 or H_2O mixtures since, within experimental error, all the results can be correlated by V-V energy transfer theory.

The theories accounting for the influence of rotation on vibrational relaxation are inadequate. Cottrell et al. (31) and Bradley-Moore's (32) theories have only a mixed success. Nikitin's (33) analysis of HI - HI collisions is probably unique to that type of molecule - the hydrogen halides are the special case of a diatomic molecule with almost all the mass centred on one atom.

Further practical and theoretical work will be required to resolve the relative contributions of rotation and vibration on the vibrational relaxation of gases. To a certain extent the emission tracer technique is unsatisfactory in such a practical role. To obtain further information, the temperature dependences of these processes must be determined. To eliminate errors in isotopic exchange, relaxation measurements should be made using higher concentrations of the collision partner.

Much attention has been focused on the laser schlieren technique (39, 40, 41) for relaxation time measurement. This technique would be ideal for the purpose discussed above : the following Chapter describes work carried out in the construction and performance of such a system.

CHAPTER 5.

THE LASER SCHLIEREN TECHNIQUE FOR MONITORING VIBRATIONAL RELAXATION.

5-1) INTRODUCTION.

Schlieren systems have for many years played an important part in the measurement of density gradients in gases. The schlieren technique is in principle simple, but the interpretation of quantitative measurements is often complex.

A parallel beam of light passes through a gas sample and is focused onto a knife edge. Any density, and hence refractive index, gradient deflects the beam of light off the edge.

The deflection may be detected electronically using a photocell or photomultiplier.

Schlieren systems represent one of the most important methods of mapping density gradients in flames (102). Flames may be run for a comparatively long period of time. The optical system can often be adjusted manually during the duration of the experiment. In shock tubes any density change e.g. due to vibrational relaxation often takes place rapidly within microseconds. The need for high intensity parallel beams of light giving measurable electronic signals has hampered the development of schlieren measurements behind shock waves.

Two types of schlieren technique have been developed for quantitative shock tube density measurements. The broad beam technique (103), as it implies, employs a wide field of light of constant intensity. The wide beam passes normally through the shock tube windows and is focused onto the knife

edge. The electrical pulse obtained from the photomultiplier is illustrated in fig. (5-1)(a). The voltage increases rapidly as the shock front enters the light beam, remains virtually constant whilst the front traverses the beam and finally decreases (often exponentially) to its equilibrium value.

Measurements of the density gradient behind the shock front are obtained from this final stage of schlieren disturbance. The deflection is a function of the average density gradient between the two edges of the beam. As one edge is in the region of equilibrium flow, the other edge - which is in the density relaxation region - will govern the magnitude of the beam displacement.

The second schlieren technique uses a laser beam as the light source. This is sufficiently narrow compared to the relaxation zone to approximate to a point source. The technique has been developed and fully discussed by Kiefer and Lutz (KL) (35, 39, 40, 41, 65). It enables one to measure density changes taking place in a few microseconds; it is roughly a factor of four more sensitive than the broad beam technique and its optical components need not be of such a critical quality.

A continuous gas laser beam passes through the shock tube onto the knife edge and photomultiplier. The deflection due to the shock front may be observed in addition to the density relaxation behind the front. A typical narrow beam schlieren pulse is illustrated in fig. (5-1) (b).

Vibrational relaxation times obtained by monitoring the density change using laser schlieren are very accurate. This chapter describes work performed on the construction and use of such a system.

FIG. 5-1

(a) BROAD BEAM SCHLIEREN PULSE

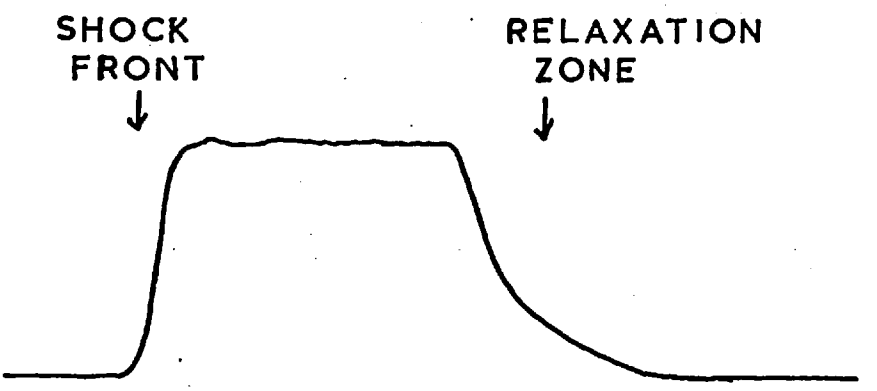

(b) NARROW BEAM SCHLIEREN PULSE

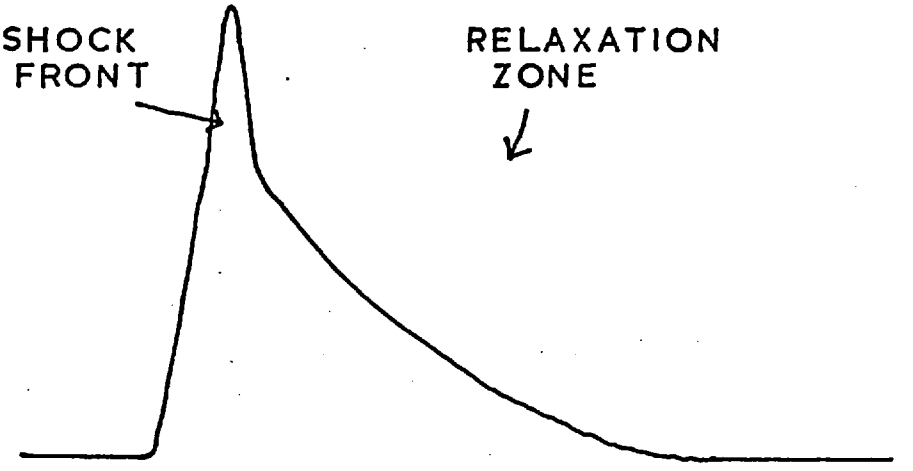

5-2) EXPERIMENTAL;

The system followed the design of Kiefer and Lutz. A narrow beam of light from a He-Ne continuous gas laser (6328Å) passed normally through the shock tube windows at observation station B. The beam was displaced slightly in the vertical plane to avoid multiple reflections off the shock tube windows. After traversing about 7 metres, the beam diverged to a spot 2" in diameter at the razor blade knife edge. The light spot was arranged so that half the light fell onto an E.M.I. 9558Q photomultiplier. The deflection due to the shock front produced a decrease in light intensity on the photomultiplier.

Initially the system was set up using an Optics Technology Inc. model 160 G. ($\frac{1}{2}$ mw.) laser. It was found that the light borne noise on the photomultiplier swamped any schlieren signal due to relaxation. Attempts to current stabilize the laser power supply did not prove successful. As emission timing signals could not be used at lower temperatures, this laser was employed in a schlieren timing apparatus.

The timing apparatus is illustrated in fig. (5-2). As the divergence of this laser beam ($> 10^{-3}$ rad.) gave an approximately 3mm. beam width in the shock tube, the width was restricted with 1mm. vertical slits. These slits were secured to the optical bench independent of the shock tube. The narrow slits of laser light passed through the shock tube exactly 1 metre apart and fell onto the knife edge/photomultipliers previously used for the light emission timing apparatus. The photomultiplier H.T. voltage was adjusted to a value near 400 volts, chosen so that statistical noise fluctuations in the laser beam were just insufficient to trigger the Racal

FIG. 5-2

LASER SCHLIEREN "TIMING" APPARATUS

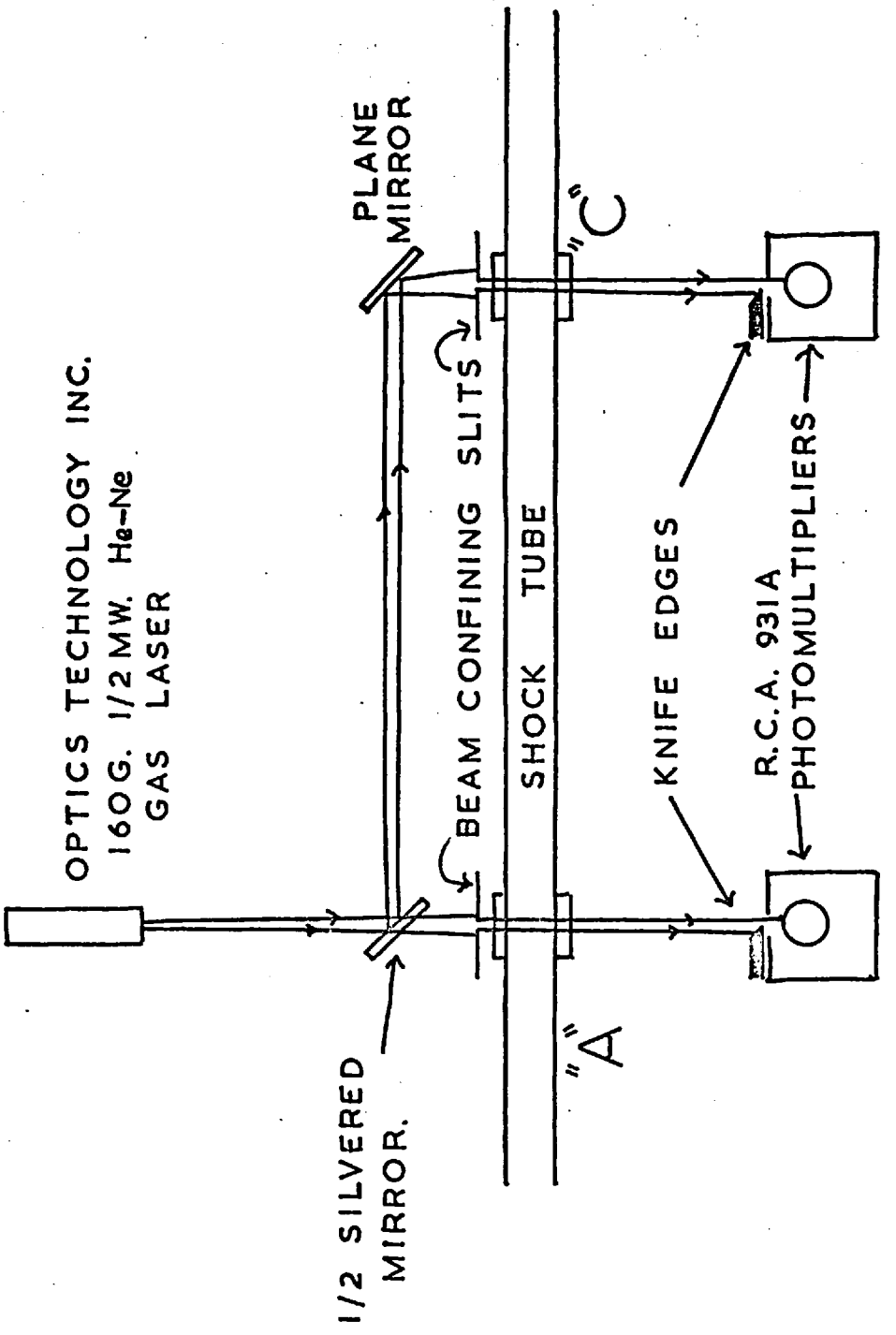

timer. Signal equalisation on start and stop channels was even more critical than with the emission technique (see Chapter 2).

5-3) ANALYSIS OF THE SCHLIEREN RECORDS. (FIG. 5-3)

The following analysis of the traces has been summarised from the derivation of Kiefer and Lutz (39). The deflection of a single ray of the beam is given by:

$$D = KLW \cdot \frac{d\rho}{dx} \qquad (5\text{-}1)$$

where

K = specific refractivity of the gas - the Gladstone-Dale constant.

L = length of the optical lever .

W = width of the shock tube.

$\frac{d\rho}{dx}$ is the density gradient at the point where the ray traverses the tube.

Provided the power distribution of the laser beam is Gaussian, then the deflection expected from the shock front may be given as

$$\frac{\Delta V}{V_0} = \text{erf}\left(\frac{D}{\sigma_K}\right)$$

where the deflection, D, is measured as ΔV - the change in voltage on the photomultiplier. V_0 is the total signal from the laser beam. σ_K is the width parameter of the Gaussian function at the knife edge.

The beam deflection due to relaxation, x, may be related to the signal obtained, V, by

$$\frac{V + \Delta V}{V_0} = \text{erf}\left[\frac{(x + D)}{\sigma_K}\right] \qquad (5\text{-}2)$$

Expanding (5-2) and ignoring the non-linear part of the expansion

FIG. 5-3

ANALYSIS OF A SCHLIEREN TRACE.

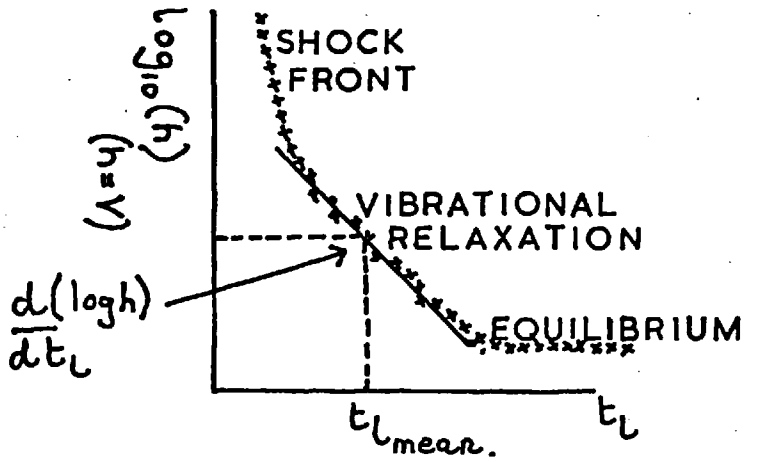

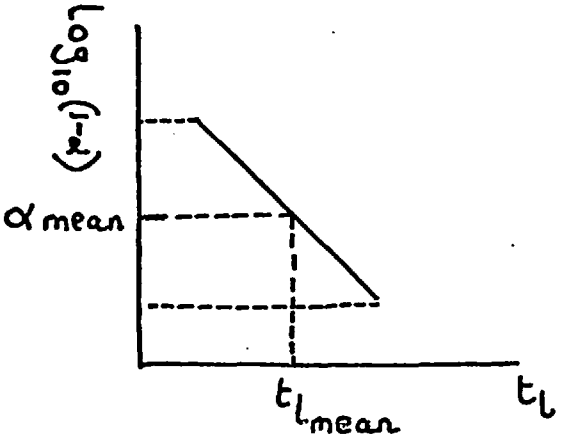

INITIALLY USE $\alpha_{mean} = \cdot 5$ WITH

$$t_{l_{mean}} = \tfrac{1}{2}(t_{l_1} + t_{l_2})$$

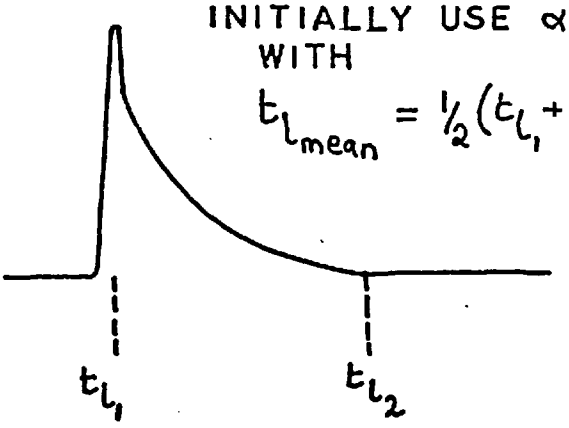

(correct to within 2% provided that $V/V_0 < 15\%$) and substituting into (5-1) leads to:

$$\frac{V}{V_0} = \frac{-KLW}{\sqrt{\pi}\,\sigma_K} \cdot \frac{d\rho}{dx}\,(0,\ t-\Delta t) \qquad (5\text{-}3)$$

where Δt is the error involved in selecting the origin of time for the density gradient change.

The density change due to vibrational relaxation is related to the relaxation time τ. Assuming an exponential density gradient in the gas:

$$\frac{d\rho}{dx}\,(x,t) = \frac{\Delta\rho}{U\tau} \exp\left[(t + x/U)/\tau\right] \qquad (5\text{-}4)$$

Combining (5-3) and (5-4) gives

$$\frac{V}{V_0} = \frac{-KLW\,(\Delta\rho)}{\sqrt{\pi}\,\sigma_K\,U\tau} \cdot e^{-t/\tau} \qquad (5\text{-}5)$$

An approximate value for the relaxation time τ_{APP}, may be obtained by plotting $\log_{10} h$, $(h = V)$, against t_1. The slope, S, of the near linear plot gives

$$\left(\tau_{APP}\right)_{\text{lab.time}} = \frac{1}{2.303|S|} \qquad (5\text{-}6)$$

KL obtained a full analysis for the variation of $P\tau_\alpha$ with α by expressing the Landau-Teller equation (1-2) in terms of the hydrodynamic shocked gas equations as well as (5-5) and (5-6).

$$P\tau_\alpha = P_\alpha \cdot \frac{\left(1 - \dfrac{d\,E^{eq}_{VIB}}{d\,E_{VIB}}\right)_\alpha}{\dfrac{d}{dt_g}\left[\ln\left(\dfrac{dE_{VIB}}{d\rho} \cdot \dfrac{h\tau}{\rho}\right)\right]_\alpha} \qquad (5\text{-}7)$$

The values $P\tau_\alpha$ were obtained from an iterative solution to (5-7) using τ_{APP} as the trial value for τ. A slightly different procedure has been adopted here. It has enabled the hydrodynamic equation computer program

previously used for the emission tracer technique (CHEMSHOCK) to be modified to intepret the laser schlieren results directly.

From eqn. (3-9)

$$\frac{d\alpha}{dt_g} = \frac{1-\alpha}{\tau} \Big/ \left(1 + \alpha \frac{d\ln\Delta H}{d\alpha}\right) \qquad (5\text{-}8)$$

where $H = H_r - H_u$.

now $h = \frac{c}{U} \cdot \frac{d\rho_2}{dt_1}$

where c is a constant for the apparatus.

$$h = \frac{c}{U} \cdot \frac{dt_g}{dt_1} \cdot \frac{d\rho_2}{d\alpha} \cdot \frac{d\alpha}{dt_g}$$

$$= \frac{c}{U} \cdot \frac{dt_g}{dt_1} \cdot \frac{d\rho_2}{d\alpha} \cdot \frac{1-\alpha}{\tau} \Big/ \left(1 + \alpha \frac{d\ln\Delta H}{d\alpha}\right) \qquad (5\text{-}9)$$

Taking the natural logarithm of both sides of (5-9) and differentiating w.r.t. α :

$$\frac{d\ln h}{d\alpha} = \frac{d\ln\left(\frac{dt_g}{dt_1}\right)}{d\alpha} + \frac{d\ln\left(\frac{d\rho_2}{d\alpha}\right)}{d\alpha} - \frac{1}{1-\alpha} - \frac{d\ln\tau}{d\alpha} - \frac{d}{d\alpha}\left(\ln\left(1 + \alpha \frac{d\ln\Delta H}{d\alpha}\right)\right) \qquad (5\text{-}10)$$

Now $$\frac{d\ln h}{dt_1} = \frac{d\ln h}{d\alpha} \cdot \frac{d\alpha}{dt_g} \cdot \frac{dt_g}{dt_1}$$

Finally substituting from (5-8) and (5-10)

$$P\tau = \frac{P \cdot (\rho_2/\rho_1)}{\left(-\frac{d\ln h}{dt_1}\right)\left(1 + \alpha \frac{d\ln\Delta H}{d\alpha}\right)} \times \left(1 + (1-\alpha)Q\right) \qquad (5\text{-}11)$$

where

$$Q = \frac{d\ln\tau}{dT} \cdot \left(\frac{T d\ln T}{d\alpha} \right) - \frac{d\ln\rho_2}{d\alpha} - \frac{\frac{d^2\rho_2}{d\alpha^2}}{\frac{d\rho_2}{d\alpha}}$$

$$+ \frac{d}{d\alpha}\left(\ln \left(1 + \alpha \frac{d\ln\Delta H)}{d\alpha}\right)\right) \qquad (5\text{-}12)$$

The approximation

$$Q \approx \frac{d\ln\tau}{dT} \cdot \left(\frac{T d\ln T}{d\alpha} \right)$$

is in fact normally good.

5-4) THE SOLUTION OF EQUATION. (5-11).

All the terms in (5-11) and Q except for $-\frac{d\ln h}{dt_1}$ and $\frac{d\ln\tau}{dT}$ are obtained from the modified CHEMSHOCK program. $\frac{d\ln h}{dt_1}$ is obtained from the slope of the semi-log plots of h against t_1. A value for $\frac{d\ln\tau}{dT}$ is obtained by including in the program data an observed relaxation time ($P_2\tau_2$) at some other temperature. (For example, in the gases examined - 10% H_2/N_2 - a relaxation time was calculated at 2500^{oK} from the emission tracer results.) The differential $\frac{d\ln\tau}{dT}$ is obtained by assuming the temperature dependence of the relaxation times to be of the form:

$$\log_{10}\left(\frac{P_1\tau_1}{P_2\tau_2} \right) = A\, T^{-1/3} \qquad (5\text{-}13)$$

The solution of (5-11) to give an exact value for $P\tau$ is obtained by substituting a trial value $\tau = 1/(d\ln h/dt_g)$ and iterating between (5-11) and (5-13) until a result constant to $\pm$ 1% is obtained. The

procedure is facilitated by writing the various differentials in polynomial form as functions of α . Solutions of (5-11) give values of $P\tau_\alpha$ as a function of the value of α at which the slope $\frac{d\ln h}{dt_g}$ was measured.

At this point the difference between KL's original analysis and ours may be noted. KL feed in as data h and t_1 values for the entire relaxation. They do not assume a linear plot of log h against t_1 and hence their program gives accurate values of $P\tau_\alpha$ corresponding to α and T_α throughout the whole relaxation region. Our results do not justify this detailed analysis; only a single mean value of $\frac{d\ln h}{dt_1}$ may be measured. This is assumed to correspond to a mean value of α , α_{MEAN}, in turn corresponding to the mean time of measurement $t_{1_{MEAN}} = \frac{1}{2}\ (t_{1_1} + t_{1_2})$ (see fig. 5-3).

The second part of the calculation is therefore the determination of α_{MEAN} by integrating the relaxation equation in the form

$$\frac{dt_1}{d\,(-\ln(1-\alpha))} = \tau_\alpha \cdot \frac{(1 + \alpha\ \frac{d\ln \Delta H}{d\alpha})}{\rho_2/\rho_1} \qquad (5\text{-}14)$$

A further iteration is required using a trial value of $\alpha_{MEAN} = \cdot 5$. The corresponding value of $P\tau$ is obtained from the first part of the analysis, together with its temperature dependence. From this and the shock solutions τ_α is obtained as a function of α ; hence $dt_1/d\,(-\ln(1-\alpha))$ as a polynomial in $(-\ln(1-\alpha))$. This is integrated to give t_1 as a polynomial in $(-\ln(1-\alpha))$. This polynomial is then inverted to give $\ln(1-\alpha)$ as a function of t_1. This also gives the first value of α_{MEAN}. The iteration is repeated: convergence of α_{MEAN} is very rapid.

5-5) THE SIMPLIFICATION OF (5-11).

Kiefer and Lutz have shown that when the semilog plots of h against t_1 are linear, a simplified form of their analysis may be used. This is esentially a modification of Blackman's (59) interpretation of his shock tube interferometric measurements. The modification may be stated

$$P\tau = P\tau_{APP}\left(\frac{\rho_2}{\rho_1}\right)\left(\frac{C_p^t}{C_p^*}\right) \qquad (5\text{-}15)$$

where C_p^t is the total heat capacity of the gas at the equilibrium temperature T^{11} and C_p^* is the heat capacity of the unrelaxed gas (3·5R for a diatomic molecule). The calculated $P\tau$, P and ρ_2 all refer to the equilibrium temperature T^{11} i.e. at $\alpha = 1{\cdot}0$.

5-6) DEMAGNIFICATION OF THE LASER BEAM.

Reduction of the laser beam width by a demagnifying telescope gives a better approximation to a point source of light. For a given density gradient this demagnification increases the size of the schlieren signal, however it increases the divergence of the beam.

It may be shown that the signal to noise ratio of the schlieren pulse is proportional to $\frac{\beta}{\alpha_1}\frac{p}{M}^{\frac{1}{2}}$ where

β = angular schlieren deflection

p = laser power

α_1 = " divergence

M = Demagnification factor of the telescope.

and hence demagnification also reduces the signal to noise ratio by the factor M. Normally the increase in signal observed by using a narrower

beam outweighs this decrease in signal to noise ratio. Some demagnification of the laser beam is therefore desirable.

5-7) RESULTS.

Quantitative relaxation measurements at station B were made using a Scientifica 5 mw. He-Ne gas laser. Initially results were obtained without demagnification of the beam through the shock tube; however, as suggested in Section 6 above, the system functioned best when a 6-1 reduction in beam width was used. The layout of the optical system is given in fig. (5-4).

The apparatus was tested using a mixture of 10% H_2, 90% N_2; the gas was shocked to about 1500-2000^{oK}, P_1 = 20 - 50 torr. From both White's results (80) and the emission tracer measurements at 2500^{oK} (Chapter 4) the observed relaxation times are expected to be about 2-3 μsec. lab. time under these conditions.

The dependence of the photomultiplier signal on beam deflection was checked experimentally by chopping the laser beam mechanically and moving the knife edge/photomultiplier combination across the beam. This dependence was found to be linear until 60% of the beam had been deflected off the knife edge.

Difficulties were experienced in distinguishing the schlieren signal due to relaxation from noise due to the laser oscillations and from mechanical noise elsewhere in the building. The laser noise was $\simeq$ 2% of the signal with a frequency of c. 1 MHz. modulated by a 10 KHz. envelope.

The noise was considerably reduced by the use of the Tektronix 1A1

FIG. 5-4

THE QUANTITATIVE SCHLIEREN APPARATUS.

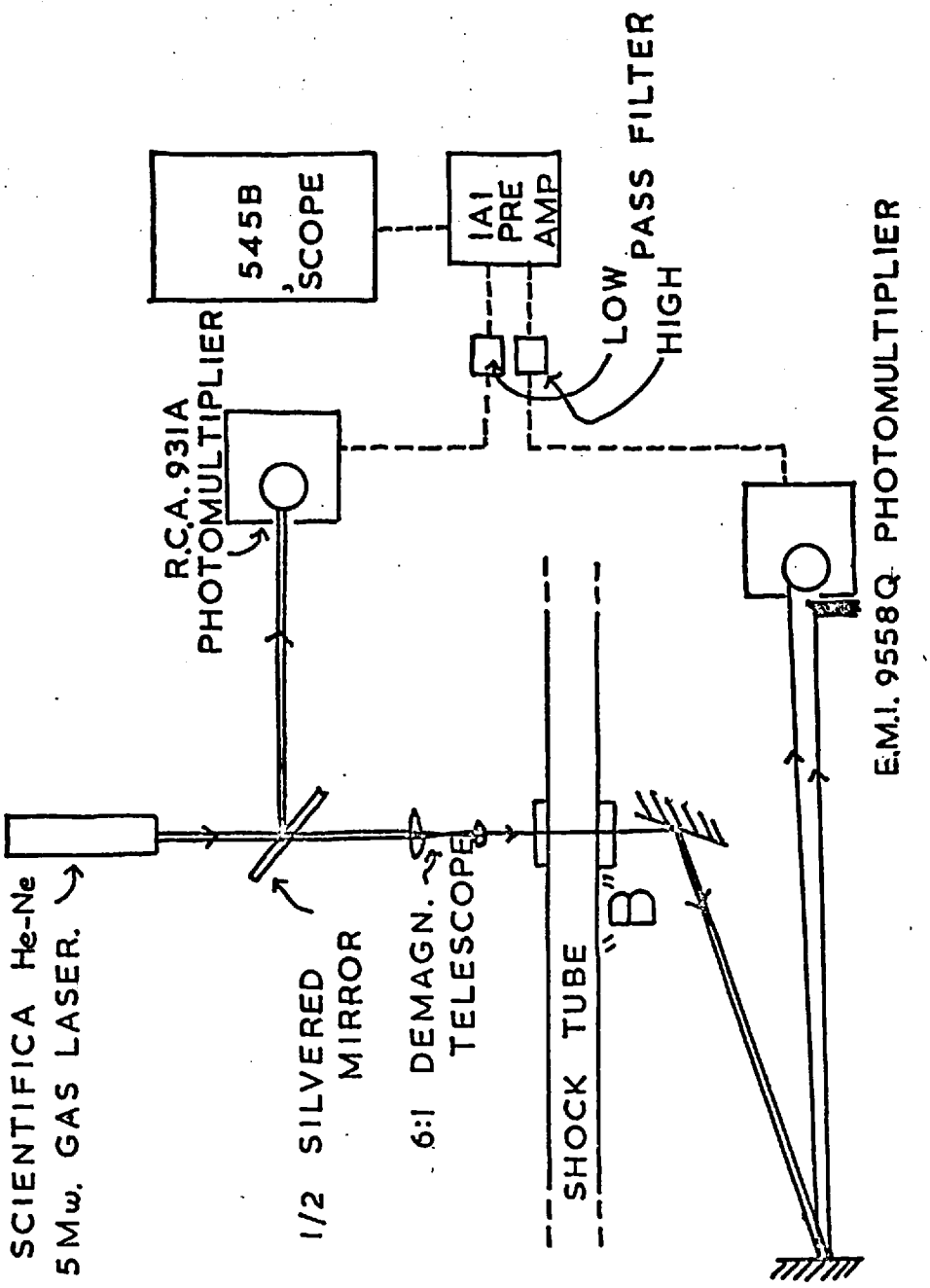

differential preamplifier. The output of the schlieren photomultiplier was passed through a high pass filter (cut off approx. 1 KHz.) to eliminate the mechanical noise and was monitored on one channel of the preamplifier.

The second channel monitored the signal from an R.C.A. 931A photomultiplier which viewed a sample of the light from the laser beam. This signal was passed through a low pass filter (cut off approx. 5 MHz.) to remove V.H.F. "fuzz".. When the 1A1 was used in the "subtract" mode the 10 KHz. noise envelope could be almost completely eliminated.

The remaining 1MHz laser noise was found to be a function of the laser cavity. This was removed by slightly adjusting one of the cavity mirrors. This involved a slight loss in laser power; as the 5mw. available from the laser exceeded the amount required for the schlieren system this was unimportant. Indeed it was necessary to check that the laser intensity did not "saturate" the photomultipliers. Examples of observed traces (i) with laser noise (ii) after processing are shown in fig. (5-5).

The schlieren traces were analysed using both (5-11) and (5-15). The comparison of the results obtained from both the simple and formal equations is shown for several runs in Table 5-1.

FIG. 5-5

OBSERVED SCHLIEREN PULSES.

(a) WITH LASER NOISE

(b) WITHOUT LASER NOISE

TIME SCALES: 2 μSEC/CM.

Table 5-1.

Calculation of $P\tau$.

$P\tau_{APP}=\left(1/\frac{d\ln h}{dt_g}\right) \times P$	eqn.(5-11)-formal $P\tau$ .atm.sec.	T^{oK}	eqn.(5-15)-simple $P\tau$ .atm.sec.	T^{oK}
$2\cdot3.\ 10^{-5}$	$2\cdot73.\ 10^{-5}$	1539	$2\cdot7.\ 10^{-5}$	1506
$1\cdot5.\ 10^{-5}$	$1\cdot83.\ 10^{-5}$	1531	$1\cdot8.\ 10^{-5}$	1514
$1\cdot3.\ 10^{-5}$	$1\cdot58.\ 10^{-5}$	1470	$1\cdot6.\ 10^{-5}$	1456
$8\cdot8.\ 10^{-6}$	$1\cdot13.\ 10^{-5}$	1978	$1\cdot1.\ 10^{-5}$	1955
$2\cdot1.\ 10^{-5}$	$2\cdot53.\ 10^{-5}$	1548	$2\cdot5.\ 10^{-5}$	1531

Fig. (5-6) shows the analysis plot for one run; fig. (5-7) gives the plot of $\log_{10} P\tau\ (N_2 - H_2)$ against $T^{-1/3}$ calculated from these results. These results are in agreement with previous measurements (80 and Chapter 4). They also agree with the Millikan and White semi-empirical formula. There is some scatter in the points - this is to be expected as the results were used both to develop and improve the system as well as to yield quantitative results.

The precautions used to reduce the laser noise left much to be desired. To obtain more accurate results it was necessary to increase the sensitivity of the system - some work has therefore been performed on a modification.

5-8) A POSSIBLE MODIFICATION TO THE LASER SCHLIEREN TECHNIQUE.

The modification is based on the R.V. Jones amplifier (104). The application of this to the laser schlieren technique is shown in fig. (5-8). Matching vertical lined grids are inserted on either side of the shock tube observation windows. The image formed by illuminating the first grid with the laser is superimposed on the second grid after traversing through the shock tube. The grids are adjusted so as to give either a half black/ half white or a totally black field of view at the photomultiplier window.

FIG. 5-6

A TYPICAL ANALYSIS

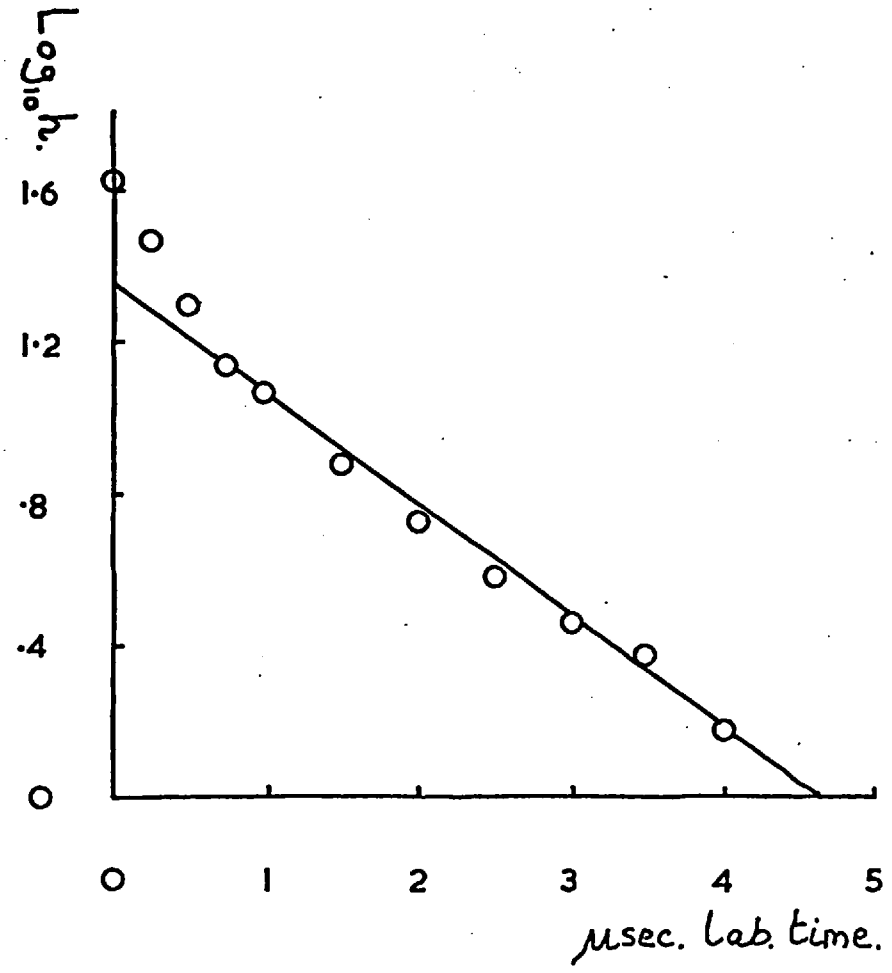

C.542 10% H_2/N_2 $P_1 = 20$ TORR. $U = 2{\cdot}09$ mm. μsec^{-1}.

$P\tau = 1{\cdot}13.10^{-5}$ ATM. SEC AT $\alpha_{mean} = {\cdot}85$

$T = 1978^{\circ}K$

FIG. 5-7

RESULTS FROM THE 10%H_2/N_2 MIXTURE.

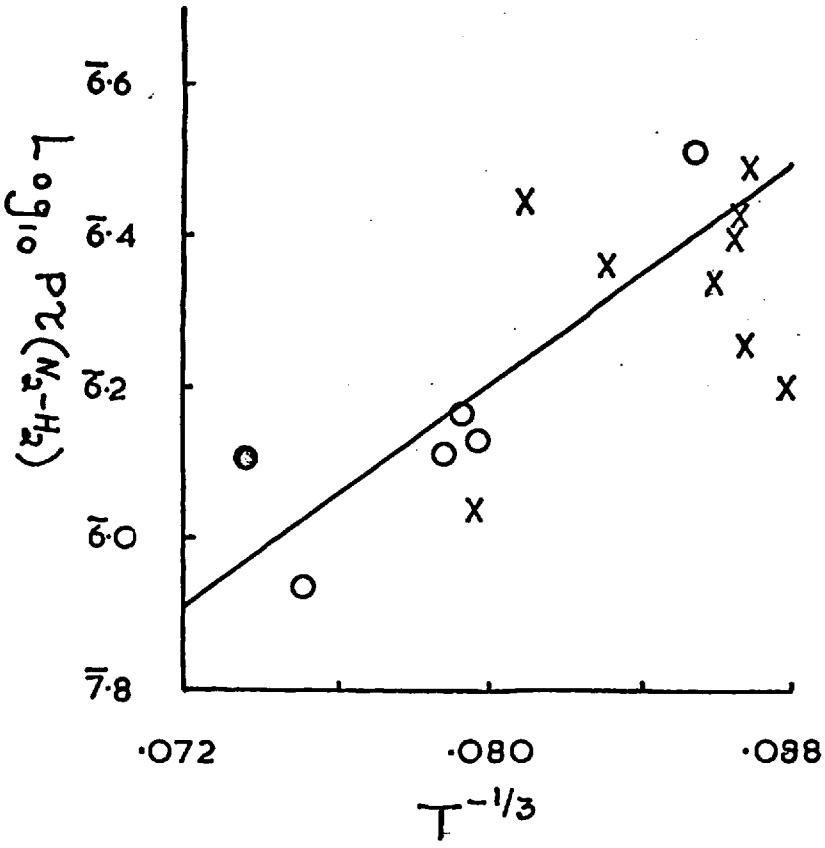

X — LASER SCHLIEREN

O — WHITE (REF. 80)

⊘ — SO_2 EMISSION 2500°K

M. & W. EQN.

FIG. 5-8

A POSSIBLE MODIFICATION TO THE APPARATUS.

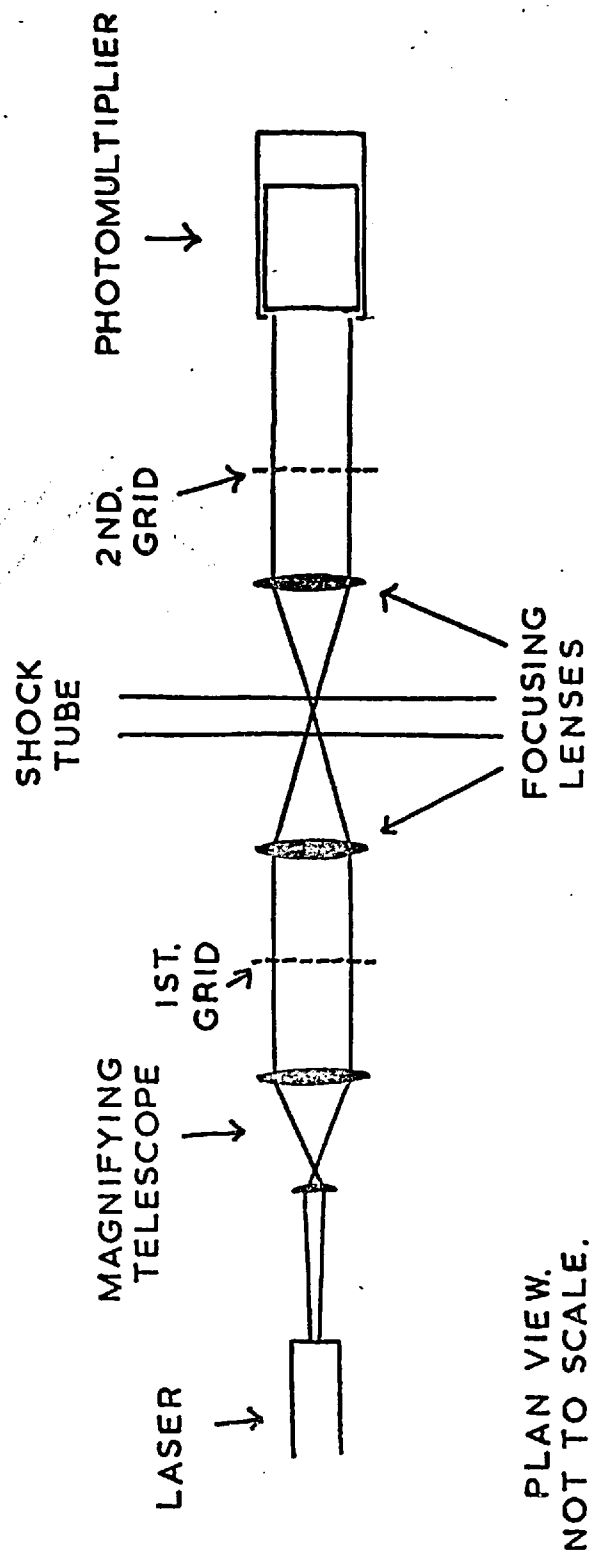

Any schlieren deflection moves the image of the first grid relative to the second grid and alters the intensity observed by the photomultiplier. In effect each line on the grid acts as a knife edge. As the sensitivity of the system is proportional to the number of knife edges then the schlieren signal is increased.

No schlieren results behind shock waves have been obtained with this system but static tests have shown the apparatus to be feasible. Initial tests suggested that grids with about 20-40 lines per inch are practical. These must be identical and drawn very accurately to avoid Moiré fringes. The best method of manufacture is to photograph a large scale grid and reduce the size of the negative. The whole apparatus must be rigidly mounted against vibration and a fine adjustment must be provided to superimpose the grids.

The beam cannot be demagnified before going through the shock tube owing to the diffraction patterns that are produced. The beam size traversing the tube is hence not of constant width; according to fig. (5-8) the beam is focused at the centre of the shock tube. The mathematical interpretation of this focused system will possibly be complex.

Time has precluded any further investigations using these laser schlieren systems, however it is hoped that further measurements of vibrational relaxation will be made using the apparatus that has been described.

APPENDIX I.

FLOW CORRECTIONS IN LOW PRESSURE SHOCK TUBES.

Boundary layer formation in small diameter, low pressure shock tubes causes considerable inaccuracies to the hydrodynamic parameters of the hot gas (68, 69, 70). The major effect that is observed is a drastic reduction of the "hot gas flow" length. This causes one to underestimate the gas particle times of the shocked gas; this effect was responsible for the non "Landau-Teller behaviour" of the relaxing gas described in Chapter 3. To a lesser extent the shocked gas temperature, pressure and density also increase over their computed values.

This appendix presents the method used to convert the laboratory times, t_l, into the correct gas particle times t_g.

For ideal, inviscid flow:

$$t_l = t_g / (\rho_2 / \rho_1)$$

and where a flow correction must be applied:

$$t_l = t_g / \left[(\rho_2 / \rho_1) \cdot C \right]$$

where C is the correction factor. Hobson et al. (70) present this factor graphically as a function of l/l_m (ref. 70. fig. 6.; $C = \frac{t_{part}}{t_{ideal}}$)

l_m is the limiting flow length - the "Mirels" length of Chapter 3.

l is the distance of the shock front from the observed gas.

$$l_m \simeq t_m . U.$$

$$l \simeq t . U.$$

where t_m is the limiting test time; t is the lab. time at the point of observation. U is the shock velocity.

Calculation of l_m.

Simplifying eqn. (3) of ref. (68) (and assuming a value of $\sqrt{3}$ for β):

$$l_m = \frac{A.P_1.U.}{T_2(W-1)} \text{ metres.} \qquad (1)$$

where $A \simeq 7{\cdot}8.\ 10^{+5}$ for air

$\simeq 8{\cdot}7.\ 10^{+5}$ for argon.

P_1 = unshocked gas pressure in torr.

T_2 = shocked gas temperature, ^{o}K.

W = density ratio, ρ_2/ρ_1.

This is for our tube diameter of $1\frac{1}{2}$". For any other diameter d", multiply l_m from (1) by $\left(\frac{d}{1{\cdot}5}\right)^2$.

This calculation enables the parameter l/l_m to be obtained. The correction factor C is then obtained from fig. 6. ref. 70.

The correction factor is only strictly exact when the gas has reached its limiting separation condition. Hobson (70) has shown, however, that the correction may be applied to gas flows before they have reached this state. In these cases the value of l_m that must be used in the correction is obtained from the observed test time. The calculated value from eqn. (1) is incorrect and will underestimate the flow correction.

Fig. 6 of reference 70 is reproduced in Fig. 3-9 of this thesis.

BIBLIOGRAPHY.

1. P. Ehrenfest. Proc. Koninkl. Ned. Akad. Wetenschap., 1914, 16, 591.

2. T.L. Cottrell & J.C. McCoubrey "Molecular Energy Transfer in Gases" (Butterworths, London, 1961).

3. S.R. Byron. J. Chem. Physics 1959, 30, 1380.

4. P. Borrell. Adv. Molecular Relaxation Processes. 1967, 1, 97.

5. A.B. Callear. Ann. Rept. Progress Chemistry. 1964, 61, 48.

6. " J. Appl. Optics. Supplement 2, 1965.

7. J.D. Lambert. Quart. Reviews 1967, 21, 67.

8. S.H. Bauer. Ann. Rev. Physic. Chemistry. 1965, 16, 245.

9. R.C. Millikan. "Molecular Relaxation Processes" (Chem. Soc. Spec. Publication No.20; Academic Press, London, 1966) p. 219.

10. A.W. Read. Progr. Reaction Kinetics 1965, 3, 203.

11. T.L. Cottrell. "Dynamic Aspects of Molecular Energy States" (Oliver and Boyd, Edinburgh, 1965).

12. L. Landau & E. Teller. Phys. Z. Sowjet Union 1936, 10, 34.

13. R.N. Schwartz, Z.I. Slawsky, & K.F. Herzfeld. J. Chem. Physics. 1952, 20, 1591.

14. J.M. Jackson & N.F. Mott. Proc. Roy. Soc. 1932. A137, 703.

15. K.F. Herzfeld & T.A. Litovitz. "Absorption and Dispersion of Ultrasonic Waves" (Academic Press, New York, 1959).

16. J.B. Calvert & R.C. Amme. J. Chem. Physics. 1966, 45, 4710.

17. J.G. Parker. ibid. 1964, 41, 1600.

18. S.W. Benson & G.C. Berend. ibid. 1962, 37, 1386.

19. " " ibid. 1966, 44, 470.

20. B. Hartmann & Z.I. Slawsky. ibid. 1967, 47, 2491.

21. H.K. Shin. ibid. 1967, 47, 3302.

22. F.I. Tanczos. ibid. 1956, 25, 439.

23. J.L. Stretton. Trans. Faraday Soc. 1965, 61, 1053.

24. R.C. Millikan & D.R. White. J. Chem. Physics. 1963, 39. 3209.

25. S.A. Losev & A.I. Osipov. Soviet Physics-Uspekhi. 1962, 4, 525.

26. D. Rapp. J. Chem. Physics. 1964, 40, 2813.

27. " ibid. 1965, 43, 316.

28. T.L. Cottrell & A.J. Matheson. Trans. Faraday Soc. 1962, 58, 2336.

29. M.G. Ferguson & A.W. Read. ibid. 1967, 63, 61.

30. J.D. Lambert & R. Salter. Proc. Roy. Soc. 1959, A253, 277.

31. T.L. Cottrell, R.C. Dobbie, J. McClain and A.W. Read. Trans. Faraday Soc. 1964, 60, 241.

32. C. Bradley-Moore. J. Chem. Physics. 1965, 43, 2979.

33. E.E. Nikitin. Teor. Eksp. Khim . 1967, 3, 185.

34. A.B. Callear & G.J. Williams. Trans. Faraday Soc. 1966, 62, 2030.

35. J.H. Kiefer & R.W. Lutz. 11th Internat. Symposium on Combustion (Berkley, California 1966). Preprint paper II-5.

36. J.N. Bradley. "Shock Waves in Chemistry and Physics". (Methuen, London, 1962).

37. A.G. Gaydon & I.R. Hurle. "The Shock Tube in High Temperature Chemical Physics". (Chapman and Hall, London, 1963)

38. E.F. Green & J.P. Toennies. "Chemical Reactions in Shock Waves". (Arnold, London, 1964).

39. J.H. Kiefer & R.W. Lutz. J. Chem. Physics. 1966, 44, 658.

40. " " ibid. 1966, 44, 668.

41. " " ibid. 1966, 45, 3888.

42. A.G. Gaydon & I.R. Hurle. 8th Internat. Symposium on Combustion. (Williams and Wilkins, Baltimore, 1962) p. 309.

43. R.L. Taylor, M. Camac & R.M. Feinberg. 11th Internat. Symposium on Combustion (Berkley, California, 1966). Preprint paper II-6.

44. B.P. Levitt & D.B. Sheen. J. Chem. Physics. 1964, 41, 584.

45. " " Trans. Faraday Soc. 1965, 61, 2404.

46. " " ibid. 1967, 63, 540.

47. " " "Molecular Relaxation Processes." (Chem. Soc. Spec. Publication No.20; Academic Press, London, 1966) p. 269.

48. D.B. Sheen. Ph.D. Thesis (London University 1966).

49. A.De Vries &F.Klein. J. Chem. Physics. 1964, 41, 3428.

50. B.P. Levitt & D.B. Sheen. Trans. Faraday Soc. 1967, 63, 2955.

51. J.D. Lambert & R. Salter. Proc. Roy. Soc. 1957, A243, 78.

52. D. Shields. J. Chem. Physics, 1967, 46, 1063.

53. B.J. McBride, S. Heimal, J.G. Ehlers & S. Gordon. "Thermodynamic Properties to 6000^{oK} for 210 Substances involving the First 18 Elements". 1963, NASA Report SP-3001.

54. I.R. Hurle, A.L. Russo, & J.G. Hall. J. Chem. Physics 1964, 40, 2076.

55. T.A. Holbeche & J.G. Woodley. Royal Aircraft Establishment Tech. Memo. Aero 937 (1966).

56. K.N.C. Bray. Publication 67-3, 1967, Fluid Mechanics Laboratory, M.I.T.

57. A.L. Russo. J. Chem. Physics. 1966, 44, 1305.

58. R.L. Taylor. Private Communication.

59. V. Blackman. J. Fluid Mechanics. 1956, 1, 61.

60. N.H. Johannesen, H.K. Zienkiewicz, P.A. Blythe & J.H. Gerrard. ibid. 1962, 13, 213.

61. " ibid. 1963, 17, 267.

62. C.J.S.M. Simpson, K.B. Bridgeman & T.R.D. Chandler. 6th Internat. Shock Tube Symposium (Amer. Phys. Soc., Freiberg, Germany, 1967), paper B.9.

63. C.J.S.M. Simpson. 18th Shock Tube Liaison Meeting (Imperial College, April 1968).

64. M. Bristow. 17th Shock Tube Liaison Meeting (Liverpool, April 1967).

65. J.H. Kiefer & R.W. Lutz. Phys. Fluids 1966, 9, 1638.

66. J.P. Appleton. J. Chem. Physics. 1967, 47, 3231.

67. I.R. Hurle. ibid. 1964, 41, 3592,

68. H. Mirels. Phys. Fluids 1963, 6, 1201.

69. " ibid. 1966, 9, 1907.

70. J.N. Fox, T.I. McLaren & R.M. Hobson. ibid. 1966, 9, 2345.

71. R.C. Millikan & D.R. White. J. Chem. Physics. 1963, 39, 98.

72. " " Amer. Inst. Ast. Aero. J. 1964, 2, 1844.

73. S .J. Lukasik & J.E. Young. J. Chem. Physics 1957, 27, 1149.

74. T.A. Jacobs. ibid. 1967, 46, 1958.

75. " J. Physic. Chem. 1963, 67, 665.

76. H.E. Avery & J.N. Bradley. Trans. Faraday Soc. 1964, 60, 857.

77. E.F. Greene, R.L. Taylor & W.L. Patterson. J. Physic. Chem. 1958, 62, 238.

78. G.B. Skinner & R.A. Ruehrwein. ibid. 1959, 63, 1736.

79. V. Kevorkian, C.E. Heath & M. Boudart. ibid. 1960, 64, 964.

80. D.R. White. J. Chem. Physics 1967, 46, 2016.

81. " ibid. 1968, 48, 525.

82. R.C. Millikan. ibid. 1964, 40, 2594.

83. D.R. White. ibid. 1966, 45, 1257.

84. B. Cary. Phys. Fluids 1965, 8, 26.

85. R.R. Boade. J. Chem. Physics. 1965, 42, 2788.

86. D.R. White & R.C. Millikan. ibid. 1963, 39, 1803.

87. J.O. Hirschfelder, C.F. Curtiss & R.B. Bird. "Molecular Theory of Gases and Liquids" (Wiley, New York, 1954).

88. E.E. Nikitin. Dokl. Akad. Nauk. S.S.S.R. 1960, 132, 395.

89. A.P. Modica & J.E. LaGraff. J. Chem. Physics 1966, 45, 4729.

90. S.J. Colgan & B.P. Levitt. Trans. Faraday Soc. 1967, 63, 2898.

91. P.W. Huber & A. Kantrowitz. J. Chem. Physics 1947, 15, 275.

92. P. Borrell. "Molecular Relaxation Processes" (Chem. Soc. Spec. Publication No. 20; Academic Press, London, 1966) p. 263.

93. J.G. Parker & R.H. Swope. J. Chem. Physics. 1965, 43, 4427.

94. L.W. Richards & D.H. Sigafoos. ibid. 1965, 43, 492.

95. R.C. Millikan & D.R. White. ibid. 1963, 38, 214.

96. D.R. White. ibid. 1965, 42, 447.

97. B.H. Mahan. ibid. 1967, 46, 98.

98. R.D. Sharma & C.A. Brau. Physic. Rev. Letters 1968, 19, 1273.

99. C. Bradley-Moore, R.E. Wood, B.L.B. Hu, & J.T. Yardley. J. Chem. Physics. 1967, 46, 4222.

100. D.G. Jones, J.D. Lambert & J.L. Stretton. Proc. Physic. Soc. 1965, 86, 857.

101. J.T. Yardley & C. Bradley-Moore. J. Chem. Physics. 1968, 48, 14.

102. F.J. Weinberg. "Optics in Flames" (Butterworths, London, 1962).

103. E.L. Resler & M.Scheibe. J. Acoust. Soc. Am. 1955, 27, 932.

104. R.V. Jones & J.C.S. Richards. J. Scien. Inst. 1959, 36, 90.

105. D.R. White Private Communication.